11-2020

Eukaryotic Initiation Factor 5A2 (EIF5A2) Contributes to Ovarian Tumor Growth and Metastasis

Guannan Zhao
University of Tennessee Health Science Center

Eukaryotic Initiation Factor 5A2 (EIF5A2) Contributes to Ovarian Tumor Growth and Metastasis

Abstract

Ovarian cancer has the highest mortality rate among all gynecological malignancies due to lack of effective biomarkers for early diagnosis. The majority of ovarian cancer patients are already at an advanced stage when diagnosed. In addition, ovarian cancers often become chemoresistant and metastatic, and recur following initial chemotherapy.

Document Type

Dissertation

Degree Name

Doctor of Philosophy (PhD)

Program

Biomedical Sciences

Research Advisor

Junming Yue, PhD

Keywords

Deoxyhypusine synthase, EIF5A, Epithelial to mesenchymal transition, Hypusination, Ovarian cancer, TGFβ

Subject Categories

Diseases | Medical Cell Biology | Medical Sciences | Medicine and Health Sciences | Neoplasms

UNIVERSITY OF TENNESSEE HEALTH SCIENCE CENTER

DOCTORAL DISSERTATION

Eukaryotic Initiation Factor 5A2 (EIF5A2) Contributes to Ovarian Tumor Growth and Metastasis

Author:
Guannan Zhao

Advisor:
Junming Yue, PhD

A Dissertation Presented for The Graduate Studies Council of
The University of Tennessee Health Science Center
in Partial Fulfillment of the Requirements for the Doctor of Philosophy degree from
The University of Tennessee

in

Biomedical Sciences: Cancer & Developmental Biology
College of Graduate Health Sciences

November 2020

ACKNOWLEDGEMENTS

I would like to express my deepest gratitude to my advisor Dr. Junming Yue for his longtime supervision and support on my PhD research project. His knowledge, endurance, and perspectives on research have always been an aspiration for me and will continue to benefit my future career. I also want to thank all the coworkers in Dr. Yue's lab for their generous and friendly support. I also want to thank my graduate committee members, Drs. Lawrence M. Pfeffer, Ramesh Narayanan, Zhaohui Wu, and Zheng Fan for their advice and mentoring during my PhD program. In addition, I would like to thank the staff in the Research Histology Core Laboratory, and Institutional Animal Care and Use Committee (IACUC) at the UTHSC.

I would like to acknowledge my family members and my friends for their unabated and continued encouragement, support and love during my PhD training.

I also would like to thank NIH/NCI for the funding support.

ABSTRACT

Ovarian cancer has the highest mortality rate among all gynecological malignancies due to lack of effective biomarkers for early diagnosis. The majority of ovarian cancer patients are already at an advanced stage when diagnosed. In addition, ovarian cancers often become chemoresistant and metastatic, and recur following initial chemotherapy.

Eukaryotic initiation factor 5A2 (EIF5A2) is an isoform of eukaryotic initiation factor (EIF5A). EIF5A2 is involved in protein translation, elongation, and termination. EIF5A2 is rarely detected in normal tissues but is highly expressed in many malignancies including ovarian cancer. EIF5A2 expression is highly correlated with poor patient survival. However, the functions of EIF5A2 and the underlying molecular mechanisms that contribute to ovarian tumor development have not been well investigated. The goal of this study was to determine the regulatory mechanisms of EIF5A2 expression in ovarian cancer and define the role of EIF5A2 in ovarian primary tumor growth and metastasis.

In this study, we found that CRISPR/Cas9 mediated knockout (KO) of EIF5A2 inhibits the epithelial to mesenchymal transition (EMT) in ovarian cancer cells and suppresses cell migration and invasion. In contrast overexpression of EIF5A2 promotes EMT, migration, and invasion. Moreover, KO of EIF5A2 inhibits primary ovarian tumor growth and metastasis in an orthotopic ovarian cancer mouse model. KO of EIF5A2 attenuates the TGFβ signaling pathway, and TGFβ induces EIF5A2 expression through transcriptional regulation in ovarian cancer cells. Our findings demonstrated that EIF5A2 promotes EMT via activating the TGFβ pathway in ovarian cancer cells, and EIF5A2 forms a positive feedback loop with TGFβ and contributes to ovarian tumor metastasis by promoting EMT.

EIF5A is the only known hypusinated protein, and hypusination is required for EIF5A2 maturation. The amino acid hypusine is formed by the post-translational modification of lysine 50 residue in the EIF5A2 molecule through deoxyhypusine synthase (DHS). N1-guanyl-1, 7-diaminoheptane (GC7), an inhibitor of DHS, blocks the hypusination of EIF5A2. Disruption of the EIF5A2-hypusination pathway, by either genetic or pharmacological approaches, suppresses ovarian tumor growth and metastasis.

In summary, this study addressed the molecular mechanisms involved in the regulation of EIF5A2 in ovarian tumor metastasis and identified novel therapeutic strategies to combat ovarian cancer by targeting EIF5A2/TGFβ/EMT axis or hypusination pathways.

TABLE OF CONTENTS

LIST OF TABLES

LIST OF FIGURES

LIST OF ABBREVIATIONS

CRISPR/Cas9	Clustered Regularly Interspaced Short Palindromic Repeats/Cas9
DFS	Disease-Free Survival
DHS	Deoxyhypusine Synthase
DOHH	Deoxyhypusine Hydroxylase
EIF5A	Eukaryotic Initiation Factor 5A
EIF5A1	Eukaryotic Initiation Factor 5A1
EIF5A2	Eukaryotic Initiation Factor 5A2
EMT	Epithelial to Mesenchymal Transition
EOC	Epithelial Ovarian Cancer
ESCC	Esophageal Squamous-Cell Carcinoma
FTE	Fallopian Tube Epithelium
GC	Gastric Cancer
GC7	N1-guanyl-1,7-diamine-heptane
HCC	Hepatocellular Carcinoma
i.p.	Intraperitoneal
i.v.	Intravenous
IHC	Immunohistochemistry
KD	Knockdown
KO	Knockout
NSCLC	Non-Small Cell Lung Cancer
NSG	NOD.Cg *Prkdcscid Il2rgtm1Wjl*/SzJ
OS	Overall Survival

OSCC	Oral Squamous Cell Carcinoma
OSE	Ovarian Surface Epithelial
SAT1	Spermidine/Spermine N(1)-Acetyltransferase
TCGA	The Cancer Genomic Atlas
TGF-β	Transforming Growth Factor-β
TGFβR1	Transforming Growth Factor-β receptor-1
TGFβR2	Transforming Growth Factor-β receptor-2
TGFβR3	Transforming Growth Factor-β receptor-3
UTR	Untranslated Region

CHAPTER 1. INTRODUCTION

Background

Ovarian cancer ranks fifth in causing death among women's malignancies. Over 300,000 ovarian cancer cases were diagnosed globally in 2018, and it is projected that by the year of 2035 the case number will rise to 371,000 per year and deaths of 254,000 per year (Bhatla and Jones, 2018). The five-year survival rate of ovarian cancer is approximately 47%, which is the lowest survival among gynecological malignances (Torre et al. 2018). The high mortality rate of ovarian cancer patients reflects the typically late stage of the cancer at time of diagnosis. More than three quarters of ovarian cancer patients are diagnosed at stages III and IV, when cancer cells already have spread throughout the abdominal cavity. Therefore, it is essential to identify novel biomarkers for early diagnosis and develop therapeutics to inhibit ovarian tumor metastasis (Brown and Palmer, 2009; Burger, 2008; Kurman et al., 2008).

Ovarian carcinoma metastasis is markedly different from other types of cancer. While the classic and well-studied hematogenous metastasis is the major approach for other cancers, ovarian carcinoma disseminates through pelvic or para-aortic lymph nodes and directly invades neighboring or distant organs, including omentum, colon and liver. This process allows ovarian tumor cells to spread easier than other carcinomas (Eisenkop and Spirtos, 2001).

Ovarian cancer development

Based on tumor cell morphology, ovarian cancer is classified into two categories: non-epithelial and epithelial ovarian cancer (EOC) (Bast et al., 2009). The majority of ovarian tumors belong to EOC, which accounts for 95% of the ovarian malignancies. The effective detection of early-stage EOC requires the understanding of the mechanisms of EOC initiation, progression, and metastatic transition (Kim et al., 2018).

EOCs were thought to originate from ovarian surface epithelial (OSE) cells (Hamilton, 1992). In the past two decades, the fallopian tube epithelium (FTE) has emerged as the new primary origin of EOC (Kindelberger et al., 2007; Nik et al., 2014). However, recent studies indicated that both OSE and FTE are the origins of epithelial ovarian cancer (Kim et al., 2018).

During initial tumor metastasis, EOC cells detach from ovaries and dissociate into single cells or form tumor spheres in the peritoneal cavity (Lengyel, 2010). While single tumor cells undergo apoptosis, the tumor spheres metastasize to distant organs, accompanied by frequent ascitic fluid accumulation, which contributes to a poor patient survival rate (Lengyel, 2010; Scalici et al., 2017; Ahmed and Stenvers, 2013).

Epithelial-to-mesenchymal transition (EMT). EMT is characterized by the loss of adherence junctions and apical-basal polarity, gain of motility, and switch into stem cell-like mesenchymal phenotype (Nieto, 2013). EMT has been found to participate in many biological processes, such as epithelial development, wound healing, organ fibrosis, and cancer metastasis (Nieto et al., 2016; Nauseef and Henry, 2011; Micalizzi et al., 2010). Experimental evidence demonstrates that EMT is essential in tumor initiation, progression, invasion and metastasis (Micalizzi et al., 2010; Drasin et al., 2011; DiMeo et al., 2009).

The role of EMT in ovarian cancer supports its participation in metastasis and chemoresistance (Lili et al., 2013; Ahmed et al., 2010). For example, EMT contributes to ovarian cancer cell survival in low oxygen conditions, and the secretion by tumor cells of soluble factors that regulate the function of surrounding stromal cells (Imai et al., 2003). Prior to their detachment and metastasis, ovarian carcinoma cells often undergo EMT, which reduces the intercellular adhesion between cancer cells and facilitates the attachment of epithelial cells to the basement membrane (**Figure 1-1**) (Farghaly, 2012). Once the ovarian tumor cells establish a metastatic colony in the omentum or peritoneum, tumor cells undergo the mesenchymal-to-epithelial transition (inverse of the process of EMT) to regain an epithelial phenotype, which permits cells to interact with paracrine growth factors and proliferate at a high growth rate (Haque and Morris, 2017).

The phenotypic switch in EMT is accompanied by alternating the gene expression profiles of both epithelial and mesenchymal markers, such as Ecadherin, Snail1 and Snail2, Twist, Vimentin, ZEB1, ZEB2, and others (Zhao et al., 2019). In epithelial cancer, the acquisition of an invasive phenotype during EMT typically correlates with the loss of Ecadherin (Kalluri and Weinberg, 2009). Ovarian tumor cells in ascites and at metastatic sites have lower Ecadherin expression than primary tumor cells, and ovarian carcinoma with lower Ecadherin is more invasive and associated with poor patient survival (Daraï et al., 1997). Furthermore, EMT is regulated by multiple signaling pathways including TGFβ, WNT, and Notch, which are activated in various human cancers (DiMeo et al., 2009; Miyamoto et al., 2013; Liu et al., 2012b; Hoffmeyer et al., 2012; Espinoza et al., 2013; Muraoka et al., 2002).

Despite the significant improvement in understanding the molecular mechanisms of EMT in the past decade, it is still unclear how EMT is regulated in ovarian tumor progression and metastasis. It is important to further identify the critical target genes or gene networks in regulating EMT and develop the novel therapy by reversing the EMT phenotypic switch.

Transforming growth factor-β (TGFβ). TGFβ is a multifunctional cytokine that regulates many biological processes, including cell growth, differentiation, apoptosis, and motility as well as extracellular matrix production, angiogenesis, and cellular immunity (Haque and Morris, 2017). The role of TGFβ in cancer development is paradoxical: TGFβ can inhibit cellular transformation and block cancer progression when cancer development is in the early stages; however, in later stages cancer cells can circumvent the inhibitory effects of TGFβ and undergo tumor progression by promoting EMT,

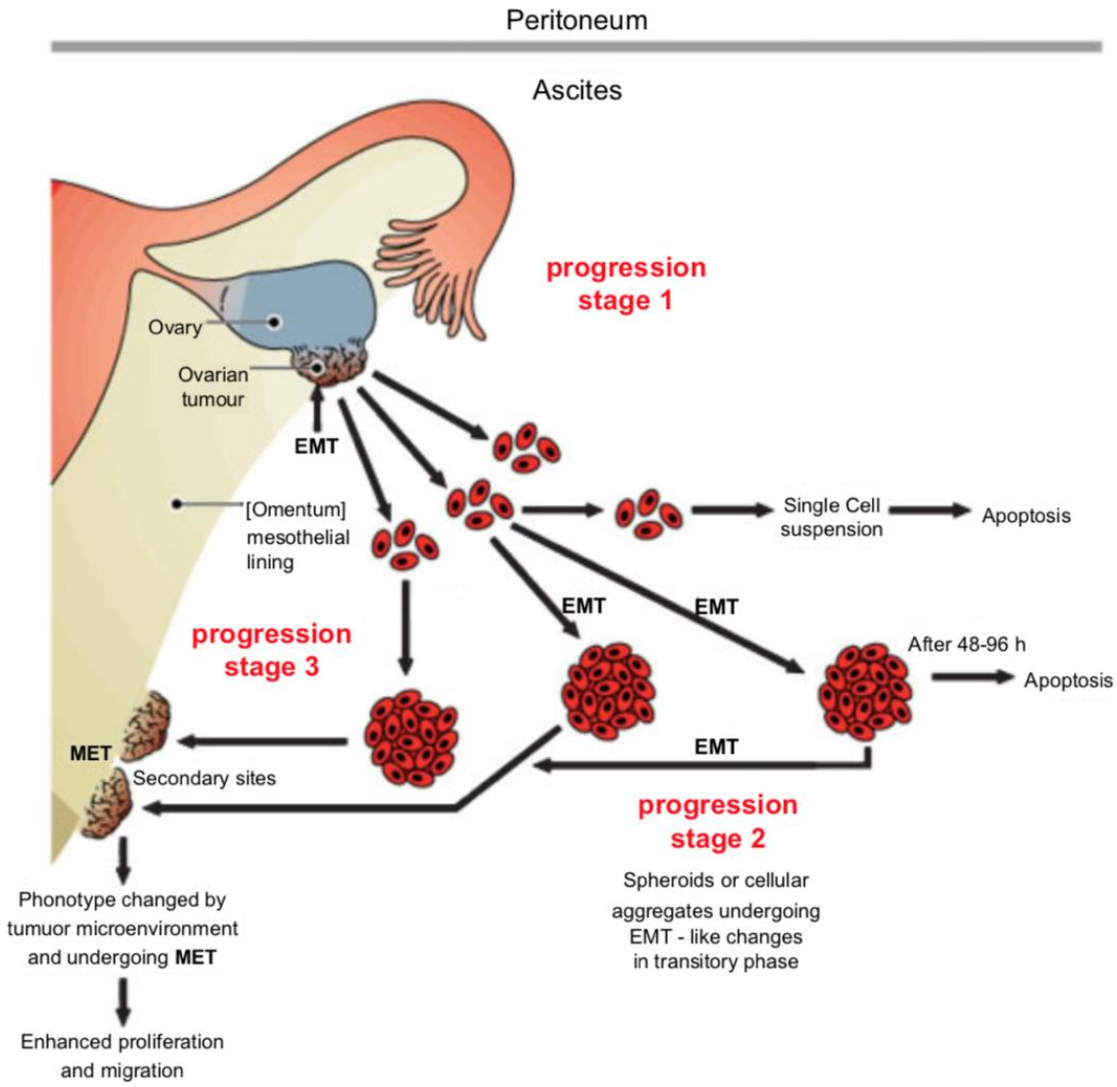

Figure 1-1. Scheme showing a working model of ovarian cancer progression. There are three stages during ovarian tumor metastasis. In stage 1, epithelial ovarian tumor cells undergo EMT to obtain motility and start to metastasize. The shed tumor cells undergo apoptosis while the other surviving tumor cells form cellular aggregates or spheroids during stage 2. The cellular aggregates and spheroids subsequently infiltrate the mesothelial lining of the abdominal cavity where they undergo MET to allow cells to attach and proliferate and migrate.
Reprinted with open access permission. Farghaly, S. (2013). "Anti-metastatic gene therapy in patients with advanced epithelial ovarian cancer (EOC)." J Cell Sci Ther, S:15, 2.

stimulating angiogenesis, and inducing immunosuppression (Yan and Sun, 2014; Haque and Morris, 2017).

TGFβ effectively induces EMT in various epithelial cells (Xu et al., 2009). TGFβ causes the phenotypic switch from cuboidal epithelial cells into elongated spindle mesenchymal cells, which is accompanied by reduced expression of epithelial markers and increased expression of mesenchymal markers (Miettinen et al., 1994). Enhanced production of active TGFβ is often observed in cancer cells. A study showed that the conversion into more invasive spindle cell carcinomas correlates with the expression of activated TGFβ (Cui et al., 1996). Enhanced TGFβ production not only triggers EMT and enables cellular invasiveness but also promotes angiogenesis in the tumor microenvironment, offering an exit route for migratory mesenchymal cells (Derynck et al., 2001).

In the TGFβ signaling pathway, TGFβ binds to transforming growth factor-β receptor-2 (TGFβR2) and initiates the signaling process. The binding process also requires transforming growth factor-β receptor-3 (TGFβR3, also known as β-glycan), which induces a conformational change in TGFβR2 that facilitates the ligand-receptor binding (López-Casillas et al., 1993; Sankar et al., 1995). TGFβ receptor-1 (TGFβR1)/ALK-5, a serine/threonine kinase, is incorporated into the TGFβ/TGFβR2 complex to phosphorylate Smad2 and Smad3 and initiate signaling. Smad2 and Smad3 are two proteins belonging to the receptor-regulated Smad family (Haque and Morris, 2017). The phosphorylated Smad2 and Smad3 combine with Smad4 to form the heteromeric Smad complex, which then translocates into the cell nucleus and interacts with various transcriptional factors to activate downstream target genes (Dou et al., 2000).

The eukaryotic initiation factor 5A (EIF5A). EIF5A is present in most of the eukaryotic cells (Park et al., 1993) and was initially identified as a translation initiation factor that acts in the final step of protein synthesis by promoting the formation of the first peptide bond (Wu et al., 2020). Recent experimental results have suggested that EIF5A also participates in translation elongation and termination (Wu et al., 2020). A positive correlation has been found between cancer cell proliferation and EIF5A expression during protein synthesis (Caraglia et al., 2013). Mounting evidence indicates that EIF5A promotes cell proliferation, cancer progression, invasiveness and metastasis, and is also associated with poor clinical prognosis (Caraglia et al., 2013; Xie et al., 2008; Lee et al., 2010; Marchet et al., 2007; Clement et al., 2006).

There are two isoforms of EIF5A, EIF5A1 and EIF5A2, which have 84% similarity in cDNA and 94% similarity in protein sequences (Clement et al., 2003; Saini et al., 2009). EIF5A1 is expressed in many normal tissues while EIF5A2 is expressed only in specific normal tissues. However, both EIF5A1 and EIF5A2 expression is elevated in a variety of cancers. The low expression of EIF5A2 in normal tissues and high expression in cancer tissues makes EIF5A2 a potentially more sensitive biomarker for cancer diagnosis than EIF5A1.

EIF5A2 is located near chromosome 3q26, which is frequently amplified in many solid tumors (Wang et al., 2013). Overexpression of EIF5A2 is associated with a more advanced and aggressive disease status in many cancers. For example, one study found that EIF5A2 expression correlates with tumor recurrence and progression in pTa/pT1 urothelial carcinoma of the bladder (Luo et al., 2009). Silencing EIF5A2 in ovarian cancer cell line UACC-1598 inhibits cell growth and blocks the oncogenic properties of EIF5A2 (Clement et al., 2006). EIF5A2 expression is also significantly correlated with tumor cell proliferation in colorectal cancer (Xie et al., 2008). In addition, a higher risk of lymph node metastasis is strongly associated with expression of EIF5A2 in colorectal carcinoma (Xie et al., 2008; Lee et al., 2010; Marchet et al., 2007). In gastric cancer, EIF5A2 is correlated with advanced clinic pathological features and reduced survival. In hepatocellular carcinoma (HCC), more than half of HCC show upregulated mRNA levels of EIF5A2 compared to normal tissues. By Kaplan–Meier analysis, EIF5A2 expression is significantly associated with shorter survival of HCC patients (Cao et al., 2017). The expression level of EIF5A2 is high in many non-small cell lung cancers and low in all tested normal lung tissue (He et al., 2011). In cervical cancer tissues, the levels of both EIF5A2 mRNA and protein are upregulated compared to adjacent non-tumor tissues, and the aggressive features of cervical cancer is associated with higher EIF5A2 expression (Yang et al., 2016b). EIF5A2 is also suggested to be a potential biomarker for shorter overall survival and disease-free survival in stage II cervical cancer patients as well as in patients with a negative pelvic lymph node status. In esophageal squamous cell carcinoma (ESCC), tumor tissues show elevated levels of EIF5A2 mRNA compared with paired non-tumor tissues, and tumor tissues have higher frequency of positive staining of EIF5A2 than in non-tumor tissues based on immunohistochemistry staining of 232 tumor tissues and 215 non-tumor tissues (Li et al., 2014). The authors also revealed that EIF5A2 contributes to metastasis and angiogenesis in ESCC, suggesting that EIF5A2 is a promising target for treatment. Overexpression of EIF5A2 in various types of human cancers are summarized in **Table 1-1**.

A previous study suggested that EIF5A2 is an important biomarker for the prognosis of many human cancers (Wang et al., 2013). Knockdown of EIF5A2 effectively suppresses tumor cell growth and migration, suggesting that EIF5A2 has potential as target for anticancer therapy (Wang et al., 2013). However, the molecular mechanisms underlying the regulation of EIF5A2 expression remain unknown. One study suggested that EIF5A2 shuttles between cell nucleus and cytoplasm (Zender et al., 2008). Experimental evidence supporting EIF5A2 as a transcriptional factor in the nucleus is still lacking. How is EIF5A2 frequently overexpressed in various human cancers? What are the upstream and downstream targets of EIF5A2 in human cancers? How does EIF5A2 regulate EMT in cancers? Those questions need to be further addressed.

EIF5A2 was first detected in ovarian cancer cell line UACC-1598 (Clement et al., 2003). In a later study, EIF5A2 was found in 7% of cystadenomas, 30% of borderline tumors, 53% of invasive ovarian carcinomas, and 16% of informative ovarian carcinomas while EIF5A2 was barely detected in normal ovaries (Yang et al., 2009). EIF5A2 expression is significantly associated with shortened patient survival (mean 39.0 months vs 69.5 months) in ovarian carcinoma (Yang et al., 2009). These findings suggest that

Table 1-1. Summary of EIF5A2-overexpression-related findings in human cancers.

Main conclusions related with high level EIF5A2 in various human cancers	Reference
Overexpression of EIF5A2 in Federation of Gynecology and Obstetrics (FIGO) stage I-II cervical cancer cells showed strong cancer progression, and patients showing high EIF5A2 expression in tumors had relatively shorter survival time.	(Yang et al., 2016b)
Silencing of EIF5A2 inhibits cell migratory and invasive capacities in non-small cell lung cancer (NSCLC) tissues.	(Chen et al., 2018), (He et al., 2011)
EIF5A2 promotes melanoma cell invasion by targeting phosphorylated Akt and was inversely correlated with the 5-year survival time of primary melanoma patients.	(Khosravi et al., 2014), (Khosravi et al., 2016)
EIF5A2 overexpression in esophageal squamous cell carcinoma (ESSC) cells can induce chemoresistance to chemotherapeutic drugs, enhances metastasis and angiogenesis, and is correlated with a shorter survival times of patients.	(Yang et al., 2015), (Li et al., 2014)
EIF5A2 affects the doxorubicin chemoresistance in breast cancer, and inhibition of EIF5A2 activation can enhance the therapeutic efficacy of doxorubicin in estrogen negative cancer cells.	(Liu et al., 2015a), (Liu et al., 2015b)
Overexpression of EIF5A2 in colorectal carcinoma cells may help the acquirement of metastatic phenotype and assist the cancer development and progression.	(Xie et al., 2008)
EIF5A2 is highly expressed in prostate cancer and significantly associated with poor progression-free survival.	(Lu et al., 2019)
EIF5A2 overexpression is correlated with tumor metastasis in bladder cancer patients and promotes aggressiveness in cancer cells.	(Wei et al., 2014), (Chen et al., 2009), (Luo et al., 2009)
EIF5A2 can target the miR-125b and regulate the fatty acid de novo biosynthesis in hepatocellular carcinoma (HCC) cells.	(Tsang et al., 2014), (Cao et al., 2017),
EIF5A2 can be a novel therapeutic target for the treatment of nasopharyngeal carcinoma patients.	(Huang et al., 2016)
EIF5A2 associated with poor overall survival time in gastric cancer patients.	(Yang et al., 2016a)

elevated EIF5A2 in ovarian carcinoma may promote the malignant phenotype. Therefore, EIF5A2 is a potential independent biomarker of shortened survival time for ovarian cancer patients (Yang et al., 2009). However, the precise role of EIF5A2 and its mechanisms in ovarian cancer metastasis are still unclear.

Hypusine and deoxyhypusine. Hypusine is an uncommon amino acid, and of human proteins only EIF5A (both EIF5A1 and EIF5A2) contains a single hypusine residue (Caraglia et al., 2013; Maier et al., 2010). There are two reactions involved in the hypusination of EIF5A. In the first reaction, deoxyhypusine synthase (DHS) catalytically cleaves polyamine spermidine and transfers the 4-aminobutyl moiety to lysine 50 residue of the EIF5A precursor to form deoxyhypusine and 1,3-diaminopropane. When the EIF5A precursor is absent, the spermidine is catalytically cleaved by DHS and produces Δ^1-pyrroline and 1,3-diaminopropane instead (Wolff et al., 1995), indicating that spermidine associates with the DHS in the early stage of the catalytic reaction and does not bind to the EIF5A protein precursor (Jakus et al., 1993). In the second reaction, a hydroxyl group is added to the deoxyhypusine residue to form hypusine and the reaction is mediated by deoxyhypusine hydroxylase (DOHH) (**Figure 1-2**) (Mathews and Hershey, 2015; Wang et al., 2013). The hypusination of EIF5A is essential for the cell growth and biological functions of EIF5A (Schnier et al., 1991). Thus, targeting the hypusination potentially blocks the activity of EIF5A2 for ovarian cancer therapy.

The hypusination process can be blocked by preventing spermidine from binding to the DHS. Thus, selective disruption of the binding between spermidine and DHS using small molecule compounds could specifically inhibit the production of biologically active EIF5A protein and eventually control the protein synthesis. This strategy has been reported in many studies (Jakus et al., 1993). The inhibitory effects of several mono-, di-, and poly-amines on DHS were also examined, and the structural features were subsequently identified (Jakus et al., 1993). Another study reported several chemical agents which structurally resemble spermidine and could be used as potential inhibitors to disrupt the association between spermidine and DHS (Jakus et al., 1993). Several types of guanidine compounds were found to be effective to inhibit DHS in cultured cells (Jakus et al., 1993).

N1-guanyl-1,7-diamine-heptane (GC7). GC7 is one of the common inhibitors routinely used to inhibit the DHS activity. GC7 was first synthesized in 1993 and is one of the most competitive inhibitors for DHS (Jakus et al., 1993). GC7 fully inhibits the hypusination at doses between 1 and 10 μM in Chinese hamster ovary cells and has the potential for drug development and cancer therapy (Jakus et al., 1993).

Recent studies showed that GC7 inhibits tumor progression in several human cancer cells. In breast cancer, inhibition of EIF5A hypusination with GC7 reduces TGFβ/Fibronectin induced metastatic dissemination (Güth et al., 2019). In oral squamous cell carcinoma cells, inhibition of EIF5A hypusination with GC7 achieves better anti-tumor effects both in vitro and in vivo when it is combined with cisplatin than cisplatin alone (Fang et al., 2018b). In hepatocellular carcinoma cells, GC7 blocks EMT and reverses hypoxia-induced chemotherapy resistance (Zhou et al., 2017) and inhibits

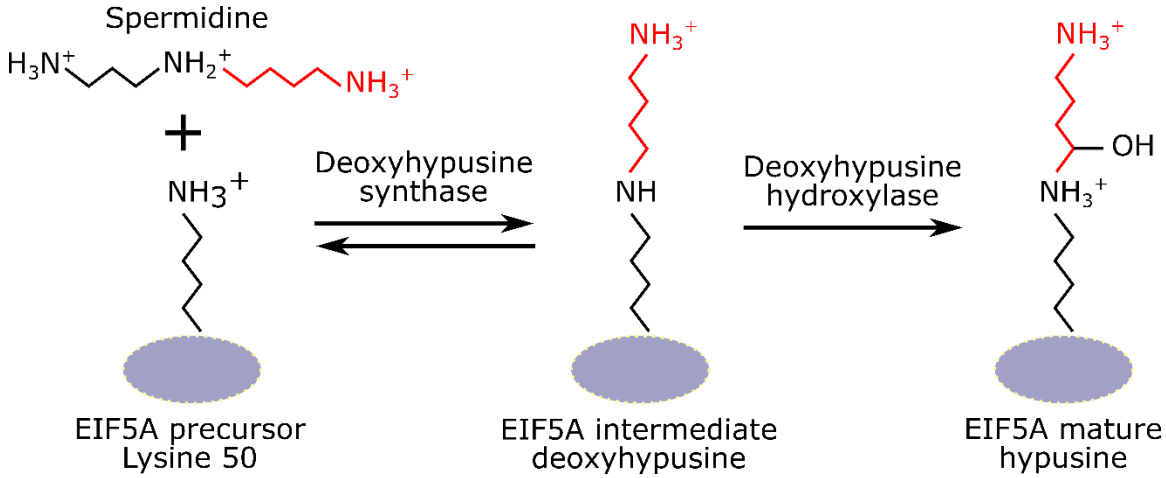

Figure 1-2. Scheme showing the chemical reactions of hypusine formation in EIF5A.

First, an amino-butyl moiety is transferred from the spermidine to the lysine 50 in EIF5A2 by the enzyme deoxyhypusine synthase (DHS) and then deoxyhypusine hydroxylase (DOHH) added a hydroxyl group to the deoxyhypusine and form the hypusine. Data source: Maier, B., et al. (2010). "Hypusine: a new target for therapeutic intervention in diabetic inflammation." Discovery Medicine, 10 (50), 18-23.

neuroblastoma (Bandino et al., 2014). GC7 also suppresses cell proliferation and induces apoptosis in immortalized and malignant human oral keratinocytes (Lee et al., 2009).

Although GC7 demonstrates a great potential as a DHS inhibitor, its specificity is still unclear and raises concerns about the clinical utility of GC7 for cancer treatment (Massagué et al., 2005). Due to the high similarity between GC7 and spermidine, GC7 could potentially influence other key targets of spermidine, such as spermidine/spermine N(1)-acetyltransferase (SAT1). SAT1 is a key regulator of the polyamine catabolism (Pegg, 2008; Liu et al., 2012a). Therefore, the molecular modification of GC7 may be required to improve the specificity of GC7.

Ovarian cancer treatment

Current treatment on ovarian carcinoma patients with advanced stage disease relies on aggressive surgery, such as cytoreduction and tumor debulking to remove all visible tumors in surgery. Cytoreduction surgery typically involves multiple surgeries to clear as much tumor as possible in the pelvis, such as an *en bloc* resection of the ovarian tumors, reproductive organs, and the sigmoid colon (Lengyel, 2010). Cytoreduction surgery has been consistently demonstrated to improve patient survival time (Bristow et al., 2002; Winter et al., 2007).

Drug administration by the intravenous (i.v.) and intraperitoneal (i.p.) routes is another factor to consider and the optimal route for drug delivery is still up for debate. Chemotherapy is typically used after surgery to kill any remaining cancer cells. Increasing experimental evidence has showed that intraperitoneal delivery of drugs leads to an increased progression-free survival and overall survival by several months for patients after tumor debulking compared with patients who underwent intravenous administration (Armstrong et al., 2006). The reason for this improvement is likely because the ovarian tumors are confined within the peritoneal cavity and intraperitoneal injection can achieve high concentrations of drugs in abdomen.

Due to the low number of cases compared with other diseases like breast and colon cancers, ovarian carcinoma has had limited number of patients for large phase III trials (Lengyel, 2010). Primary therapy is mainly cytoreductive surgery and platinum-based chemotherapy, which has been largely unchanged over the years. Other drugs to target DNA repair, immunoregulatory pathways, and stem cell biology are also on clinical trials for targeted gene therapy. Due to genetic similarity in primary tumors and metastasis from other cancers, ovarian cancer can also benefit from the diagnosis and treatment developed for other cancers. Identifying effective biomarkers for early diagnosis of ovarian cancer can greatly help reduce mortality rate.

Summary and Aims of Dissertation

Ovarian cancer is the most lethal gynecological cancer and most patients are diagnosed at advanced stages. A critical barrier to progress for the treatment of ovarian cancer is the lack of effective biomarkers for diagnosis, and the lack of mechanistic understanding of ovarian cancer metastasis and chemoresistance. EIF5A is one of the eukaryotic translation initiation factors and functions in both initiation and elongation of protein synthesis. Hypusination is the key step of posttranslational modification of EIF5A for EIF5A maturation and function. The EIF5A2 isoform of EIF5A is frequently amplified in various solid tumors. We recently found that EIF5A2 is highly expressed in ovarian cancer patients, and EIF5A2 expression correlates with poor patient survival. The aim of this study is to understand the function of EIF5A2 in ovarian cancer and the molecular mechanisms underlying tumor metastasis. We found that CRISPR/Cas9 nickase mediated EIF5A2 knockout inhibits EMT in ovarian cancer cells. We also found that EIF5A2 and TGFβ signaling pathway form a positive feedback loop in ovarian cancer cells.

Our goal was to elucidate the role of the EIF5A2/TGFβ/EMT axis in ovarian cancer. The results of this study will provide novel insights on the molecular mechanisms underlying the regulation of EIF5A2 and how the EIF5A2/TGFβ axis regulates EMT in ovarian cancer. The overall goal of this work was to develop novel therapeutics for ovarian cancer by targeting the EIF5A2/TGFβ axis to inhibit ovarian primary tumor growth and metastasis.

CHAPTER 2. METHODS AND MATERIALS

Methods and Materials Related to EIF5A2 Enhances Ovarian Tumor Growth and Metastasis by Promoting EMT via Activating the TGFβ Pathway

Cell culture

Ovarian cancer cell lines, SKOV3 and OVCAR3, were obtained from ATCC and cultured in Dulbecco's Modified Eagle Medium (DMEM) supplemented with 10% FBS (Hyclone; Logan, UT), 100 U/ml penicillin/streptomycin (PS, Invitrogen; Carlsbad, CA). OVCAR8 cell line was purchased from National Cancer Institute and cultured in RPMI 1640 with 10% FBS (Hyclone; Logan, UT), 1% penicillin/streptomycin (PS, Invitrogen; Carlsbad, CA). Three ovarian cancer cell lines were grown using standard cell culture techniques at 37°C under 5% carbon dioxide (CO_2) and 15% oxygen (O_2). Cell lines were authenticated using Short Tandem Repeat (STR) analysis by ATCC and tested negative for mycoplasma contamination using luciferase assay (Lonza, Allendale, NJ). Cells were frozen at early passages and used in less than 4 weeks in continuous culture.

Lentiviral vector production

The lentiviral CRISPR/Cas9 nickase-mediated EIF5A2 gene editing vectors were constructed by annealing two gRNA oligonucleotides and subcloning them into BsmII site of lentiviral vector Lentiguide-puro vector (#52963, Addgene), and gRNAs were driven by human U6 promoter. Two gRNA sequences, 5' AACGGCTTCGTGGTGCTCAA and 5' CGCAAGGCCGAGCACTGCAT were designed to target exon 1 of EIF5A2 gene. The lentiviral CRISPR/Cas9 nickase-mediated TGFβR2 gene editing vectors were constructed using the same method as we described previously (Zhao et al., 2017) by annealing two gRNA oligonucleotides 5'TTCCAGAATAAAGTCATGGT and 5'TTCTCCAAAGTGCATTATGA to target exon 4. EIF5A2 and EGFP lentiviral vectors were purchased from APPLIED Biological Materials Inc. Lentivirus was produced by packaging in 293FT cells, as published previously (Yue et al., 2010). EIF5A2 KO and TGFβR2 KD stable cell lines were generated by transducing the ovarian cancer SKOV3 and OVCAR8 cells with the lentiviral CRISPR/Cas9 nickase vector and selected with 2 μg/ml puromycin or 10 μg/ml blasticidin. LentiCas9-blast was used as the control vector without gRNAs. EGFP control and EIF5A2 expressing cell lines were established by transducing OVCAR3 with EIF5A2 overexpression vector, and stable cell lines were established by selecting with 2 μg/ml puromycin.

MTT assay

SKOV3, OVCAR8 or OVCAR3 cells (3000/well) transduced with lentiviral CRISPR/Cas9 nickase EIF5A2 gRNA and control or EIF5A2 OE and EGFP vectors were plated into 96-well plates and cultured at different time points (24, 48 and 72 h). Thereafter, 10 µl of MTT reagent was added to each well and incubated for ~4 h and then terminated by adding 100 µl detergent reagent to incubate at 22°C in the dark for 2 h. Cell proliferation was assessed by measuring the absorbance at 570 nm wavelength.

Cell clonogenic survival assay

Four hundred EIF5A2 expressing and EGFP control OVCAR3 cells, EIF5A2 KO and control SKOV3 and OVCAR8 cells were seeded on 6-well plates and cultured for 2 weeks and then fixed with 70% ethanol and stained with crystal blue. Colonies were counted for statistical analysis in triplicate.

Cell migration assay

The cell migration assay was assessed using a transwell chambers (BD Falcon™, San Jose, CA) inserted into 24-well cell culture plates. SKOV3, OVCAR8 and OVCAR3 cells (5×10^4) in 300 µl serum-free culture medium were added into the upper chamber. Culture medium containing 10% of FBS as the chemoattractant was added into the lower chamber of each well and cultured for 8 h. The medium and non-migrated cells in the upper chamber were removed, while the migrated cells on the lower side of the membranes were fixed with methanol and stained with crystal violet. Pictures were taken at 10X magnification, and cells from at least three different fields were counted.

Cell invasion assay

SKOV3, OVCAR3 and OVCAR8 (3×10^5) cells were seeded in 300 µl serum-free culture medium onto transwell plates precoated with Matrigel (BD BioSciences, San Jose, CA). The medium containing 10% of FBS was added to the bottom chamber of the invasion system as the chemoattractant. The transwell inserts were stained for 10 min with hematoxylin and eosin following methanol fixation for 20 mins following overnight incubation. Pictures were taken at 10X magnification. Invaded cells were counted from at least three different fields.

Smad-dependent reporter gene luciferase assay

The lentiviral vector pGF-Smad2/3/4-mCMV-Luciferase-EF1a-puro (System Biosciences, CA) containing Smad2/3/4 transcriptional response elements (TRE) was used to transduce EIF5A2 KO and control SKOV3 and OVCAR8 cells using 10 MOI

(multiplicity of infection). EIF5A2 KO and control cells were treated with 6 ng/ml TGFβ for 12 h to activate Smad2/3/4 pathway. Luciferase activity was measured and normalized by comparing to control cells.

Immunofluorescent staining

The paraffin-embedded (FFPE) blocks of fully de-identified ovarian serous carcinoma were obtained from the Tissue Services Core of the University of Tennessee Health Science Center (UTHSC). Hematoxylin and eosin (H&E) staining was performed by the Histology Core of UTHSC. To detect EIF5A2 gene expression, ovarian serous carcinoma sections were antigen-retrieved and incubated with blocking buffer (5% normal goat serum, 3% bovine serum albumin, and 0.1% Triton-X100 in PBS) for 1 h. The slides were incubated overnight with primary antibodies to EIF5A2, Cytokeratin-7 (1:200 dilution, Abcam, Cambridge, UK) and Vimentin (1:200 dilution, Cell Signaling, Danvers, MA). After rinsing three times for 5 mins with PBST, Alexa 488- or 594-conjugated goat anti-rabbit or –anti-mouse (Invitrogen, Carlsbad, CA) antibodies were added and incubated for 1 h at room temperature. Cell nuclei were counterstained with DAPI (Vector Laboratories, Inc.; Burlingame, CA). Images were captured on a Zeiss LSM700 laser scanning confocal microscope.

Western blot

Ovarian cancer cells were collected in RIPA buffer (Thermo Scientific; Rockford, IL) containing 1% Halt Proteinase Inhibitor Cocktail (Thermo Scientific; Rockford, IL). An equal amount of protein (100 μg/lane) was loaded onto 10% SDS-PAGE gels and transferred onto nitrocellulose membranes. The membranes were blocked with 5% nonfat milk for 1 h and incubated with primary antibodies against EIF5A2, Cytokeratin-7(Abcam), GAPDH (Santa Cruz; St. Louis, MO), Vimentin, Ecadherin, β-catenin, snail2, Smad2 or p-Smad2 (Cell Signaling).

Orthotopic ovarian cancer mouse model

To test the effect of EIF5A2 KO in ovarian cancer cells on ovarian tumor metastasis, EIF5A2 KO and control SKOV3 cells were labeled with luciferase. 5×10^5 EIF5A2 KO and control SKOV3 cells were intrabursally injected into 10 of two-months-old immunocompromised NOD.Cg *Prkdcscid Il2rgtm1Wjl*/SzJ (NSG) female mice (n=5/group) (#005557, Jackson Laboratory). Tumor growth and metastasis was monitored using the Xenogen bio-imaging system once a week. Mice were sacrificed at 5 weeks after cell injection. Primary tumors from ovaries and metastatic tumors from peritoneal organs were collected. Xenograft tumors and the peritoneal organs of each mice were subjected to double-blind histopathologic analysis by a pathologist.

Quantification and statistical analysis

All the statistical analysis of experimental data was carried out in Excel unless otherwise indicated.

Western blot experiments were repeated independently for three times. The protein bands from Western blot were quantified using the ImageJ software and GAPDH was used as a loading control. SKOV3 and OVCAR8 cells treated with TGFβ for different time points (6, 12 and 24 h) were all compared to vehicle. SKOV3 and OVCAR8 cells treated with SB431542 in different doses (10, 20 and 40 μM) were all compared to vehicle. Statistical significance was determined by the Student's t-test between two groups. $^{*}p < 0.05$, $^{**}p < 0.01$, $^{***}p < 0.001$, $^{****}p < 0.0001$.

The cell survival assay and MTT were performed using three biological repeats. The comparisons between two groups were performed using Student's t-test.

For the migration and invasion assays, cells were counted from three different fields using the ImageJ software. The comparisons between two groups were performed using the Student's t-test.

The luciferase reporter assays were performed using three biological repeats. EIF5A2 KO with or without TGFβ stimulation was compared to control with or without TGFβ stimulation respectively; EIF5A2- overexpression with or without TGFβ stimulation was compared to control with or without TGFβ stimulation respectively. The statistical comparisons between two groups were performed using Student's t-test.

Methods and Materials Related to Disruption of Hypusination Pathway Inhibiting Primary Ovarian Tumor Growth and Metastasis

Cell culture

Ovarian cancer cell lines, SKOV3 was obtained from ATCC and cultured in Dulbecco's Modified Eagle Medium (DMEM) supplemented with 10% FBS (Hyclone; Logan, UT), 100 U/ml penicillin/streptomycin (PS, Invitrogen; Carlsbad, CA). OVCAR8 cell line was purchased from National Cancer Institute and cultured in RPMI 1640 with 10% FBS (Hyclone; Logan, UT), 1% penicillin/streptomycin (PS, Invitrogen; Carlsbad, CA). Both ovarian cancer cell lines were grown using standard cell culture techniques at 37°C under 5% carbon dioxide (CO_2) and 15% oxygen(O_2). Cell lines were authenticated using Short Tandem Repeat (STR) analysis by ATCC and tested negative for mycoplasma contamination using luciferase assay (Lonza, Allendale, NJ). Cells were frozen at early passages and used in less than 4 weeks in continuous culture. N1-guanyl-1, 7-diaminoheptane (GC7) was purchased from Millipore Sigma Inc.

Lentiviral vector production

The lentiviral CRISPR/Cas9 nickase-mediated DHS gene editing vectors were constructed by annealing two gRNA oligonucleotides and subcloning them into BsmII site of lentiviral vector Lentiguide-puro vector (#52963, Addgene), and gRNAs were driven by human U6 promoter. Two gRNA sequences, 5'AGGAAGTAGGGAACGTGCTT and 5'TTGCGGAGACGCGCGCGTCG were designed to target exon 1 of DHS gene. Lentivirus was produced by packaging in 293FT cells, as published previously (Yue et al., 2010). DHS KO stable cell lines was generated by transducing the ovarian cancer SKOV3 and OVCAR8 cells with the lentiviral CRISPR/Cas9 nickase vector and selected with 2 μg/ml puromycin or 10 μg/ml blasticidin. LentiCas9-blast was used as the control vector without gRNAs.

MTT assay

SKOV3 and OVCAR8 (3000/well) transduced with lentiviral CRISPR/Cas9 nickase DHS editing and control or wildtype cells treated with GC7 were plated into 96-well plates and cultured at different time points (24, 48 and 72 h). Thereafter, 10 μl of MTT reagent was added to each well and incubated for ~4 h and then terminated by adding 100 μl detergent reagent to incubate at 22°C in the dark for 2 h. Cell proliferation was assessed by measuring absorbance at 570 nm wavelength.

Cell clonogenic survival assay

400 DHS KO and control SKOV3 and OVCAR8 cells or wildtype cells treated with GC7 were seeded on 6-well plates and cultured for 2 weeks and then fixed with 70% ethanol and stained with crystal blue. Colonies were counted for statistical analysis in triplicate.

Cell migration assay

The cell migration assay was assessed using transwell chambers (BD Falcon™, San Jose, CA) inserted into 24-well cell culture plates. SKOV3 and OVCAR8 cells (5×10^4) transduced with lentiviral CRISPR/Cas9 nickase DHS editing and control or wildtype cells treated with GC7 were seeded in 300 μl serum-free culture medium and added to the upper chamber. Culture medium containing 10% of FBS as the chemoattractant was added into the lower chamber of each well and cultured for 8 h. The medium and non-migrated cells in the upper chamber were wiped away, while the migrated cells on the lower side of the membranes were fixed with methanol and stained with crystal violet. Pictures were taken at 10X magnification and cells were counted from at least three different fields.

Cell invasion assay

SKOV3 and OVCAR8 (3×10^5) cells transduced with lentiviral CRISPR/Cas9 nickase DHS editing and control or wildtype cells treated with GC7 were seeded in 300 μl serum-free culture medium and put into transwell plates precoated with Matrigel (BD BioSciences, San Jose, CA). The medium containing 10% of FBS was added to the bottom chamber of the invasion system as the chemoattractant. The transwell inserts were stained for 10 min with hematoxylin and eosin following methanol fixation for 20 mins following overnight incubation. Pictures were taken at 10X magnification. Invaded cells were counted in at least three different fields.

Immunofluorescent staining

The paraffin-embedded (FFPE) blocks of fully de-identified ovarian serous carcinoma were obtained from the Tissue Services Core of the University of Tennessee Health Science Center (UTHSC). Hematoxylin and eosin (H&E) staining was performed by Histology Core of UTHSC. To detect DHS, hypusine and EMT genes expression, ovarian serous carcinoma sections were antigen-retrieved and incubated with blocking buffer (5% normal goat serum, 3% bovine serum albumin, and 0.1% Triton-X100 in PBS) for 1 h. The slides were incubated overnight with primary antibodies to DHS, Cytokeratin-7 (1:200 dilution, Abcam, Cambridge, UK), hypusine (1:200 dilution, Millipore Sigma, US), and Vimentin (1:200 dilution, Cell Signaling, Danvers, MA). After rinsing three times for 5 mins with PBST, Alexa 488- or 594- conjugated goat anti-rabbit or –anti-mouse (Invitrogen, Carlsbad, CA) antibodies were added and incubated for 1 h at room temperature. Cell nuclei were counterstained with DAPI (Vector Laboratories, Inc.; Burlingame, CA). Images were captured on a Zeiss LSM700 laser scanning confocal microscope.

Western blot

Ovarian cancer cells were collected in RIPA buffer (Thermo Scientific; Rockford, IL) containing 1% Halt Proteinase Inhibitor Cocktail (Thermo Scientific; Rockford, IL). An equal amount of protein (100 μg/lane) was loaded onto 10% SDS-PAGE gels and transferred onto nitrocellulose membranes. The membranes were blocked with 5% nonfat milk for 1 h and incubated with primary antibodies against DHS, hypusine, EIF5A2, Cytokeratin-7(Abcam), GAPDH (Santa Cruz; St. Louis, MO), Vimentin, Ecadherin, β-catenin, snail2, Smad2 or p-Smad2 (Cell Signaling).

Orthotopic ovarian cancer mouse model

To test the effect of DHS KO in ovarian cancer cells on ovarian tumor metastasis, DHS KO and control OVCAR8 cells were labeled with luciferase. 5×10^5 DHS KO and control OVCAR8 cells were intrabursally injected into 10 two-months-old

immunocompromised NOD.Cg *Prkdcscid Il2rgtm1Wjl*/SzJ (NSG) female mice (#005557, Jackson Laboratory), (n=5/group). To test the efficacy of GC7, 10 NSG female mice were intrabursally injected with 5×10^5 wildtype OVCAR8 cells and randomly divided into two groups after one-week post-injection. One group of mice were treated with GC7 (16 mg/kg) and another group of mice were treated with vehicle for 5 days a week through intraperitoneal injection for 4 weeks. Tumor growth and metastasis were monitored using the Xenogen bio-imaging system once a week. Mice were sacrificed at 5 weeks after cell injection and primary tumor from ovaries and metastatic tumors from other peritoneal organs were collected. Xenograft tumors and the peritoneal organs of each mice were subjected to double-blind histopathologic analysis by a pathologist.

Quantification and statistical analysis

All the statistical analysis of experimental data was carried out in Excel unless otherwise indicated.

Western blot experiments were repeated independently for three times. SKOV3 and OVCAR8 cells treated with different doses of GC7 (10 μM, 50 μM and 100 μM) were all compared to vehicle. The protein bands from Western blot were quantified using ImageJ software and GAPDH was used as a loading control. The statistical significance of comparisons between two groups was determined by Student's t-test. $^{*}p < 0.05$, $^{**}p < 0.01$, $^{***}p < 0.001$, $^{****}p < 0.0001$.

The cell survival assay and MTT were performed using three biological replicates. GC7 treatment with doses of 10 μM and 50 μM were all compared to vehicle. The comparisons between two groups were performed using Student's t-test.

For the migration and invasion assays, cells were counted from three different fields using ImageJ software. The comparisons between two groups were performed using Student's t-test.

CHAPTER 3. EIF5A2 ENHANCES OVARIAN TUMOR GROWTH AND METASTASIS BY PROMOTING EPITHELIAL TO MESENCHYMAL TRANSITION VIA ACTIVATING THE TGFβ PATHWAY

Introduction

Ovarian cancer has the highest mortality rate among gynecological malignancies (Siegel et al., 2019). Ovarian cancer patients have few obvious symptoms at early stages and are often diagnosed at later stage III and IV when tumors have already metastasized to the peritoneal cavity or other distant abdominal organs such as the omentum, intestine, liver, spleen and kidney. Early stage ovarian cancer patients respond to chemotherapy, but eventually become chemotherapy resistant at late stages. Although combinational approaches are applied for ovarian cancer therapy including debulking surgery, chemotherapy, targeted therapy and immunotherapy, the five-year survival rate of 35 to 40% is poor (Scalici et al., 2017; Terraneo et al., 2020; Ahmed and Stenvers, 2013; Lengyel, 2010). The molecular mechanisms underlying ovarian cancer metastasis and chemoresistance remain unclear. Thus, it is essential to identify new biomarkers for early diagnosis for ovarian cancer and develop new drugs to improve therapy.

EIF5A is a eukaryotic translation initiation factor that participates in the initiation and elongation process of protein synthesis. EIF5A is the only protein that undergoes hypusination through posttranslational modification. The two isoforms of EIF5A, EIF5A1 and EIF5A2, share sequence similarity of 84% mRNA and 94% protein (Clement et al., 2003). EIF5A1 is expressed in majority of cell types and is required for embryonic development, while EIF5A2 is expressed in specific cell types and is not required for embryonic development (Pällmann et al., 2015). Interestingly, EIF5A2 is aberrantly amplified or upregulated in many cancers including ovarian cancer, lung, pancreatic cancer and hepatocellular carcinoma, and contributes to tumor growth and metastasis (Fujimura et al., 2015; He et al., 2011; Shek et al., 2012; Clement et al., 2003). Therefore, EIF5A2 is an attractive drug target for cancer therapy based on its aberrant expression in various cancer types. Although EIF5A2 is upregulated in ovarian cancer, its functional role has not been well characterized. Previous studies demonstrated that EIF5A2 contributes to EMT in colorectal, gastric and breast cancer (Zhu et al., 2012; Sun et al., 2018; Liu et al., 2015b). EMT contributes to tumor initiation, progression, invasion and metastasis, and EMT is regulated by multiple signaling pathways including ERK1/2, AKT, WNT in different cancer types (Micalizzi et al., 2010; Drasin et al., 2011; DiMeo et al., 2009). Although EMT contributes to tumor metastasis, the role of EMT in ovarian cancer is somewhat controversial due to the similar expression levels of Ecadherin in ovaries and other distant organs (Ahmed et al., 2007). However, accruing evidence indicates that EMT plays a key role in ovarian tumor metastasis (Bozhkova and Poryazova-Markova, 2019; Bhuyan et al., 2019; Antony et al., 2019; Solheim et al., 2017; Rafehi et al., 2016), our previous studies showed that TGFβ promoted EMT in ovarian cancer cells (Chen et al., 2014), and activation of the TGFβ pathway contributes to ovarian tumor metastasis in orthotopic ovarian cancer mouse models (Zhao et al., 2019).

Our results identified that EIF5A2 contributes to ovarian tumor growth and metastasis by promoting EMT. We further uncovered the molecular mechanisms underlying EIF5A2 mediated EMT in ovarian tumor metastasis.

Results

EIF5A2 expression is amplified or upregulated in ovarian cancer and associated with poor patient survival

To assess the expression of EIF5A2 in ovarian cancer, we analyzed 607 serous ovarian carcinomas and 561 normal tissues including 130 ovaries and 431 blood samples in the Oncomine database (Kandoth et al., 2013). EIF5A2 copy numbers were significantly amplified in ovarian tumors as compared to normal tissues ($p<0.001$) (**Figure 3-1A**). We also analyzed EIF5A2 expression in multiple cancer types from TCGA database, and EIF5A2 was amplified across multiple cancer types with the highest percentage found in lung and ovarian cancer patients (**Figure 3-1B**). We further examined the correlation of EIF5A2 copy number and mRNA expression in two different datasets of TCGA database including 629 serous carcinomas from Firehose Legacy and 608 from PanCancer Atlas. The copy number alteration of EIF5A2 was well-correlated with mRNA expression based on RNA-seq data (**Figure 3-1C**). We also examined EIF5A2 expression from CPTAC (Clinical Proteomic Tumor Analysis Consortium) database including 100 specimens from ovarian cancer patients and 25 normal ovaries, which was also found significantly higher in ovarian cancer tissue than that in normal ovaries at the protein level (**Figure 3-1D**). We then examined the expression of EIF5A2 in highly invasive SKOV3 and OVCAR8 ovarian cancer cells, and low invasive OVCAR3 cells using Western blot, and EIF5A2 expression was significantly higher in both SKOV3 and OVCAR8 cells than that in OVCAR3 cells (**Figure 3-2A**). To verify the expression of EIF5A2 in ovarian cancer tissues, we performed immunofluorescent staining on sections from three ovarian serous carcinoma patients that were verified by H&E staining. EIF5A2 was strongly stained in the cytoplasm of tumor cells but weakly stained in the adjacent normal tissues (**Figure 3-2B**). To determine whether EIF5A2 expression is associated with patient overall survival (OS), we examined the correlation of EIF5A2 expression with ovarian cancer patient survival based on Kaplan Meier Plotter of 655 ovarian cancer samples including 383 with high EIF5A2 expression and 272 with low expression (Győrffy et al., 2012). The OS was significantly reduced in patients with EIF5A2 high expression as compared to low expression patients (**Figure 3-1E**). We also examined additional 415 ovarian carcinoma including 207 EIF5A2 high and 208 low in the SurvExpress database (Aguirre-Gamboa et al., 2013) and EIF5A2 expression was analyzed based on risk groups. EIF5A2 expression was significantly higher in the high-risk group than that in low-risk group (**Figure 3-2C**), and the OS was significantly reduced in high-risk compared to low-risk group (**Figure 3-1F**). EIF5A2 expression was well-correlated with poor ovarian patient survival.

Figure 3-1. EIF5A2 expression is amplified or upregulated in ovarian cancer and associated with poor patient survival.
(A) EIF5A2 copy numbers in normal and cancer tissues. 1: normal ovaries (n=130); 2: normal blood (n=431); 3: ovarian cancer (n = 607), $p<0.001$. (B) EIF5A2 is amplified in majority of cancer types from in TCGA database. (C) EIF5A2 copy number is correlated with EIF5A2 mRNA expression from RNA-seq in two different datasets including TCGA PanCancer and firehose legacy. (D) Protein expression of EIF5A2 in normal and ovarian cancer tissues. Normal ovaries (n=25), Ovarian cancer (n=100), $p<0.001$. (E) EIF5A2 expression is associated with overall survival of ovarian cancer patients in Kaplan Meier Plotter database, $p<0.001$. (F) Ovarian cancer patients displayed significantly reduced patient survival in the high-risk compared to the low-risk group, $p<0.01$.

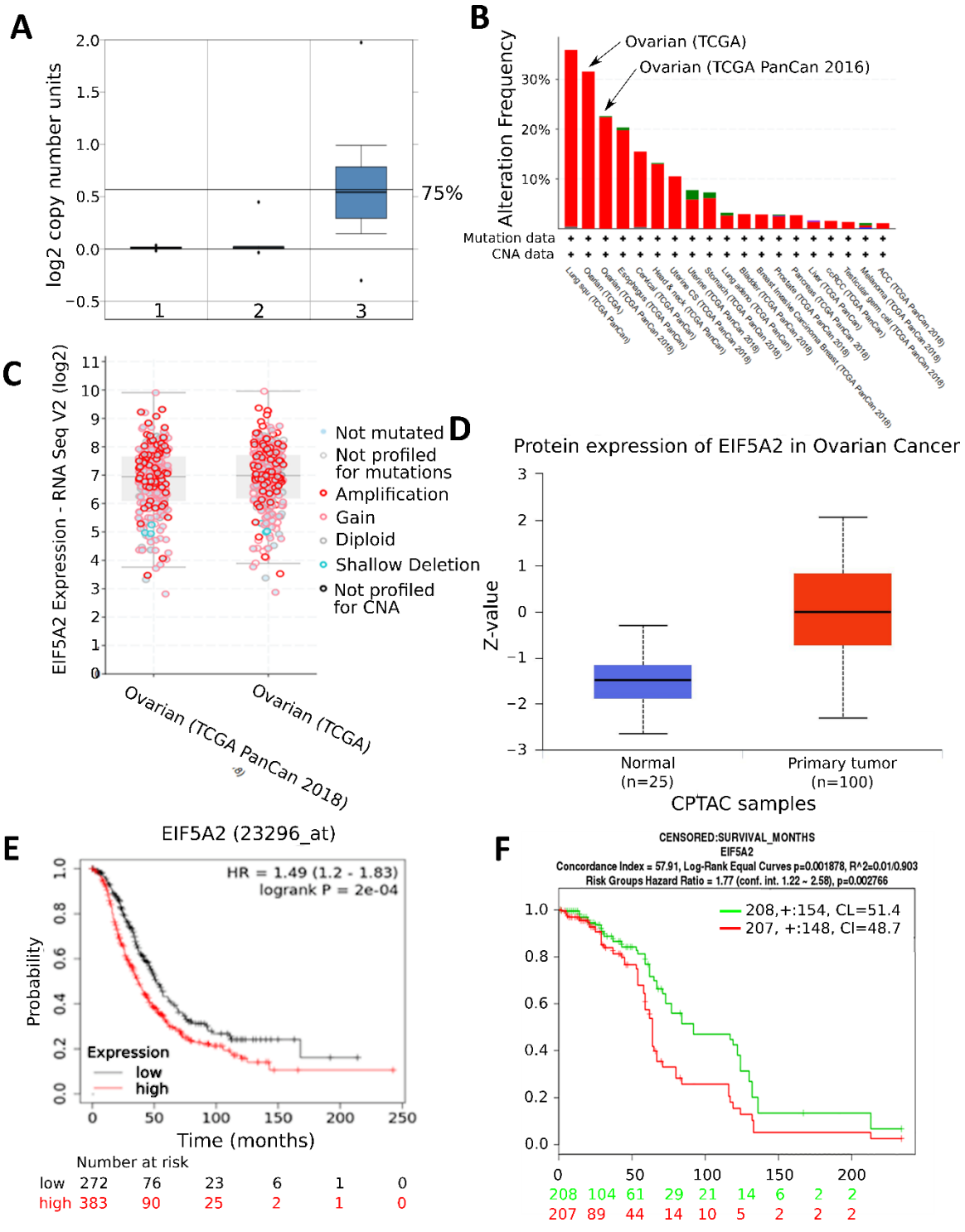

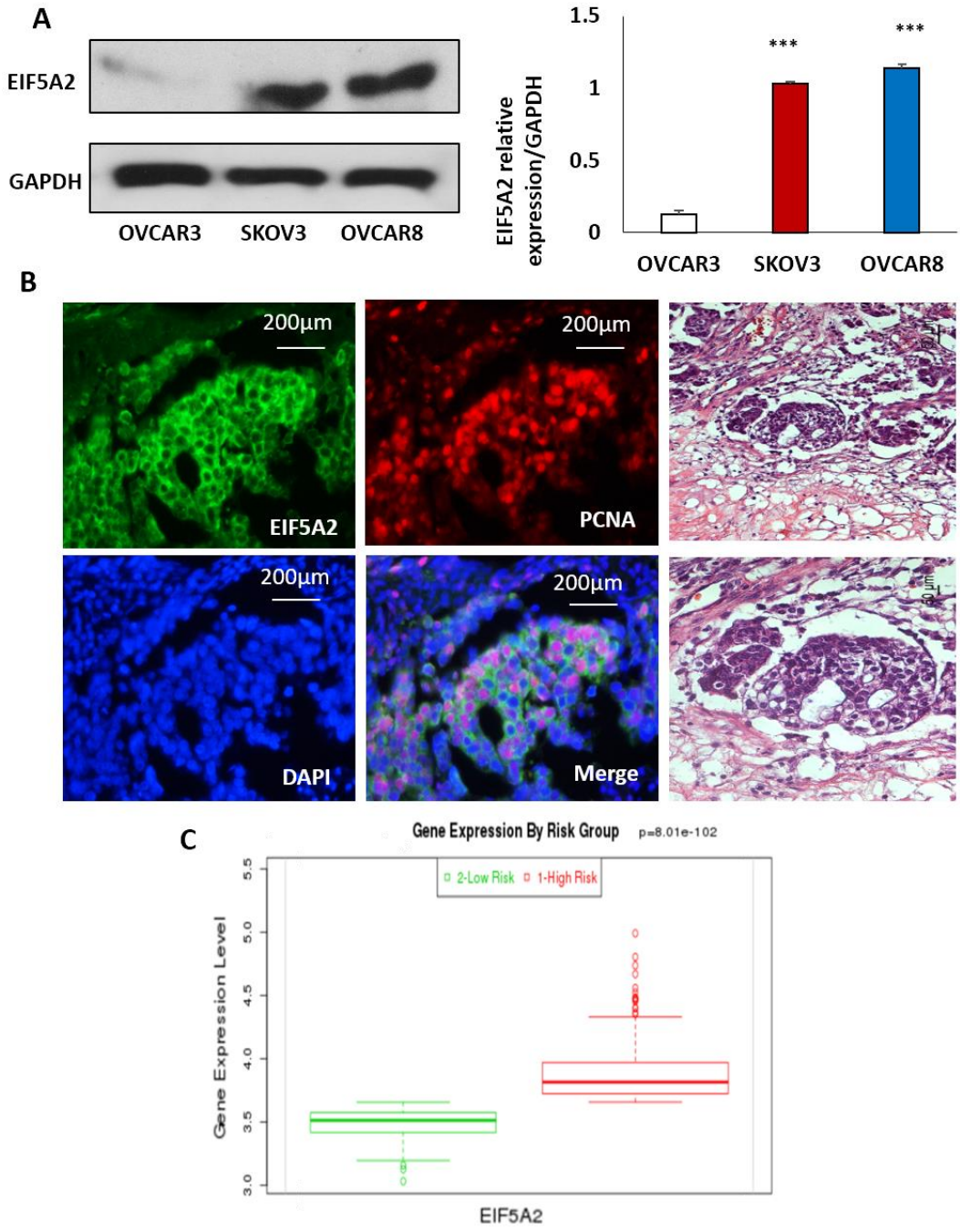

Figure 3-2. EIF5A2 expression in ovarian cancer cell line and tissues.
(A) Endogenous EIF5A2 expression in OVCAR3, SKOV3 and OVCAR8 cells. One representative Western blot was presented from three similar independent experiments. Band intensity was measured using ImageJ and the significance was determined by student's T-test. (***p<0.001). (B) Ovarian cancer sections immunofluorescent stained with EIF5A2 (green) and PCNA (red) antibodies and cell nuclei were counterstained with DAPI (blue) (n=3). (C) EIF5A2 expression is significantly higher in the high-risk group than that in the low risk group in 415 ovarian carcinoma samples in the SurvExpress database, p<0.001.

EIF5A2 promotes EMT in ovarian cancer cells

Based on their expression level of EIF5A2, to determine whether EIF5A2 contributes to EMT phenotypic switch, we knocked out EIF5A2 in highly invasive SKOV3 and OVCAR8 cells using lentiviral CRISPR/Cas9 nickase vector, and overexpressed EIF5A2 in low invasive OVCAR3 cells using lentiviral vector under the control of EF1α promoter. EIF5A2 was undetectable in both SKOV3 and OVCAR8 KO cells, while EIF5A2 expression was remarkably increased in EIF5A2 overexpression OVCAR3 cells compared to control cells. The EMT markers including the epithelial cell marker Cytokeratin-7 and Ecadherin were upregulated while mesenchymal markers including β-catenin, Vimentin and snail2 were downregulated in both SKOV3 and OVCAR8 KO compared to control cells (**Figure 3-3A**). In contrast, overexpression of EIF5A2 in OVCAR3 cells resulted in the downregulation of epithelial cell markers Cytokeratin-7 and Ecadherin, while mesenchymal markers including β-catenin, Vimentin and snail2 were upregulation compared to control cells (**Figure 3-3B**).

Loss of EIF5A2 expression inhibits ovarian cancer cell proliferation and survival

To determine the functional outcome of loss of EIF5A2 expression in ovarian cancer cells, we examined cell survival in EIF5A2 knockout and control SKOV3 and OVCAR8 cells by cell colony formation assays. Results show that loss of EIF5A2 expression led to significant inhibition in both SKOV3 (**Figure 3-4A**) and OVCAR8 (**Figure 3-4B**). Gain function of EIF5A2 enhanced cell survival in OVCAR3 cells (**Figure 3-4C**). In addition, we examined cell proliferation in EIF5A2 KO and control SKOV3 and OVCAR8 cells by performing MTT assays. Disruption of EIF5A2 by CRISPR/Cas9 nickase significantly reduced cell proliferation compared to controls at all three time points (24, 48, and 72 h) in both SKOV3 and OVCAR8 cells (**Figure 3-4D, E**). EIF5A2-expressing OVCAR3 cells promoted cell proliferation at a time-dependent manner (**Figure 3-4F**).

Loss of EIF5A2 expression inhibits ovarian cancer cell migration and invasion

EMT contributes to tumor cell migration and invasion. Since we found that EIF5A2 promoted EMT in ovarian cancer cells (**Figure 3-3**), we determine the role of EIF5A2 in migration and invasion of ovarian cancer cells using transwell plates. KO of EIF5A2 significantly inhibited migration (**Figure 3-5A**) and invasion (**Figure 3-5B**) in SKOV3 and OVCAR8 cells, while overexpression of EIF5A2 significantly enhanced migration (**Figure 3-5C**) and invasion in OVCAR3 (**Figure 3-5D**).

Figure 3-3. Disruption of EIF5A2 expression using lentiviral CRISPR/Cas9 nickase-mediated editing resulted in the inhibition of EMT in ovarian cancer cells. (A) Western blot analysis of EIF5A2 and EMT markers in EIF5A2 KO and control (Con) SKOV3 and OVCAR8 cells (n=3). (B) Western blot analysis of EIF5A2 and EMT markers in EIF5A2 expression and control OVCAR3 cells (n=3). Band intensity was measured using ImageJ and the significance was determined by student's T-test. One representative Western blot was presented from three similar independent experiments. (*$p<0.05$, **$p<0.01$, *** $p<0.001$).

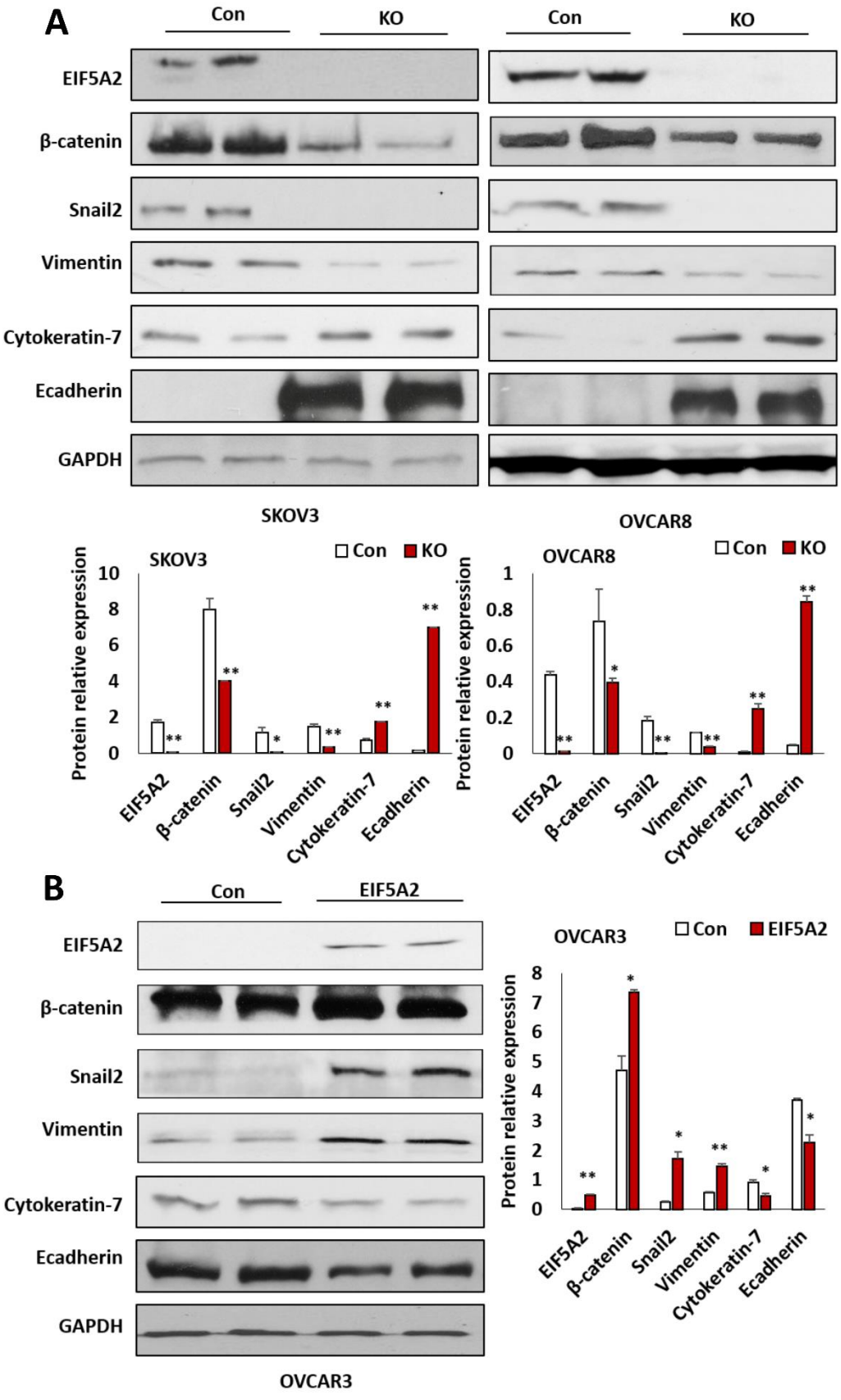

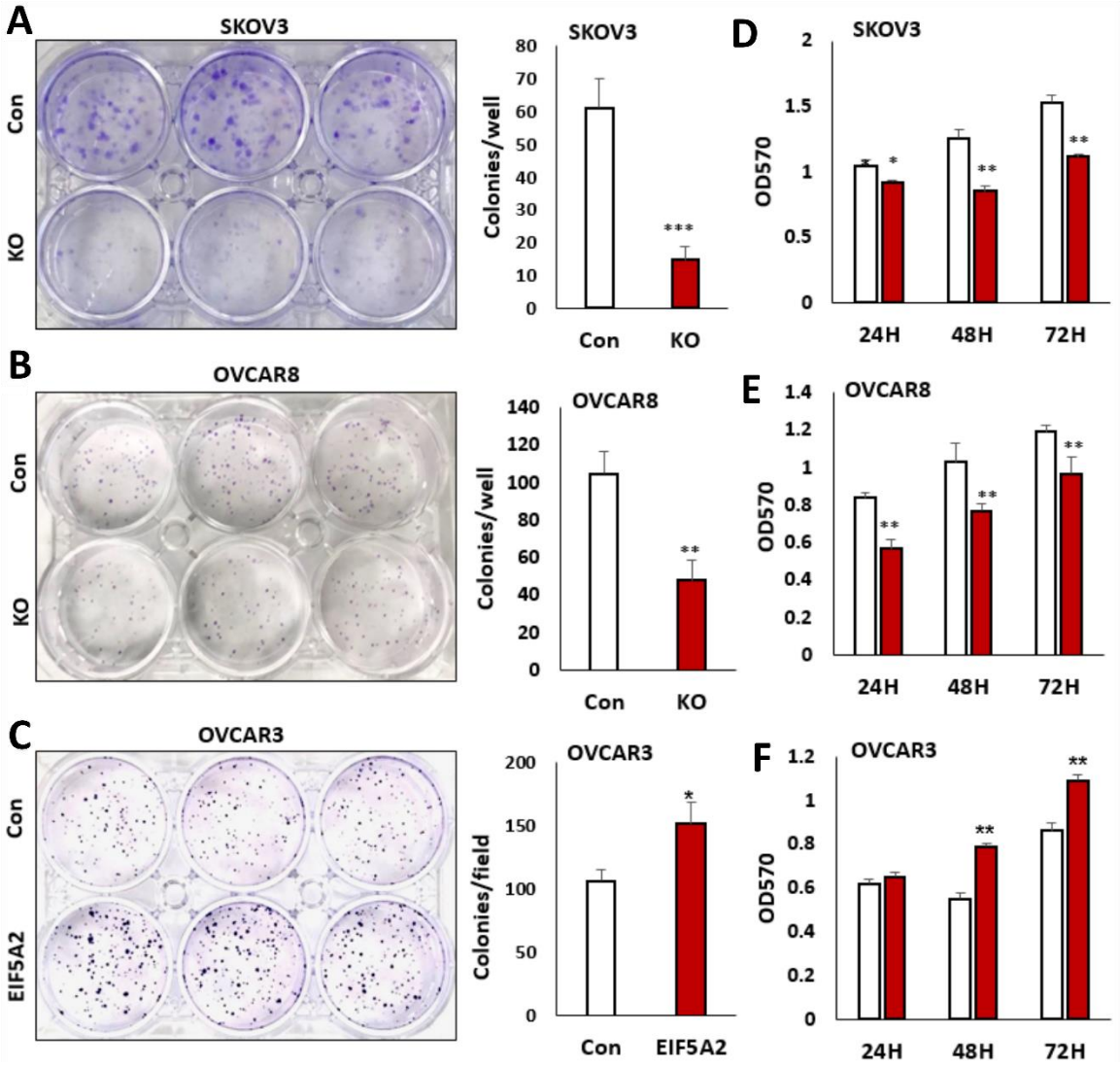

Figure 3-4. Disruption of EIF5A2 expression led to the inhibition of cell proliferation and survival in ovarian cancer cells.

(A, B) Cell survival in EIF5A2 knockout and control SKOV3 and OVCAR8 cells was determined by colony formation assay (n=3, **p<0.01; ***p<0.001). (C) Cell survival in EIF5A2-expressing and control OVCAR3 cells was determined by colony formation assay (n=3, *p <0.05). (D, E) Cell proliferation in EIF5A2 knockout and control SKOV3 and OVCAR8 cells was determined by MTT assay (n=3, *p <0.05; **p <0.01). (F) Cell proliferation in EIF5A2-expressing and control OVCAR3 cells was determined by MTT assay (n=3, **p<0.01).

Figure 3-5. Disruption of EIF5A2 expression led to the inhibition of cell migration and invasion in ovarian cancer cells.
(A**)** Cell migration in EIF5A2 knockout and control SKOV3 or OVCAR8 cells was examined using transwell plates, and migrated cells were stained with crystal blue and counted (n=3, **p<0.01). (B) Cell invasion in both EIF5A2 knockout and control SKOV3 or OVCAR8 cells was examined using Matrigel-coated plates, and invaded cells were stained with H&E and counted (n=3, **p<0.01; ***p <0.001). (C) Cell migration in EIF5A2-expressing and control OVCAR3 cells was examined using transwell plates, and migrated cells were stained with crystal blue and counted (n=3, **p<0.01). (D) Cell invasion in EIF5A2-expressing OVCAR3 cells was examined using Matrigel-coated plates, and invaded cells were stained with H&E and counted (n=3, **p<0.01).

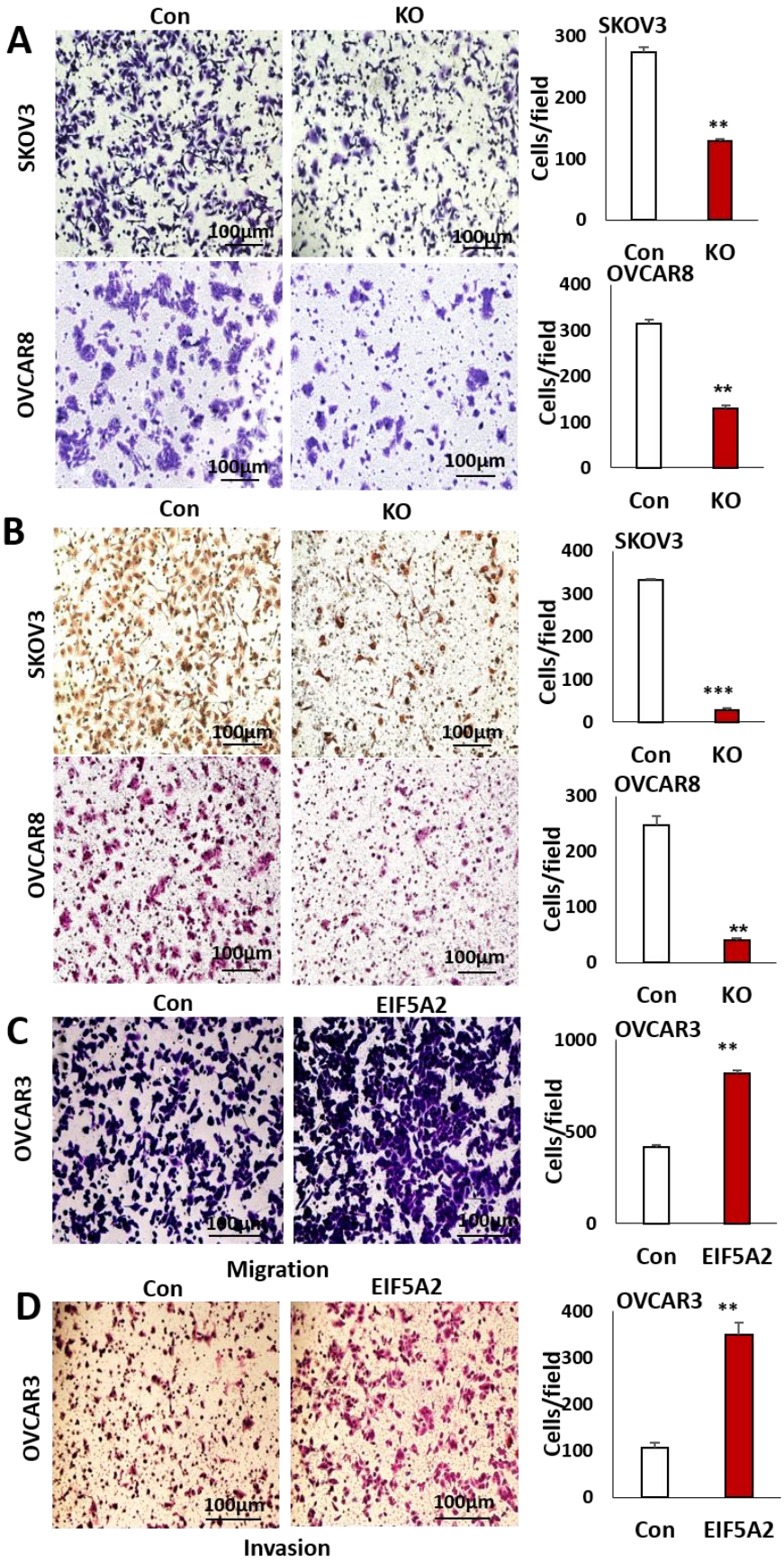

EIF5A2/TGFβ forms a positive feedback loop in promoting EMT in ovarian cancer cells

Previously, we reported that TGFβ promoted EMT in ovarian cancer cells (Chen et al., 2014). To understand how EIF5A2 contributed to EMT in ovarian cancer cells, we examined the correlation between EIF5A2 and TGFβ pathway in ovarian cancer cells by treating both SKOV3 and OVCAR8 cells with 6 ng/ml TGFβ. As shown in **Figure 3-6A**, TGFβ induced EIF5A2 expression in a time-dependent manner in both cell lines. We also treated both SKOV3 and OVCAR8 cells for 24 h with different doses of TGFβR1/2 inhibitor SB431542 and EIF5A2 expression was inhibited in a dose-dependent manner in both cell lines (**Figure 3-6B**). In addition to pharmacological approach, we used genetic approach by knocking down (KD) TGFβ receptor 2 (TGFβR2) using a lentiviral CRISPR/Cas9 nickase vector and then treated both TGFβR2 KD and control cells with 6 ng/ml TGFβ for 24 h and examined EIF5A2 expression. KD of TGFβR2 significantly reduced EIF5A2 protein levels in both SKOV3 and OVCAR8 cells, while TGFβ induced EIF5A2 expression in control but not in the KD cells (**Figure 3-6C**), indicating that TGFβ promoted EIF5A2 expression.

To examine how EIF5A2 regulates the TGFβ pathway, EIF5A2 KO SKOV3 and OVCAR8 cells and control cells were treated with 6 ng/ml TGFβ. Phospho- and total Smad2 in EIF5A2 KO and control ovarian cancer cells were examined by Western blot. Loss of EIF5A2 attenuated the TGFβ pathway as shown by the reduced phospho-Smad2 in both SKOV3 and OVCAR8 compared to control cells (**Figure 3-6D**). We further examined the TGFβ signaling by treating both EIF5A2 overexpression and control OVCAR3 cells with 6 ng/ml TGFβ. As we expected, overexpression of EIF5A2 activated the TGFβ pathway as shown by increased phospho-Smad2 in EIF5A2 overexpression OVCAR3 cells compared to control cells (**Figure 3-6E**).

To further examine the interaction of EIF5A2 and TGFβ signaling pathway, we transduced EIF5A2 KO, overexpression and control cells with a lentiviral luciferase reporter construct containing six Smad2/3/4 response elements upstream of CMV mini-promoter and then treated transduced cells with 6 ng/ml TGFβ for 12 h. Loss of EIF5A2 significantly inhibited the luciferase activity in both SKOV3 and OVCAR8 cells while overexpression of EIF5A2 enhanced luciferase activity in OVCAR3 cells (**Figure 3-7**). Our data indicated that EIF5A2 forms a positive feedback loop with TGFβ pathway in ovarian cancer cells.

Loss of EIF5A2 suppresses primary ovarian tumor growth and metastasis by inhibiting EMT and attenuating TGFβ pathway in an orthotopic ovarian cancer mouse model

To determine whether EIF5A2 contributes to primary ovarian tumor growth and metastasis, we intrabursally injected 5×10^5 ovarian cancer SKOV3 EIF5A2-KO and control cells into two-month-old immunocompromised NSG female mice. The primary ovarian tumors were significantly reduced in mice injected with EIF5A2 KO cells than

Figure 3-6. The association of EIF5A2 with the TGFβ pathway and inhibition of EIF5A2-attenuated TGFβ signaling pathway in ovarian cancer cells.
(A) TGFβ induced EIF5A2 in SKOV3 and OVCA8 cells at the indicated time points as detected by Western blot (n=3, **p<0.01). (B) TGFβR1/2 inhibitor SB431542 reduced EIF5A2 expression in SKOV3 and OVCAR8 cells at the indicated dose points for 24 has detected by Western blot (n=3, *p<0.05, **p <0.01). (C) Western blot analysis and comparison of EIF5A2 in TGFβR2 KD and control SKOV3 and OVCAR8 cells following 6 ng/ml TGFβ treatment for 24 h, respectively (n=3, **p<0.01, ***p<0.001). (D) The expression of phospho- and total Smad2 in EIF5A2 knockout and control SKOV3 and OVCAR8 cells was detected by Western blot following 6 ng/ml TGFβ treatment at the indicated time points (n=3, *p<0.05; **p <0.01; *** p<0.001). (E) The expression of phosphor- and total Smad2 in EIF5A2 overexpression and control OVCAR3 cells was detected by Western blot following 6 ng/ml TGFβ treatment at the indicated time points (n=3, **p<0.01). One representative Western blot was presented from three similar independent experiments. Band intensity was measured using ImageJ and the significance was determined by student's T-test.

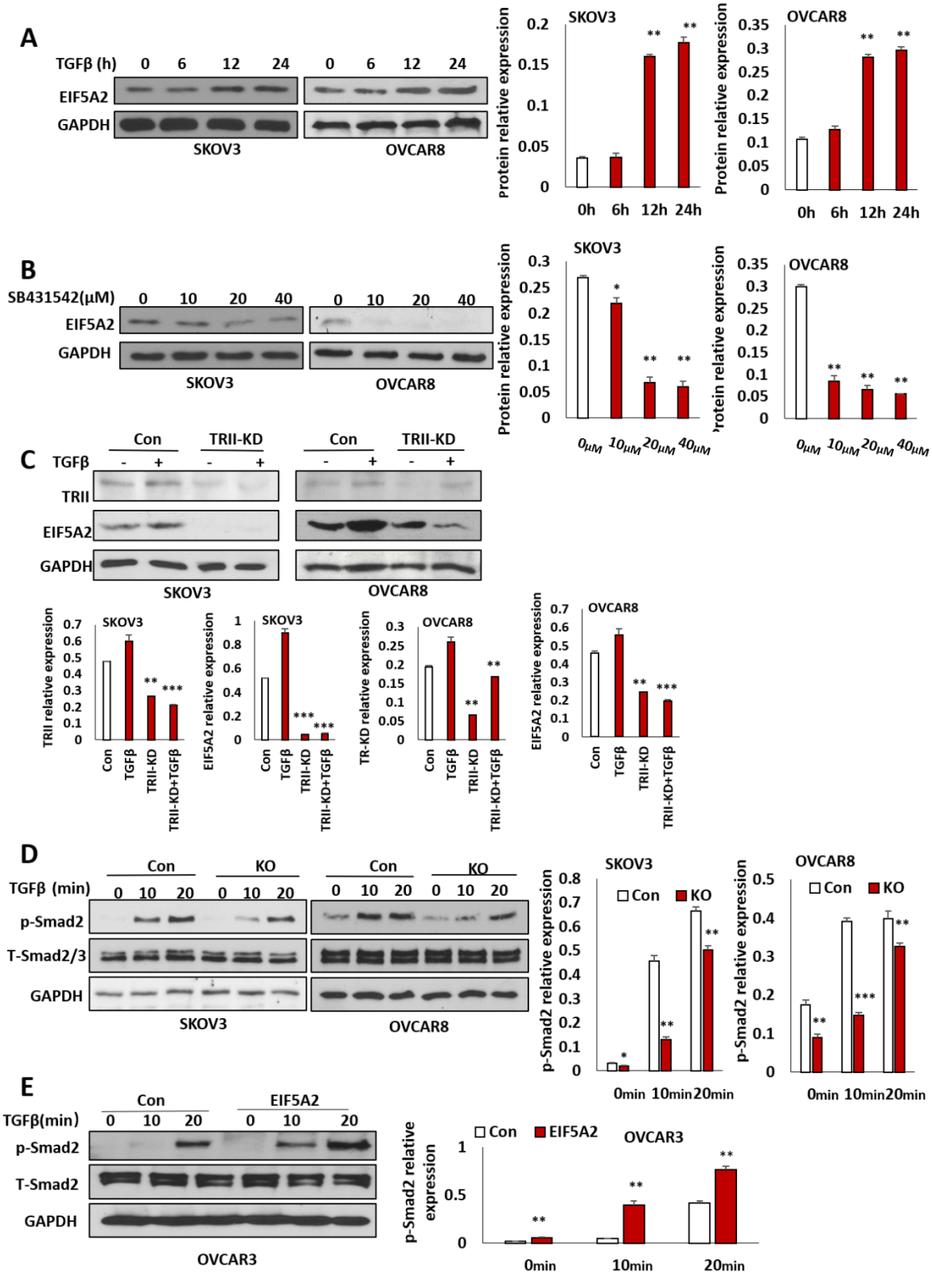

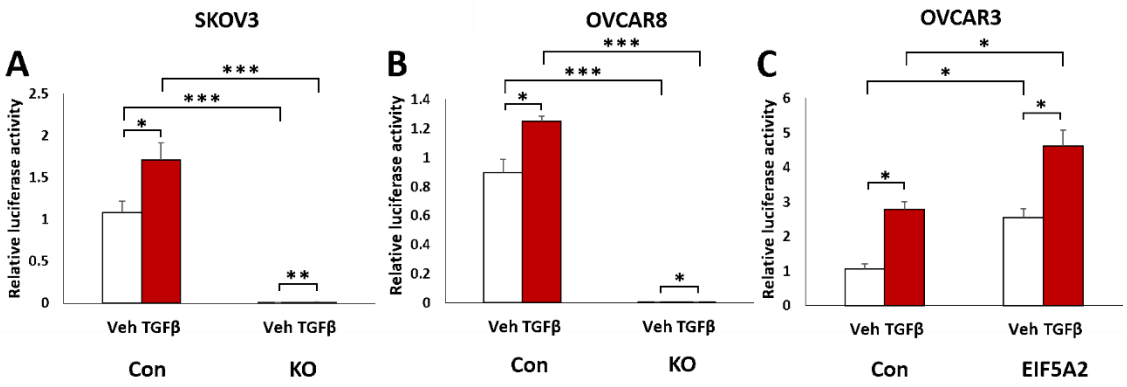

Figure 3-7. Smad-dependent reporter gene luciferase activity.
Luciferase activity in EIF5A2 KO and control SKOV3 and OVCAR8 cells (A, B) or EIF5A2 expressing and control OVCAR3 cells (C) transduced with pGreenFire1-Smad2/3/4-GF-EF1-puro lentiviral vector following 6 ng/ml TGFβ treatment for 12 h (n=3, *p<0.05, *** p<0.001).

control mice as shown by tumor weight (**Figure 3-8A**). We then examined EIF5A2, EMT markers and p-Smad2 expression in primary ovarian tumors by Western blot. EIF5A2 and mesenchymal markers including β-catenin, snail2, and Vimentin and p-Smad2 were downregulated, while the epithelial markers Cytokeratin-7 and Ecadherin were upregulated in tumors of mice implanted with EIF5A2 KO SKOV3 compared to control cells (**Figure 3-8B**). Ovarian tumors were also characterized by H&E staining (**Figure 3-8C**). Ovarian tumor sections were immunostained with EIF5A2, Vimentin and Cytokeratin-7 antibodies. EIF5A2 and Vimentin were weakly stained, while Cytokerain-7 was strongly stained in tumors from mice xenografted with KO cells than control cells (**Figure 3-9**). We further found metastatic tumors in multiple peritoneal organs including the liver and spleen of mice injected with control cells, but less metastasis in mice implanted with EIF5A2 KO cells as shown by bioluminescence and H&E staining (**Figure 3-10**). Our results indicated that loss of EIF5A2 suppressed primary ovarian tumor growth and tumor metastasis by inhibiting EMT and attenuating TGFβ pathway in orthotopic ovarian cancer mouse models.

Discussion

Lacking an effective biomarker is a major issue for early diagnosis of ovarian cancer patients. We report that EIF5A2 is a potential biomarker for early diagnosis of ovarian cancer and prognosis following chemotherapy. In particular, EIF5A2 is correlated with poor ovarian cancer patient survival. For the first time we demonstrated that EIF5A2 contributes to ovarian tumor metastasis by promoting EMT and activating the TGFβ pathway. EIF5A2 was shown to associate with metastasis, developmental stages, histological types and poor patient survival in gallbladder cancer, oral squamous cell carcinoma (Lin et al., 2020), prostate cancer (Lu et al., 2019), cervical cancer (Yang et al., 2016b), and hepatocellular carcinoma (Lee et al., 2010). In the present study, we analyzed the expression of EIF5A2 in high grade serous ovarian carcinoma in TCGA and other databases and found that EIF5A2 was associated with tumor metastasis and poor patient survival. It remains to be addressed on the correlation between EIF5A2 expression level and different stages or grades in other types of ovarian cancer including clear cell, endometrioid and mucinous carcinomas. Our studies indicate that EIF5A2 is a potential biomarker for diagnosis and prognosis as well as an attractive drug target due to its low expression in normal tissues and high expression in ovarian tumors.

Using gain and loss of functional approaches through lentiviral vector-based gene editing and overexpression, we showed for the first time that EIF5A2 promoted EMT in ovarian cancer cells, suggesting that EIF5A2 may contribute to ovarian cell invasion and metastasis. KO of EIF5A2 not only inhibited primary ovarian tumor growth and clonogenicity but also inhibited ovarian tumor metastasis in orthotopic ovarian cancer mouse models (**Figure 3-8 through 3-10**). Our finding is consistent with previous studies that EIF5A2 was also shown to promote EMT and contribute to cell invasion, chemoresistance and metastasis in several caner types including HCC (Tang et al., 2010), colorectal cancer (Zhu et al., 2012), bladder cancer (Wei et al., 2014) and OSCC (Lin et al., 2020). Therefore, targeting EIF5A2 may inhibit tumor metastasis and overcome

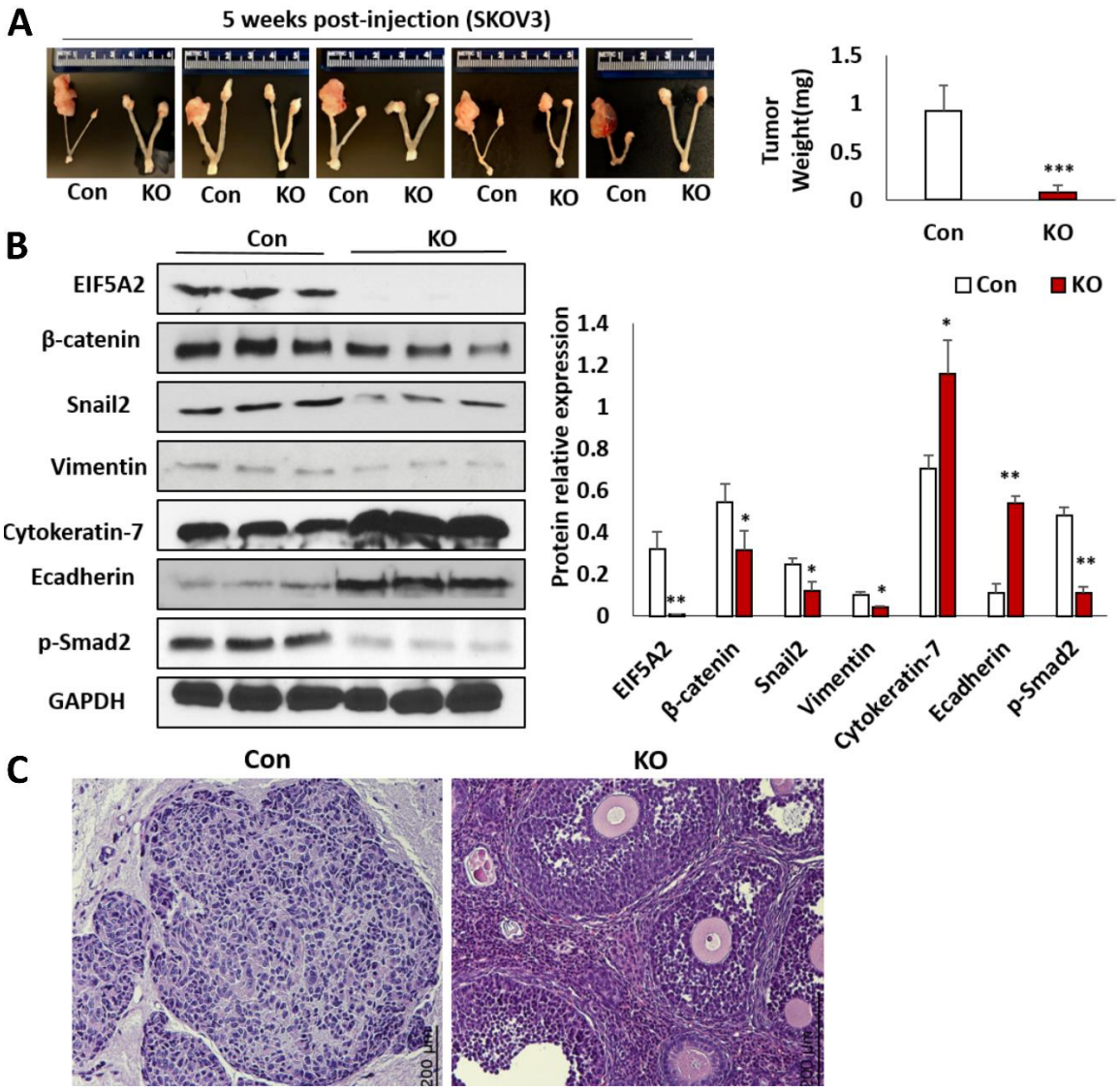

Figure 3-8. Knockout of EIF5A2 using lentiviral CRISPR/Cas9 nickase vector suppressed primary ovarian tumor growth in an orthotopic ovarian cancer mouse model.

(A) Primary ovarian tumors dissected at one month following intrabursally injection of EIF5A2 KO and control SKOV3 cells. Tumor weight in EIF5A2-KO is significantly less than in control (n=5, ***p<0.001). (B) Western blot and densitometry analysis of EIF5A2, p-Smad2 and EMT markers from primary tumor of mice xenografted with EIF5A2 KO and control cells (n=3, *p<0.05, **p<0.01). Band intensity was measured using ImageJ and the significance was determined by student's T-test. (C) Sections of primary ovarian tumors were stained with H&E.

Figure 3-9. EIF5A2 and EMT markers were stained in sections of ovarian tumor of EIF5A2 KO and control mice.

(A, B, C) Ovarian cancer sections were stained by EIF5A2, Vimentin and Cytokeratin-7 antibodies (green) and for cell proliferation was stained with PCNA antibody (red). Cell nuclei were counterstained with DAPI. Sections were also stained with H&E.

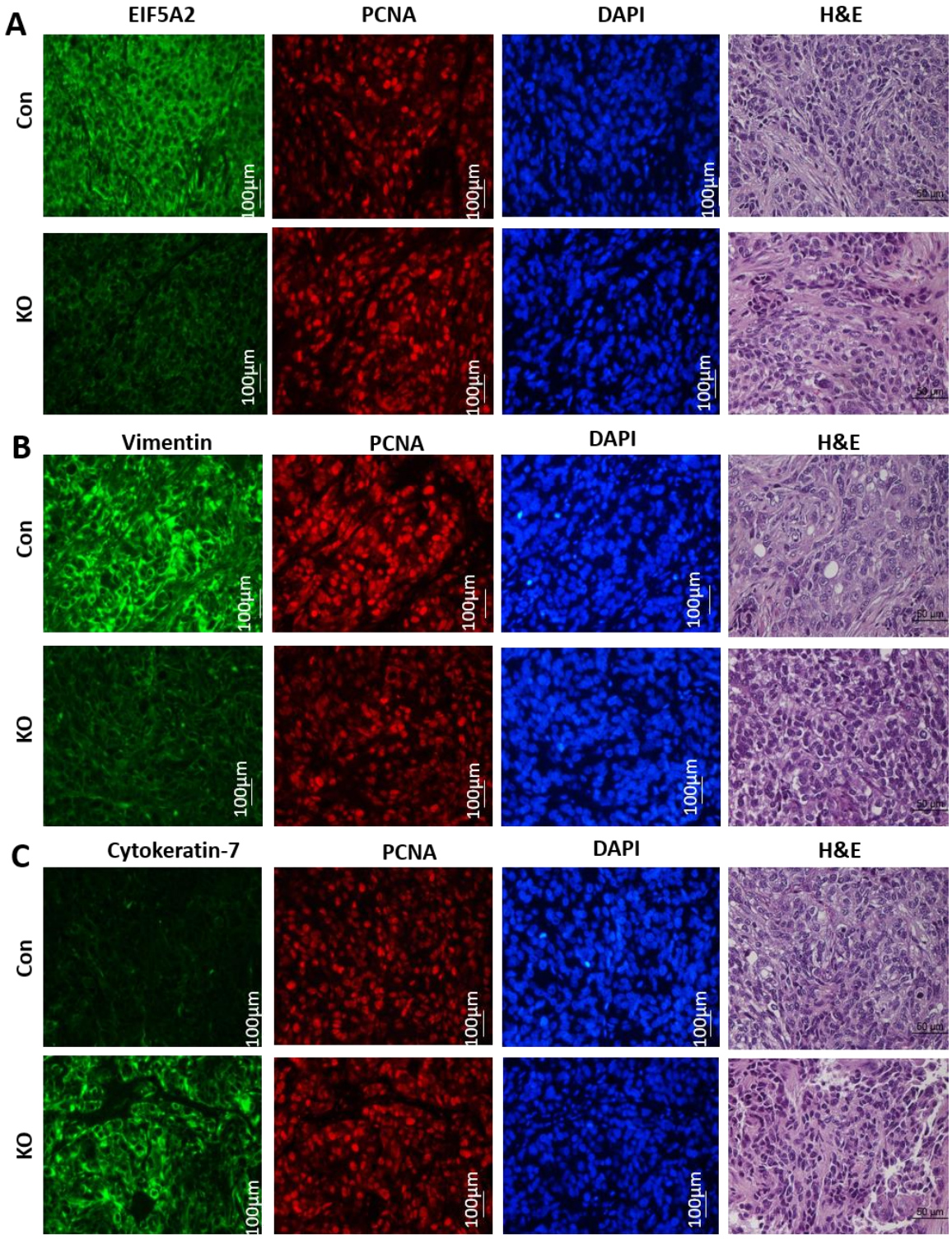

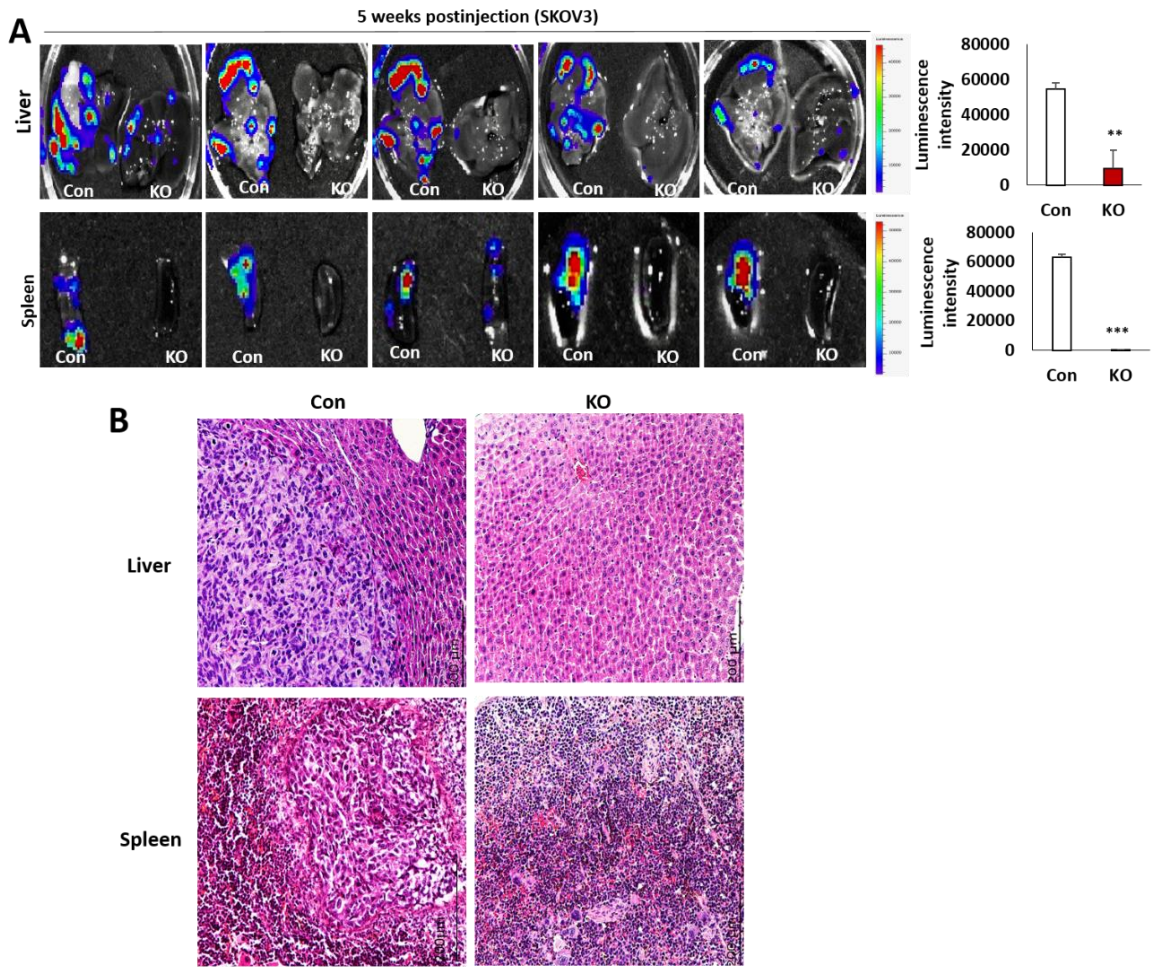

Figure 3-10. Knockout of EIF5A2 using lentiviral CRISPR/Cas9 nickase vector suppressed ovarian tumor metastasis in an orthotopic ovarian cancer mouse model. (A) Metastatic tumors in liver and spleen of mice xenografted with EIF5A2 KO and control (Con) cells (n=5, **p<0.01; ***p<0.001). (B) Sections of metastatic tumors in liver and spleen were stained with H&E.

chemoresistance by reversing EMT in cancer cells. EIF5A2 is the only hypusinated protein and matured through hypusination pathway and DHS is the first enzyme in the pathway leading to EIF5A2 maturation. A DHS small molecular inhibitor GC7 has been used to disrupt the hypusination pathway. GC7 has been shown to inhibit EMT in hepatocellular carcinoma (Lou et al., 2013), bladder cancer (Wei et al., 2014) and breast cancer (Liu et al., 2015b). Inhibition of EIF5A2 maturation may suppress tumor metastasis by reversing EMT using GC7 (Liu et al., 2015b; Zhou et al., 2017). Therefore, targeting EIF5A2 hypusination using DHS inhibitor may be a new approach for cancer therapy including ovarian cancer.

Although we showed that EIF5A2 promoted EMT in ovarian cancer cells, the molecular mechanisms by which EIF5A2 regulates EMT remains unclear. We previously showed that TGFβ promotes EMT in ovarian cancer (Chen et al., 2014). Interestingly, we found that TGFβ induced EIF5A2 expression, while inhibition of TGFβR1/2 using SB431542 or knockdown of TGFβR2 suppressed EIF5A2 expression. KO of EIF5A2 attenuated TGFβ pathway, while overexpressing EIF5A2 activated TGFβ pathways. Our studies indicated a positive feedback loop between EIF5A2 and the TGFβ pathway in ovarian cancer cells. Previous studies also showed that EIF5A2 is involved in TGFβ pathway (Hao et al., 2020; Wei et al., 2014). TGFβ increases and sustains the hypusination of EIF5A1 and EIF5A2 in high-grade metastatic breast cancer (Güth et al., 2019). However, EIF5A2 is negatively correlated with TGFβ signaling in the anaplastic thyroid carcinoma (Hao et al., 2020) whereas EIF5A2 was positively correlated with TGFβ signaling in bladder cancer by stabilizing STAT3 binding the TGFβR1 promoter (Wei et al., 2014). EIF5A2 was also post-transcriptionally upregulated by hnRNPE1 through binding 3' untranslated region in a TGFβ-dependent manner in NMuMG cells (Hussey et al., 2012). Our studies indicated a positive feed-back loop between EIF5A2 and TGFβ signaling pathway, which may contribute to ovarian cancer cell invasion and metastasis by promoting EMT. However, it is still not clear how EIF5A2 interacts with TGFβ pathway. Based on luciferase reporter gene assay, it is possible that Smad2/3/4 may bind the promoter of EIF5A2 and activate EIF5A2 expression as we showed that TGFβ induced luciferase reporter expression in EIF5A2 expressing cells, but not the EIF5A2 KO cells (**Figure 3-7**).

Collectively, our study demonstrated that EIF5A2 is highly expressed in ovarian HGSC and associated with poor patient survival. EIF5A2 promotes primary ovary tumor growth and metastasis by promoting EMT and activating the TGFβ pathway.

CHAPTER 4. DISRUPTION OF HYPUSINATION PATHWAY INHIBITS PRIMARY OVARIAN TUMOR GROWTH AND METASTASIS

Introduction

Ovarian cancer accounts for more deaths than any other types of gynecologic cancer and is therapeutically challenging. The majority of ovarian cancer patients die from advanced, high-grade serous carcinoma with widespread metastasis in the peritoneal cavity (Chandra et al., 2019). One of the reasons why ovarian cancer is rarely detected at early stages is because it metastasizes early and mostly through intraperitoneal dissemination to directly invade either neighboring or distant organs (Eisenkop and Spirtos, 2001; Lengyel, 2010). Therefore, understanding the regulatory mechanisms underlying ovarian cancer metastasis is crucial for ovarian cancer treatment.

EMT has recently received great attention in ovarian research and many studies support the role of EMT in ovarian cancer metastasis (Lili et al., 2013; Ahmed et al., 2010; Yan and Sun, 2014). In Chapter 3, our results found that EIF5A2 is highly expressed in ovarian cancer patients and correlated with poor patient survival. We also demonstrated that EIF5A2 contributes to EMT via activating the TGFβ pathway and KO of EIF5A2 suppresses ovarian primary tumor growth and metastasis.

The posttranslational hypusine modification is required for EIF5A to be maturated and functional (Caraglia et al., 2013). Hypusine was firstly isolated from bovine brain extracts by Shiba and coworkers in 1971 (Shiba et al., 1971). The EIF5A hypusination of was first discovered in Park's laboratory from human lymphocytes cultured in a medium containing radioactive spermidine and analyzed the radiolabeled proteins using two-dimensional gel electrophoresis in 1981 (Park et al., 1981). Later studies found that hypusine formation occurs at the Lys50 of N-terminal of precursor-EIF5A (Park et al., 1993).

DHS and DOHH are enzymes involved in the posttranslational modification of hypusine in EIF5A (Mathews and Hershey, 2015; Wang et al., 2013). DHS and DOHH apparently only function in the hypusination of EIF5A (Park and Wolff, 2018). This unique feature makes the polyamine-hypusine pathway an attractive target for cancer prognosis, prevention, and therapeutic treatment.

The hypusination pathway can be blocked by inhibiting the association of spermidine with DHS to specifically control EIF5A maturation and suppress tumor progression in several human cancers (Jakus et al., 1993). GC7 is one of the most competitive DHS inhibitors (Jakus et al., 1993). Multiple studies show that GC7 can reduce the metastatic dissemination of tumor cells through the inhibition of EIF5A hypusination in different human cancers, including breast cancer (Güth et al., 2019), oral squamous cell carcinoma (Fang et al., 2018b), and neuroblastoma (Bandino et al., 2014). Also blocking EMT by GC7 reverses hypoxia-induced chemotherapy resistance in

hepatocellular carcinoma cells (Zhou et al., 2017). However, it is not known whether GC7 inhibits EIF5A2 expression in ovarian cancer cells.

Our results identified that disruption of hypusination pathway by inhibition of DHS suppresses primary ovarian tumor growth and metastasis. We also demonstrated that KO of DHS or using GC7 can inhibit hypusination of EIF5A2 and reduce ovarian tumor growth and metastasis in an orthotopic ovarian cancer mouse model.

Results

Disruption of DHS expression using lentiviral CRISPR/Cas9 nickase-mediated editing inhibits hypusinated EIF5A, EIF5A2, and EMT in ovarian cancer cells

As discussed in Chapter 3, SKOV3 and OVCAR8 cell lines have high endogenous EIF5A2 expression. To determine whether blocking the hypusination modification of EIF5A2 inhibits EMT in ovarian cancer cells, we constructed lentiviral CRISPR/Cas9 nickase by using two gRNAs targeting the region of exon 1 of DHS. The lentiviral CRISPR/Cas9 nickase vector was then transduced into both SKOV3 and OVCAR8 cells and selected with 2 μg/ml puromycin following 10 μg/ml blasticidin selection. Using Western blot, we examined the alteration of DHS, hypusinated EIF5A, and EIF5A2, and EMT-associated markers in SKOV3 and OVCAR8 cells. DHS was remarkably depleted in both SKOV3 and OVCAR8 cells transduced with lentiviral DHS gRNA vector compared to control cells. Accordingly, hypusinated EIF5A was reduced in both DHS KO SKOV3 and OVCAR8 cells. EIF5A2 expression and EMT markers were also altered by upregulation of epithelial cell markers Cytokeratin-7 and Ecadherin and downregulation of mesenchymal cell marker β-catenin, Vimentin, and Snail2 compared to control cells (**Figure 4-1A, B**). We further examined hypusinated EIF5A, EIF5A2, and EMT marker gene expressions by treating both SKOV3 and OVCAR8 cells with different doses of GC7. Hypusinated EIF5A, EIF5A2, and the mesenchymal markers β-catenin, Vimentin, and Snail2 were downregulated while the epithelial markers Cytokeratin-7 and Ecadherin were upregulated following dose-dependent inhibition of DHS (**Figure 4-2A, B**).

Disruption of DHS expression inhibits cell proliferation and survival in ovarian cancer cells

To determine the functional role of the loss of DHS expression in ovarian cancer cells, we examined cell survival in DHS KO and control SKOV3 and OVCAR8 cells by using cell colony formation assay. Results showed that loss of DHS expression led to significant inhibition of cell survival in both SKOV3and OVCAR8 cells (**Figure 4-3A, B**). We examined cell proliferation in DHS KO and control SKOV3 and OVCAR8 cells by performing the MTT assays. KO of DHS significantly reduced proliferation compared

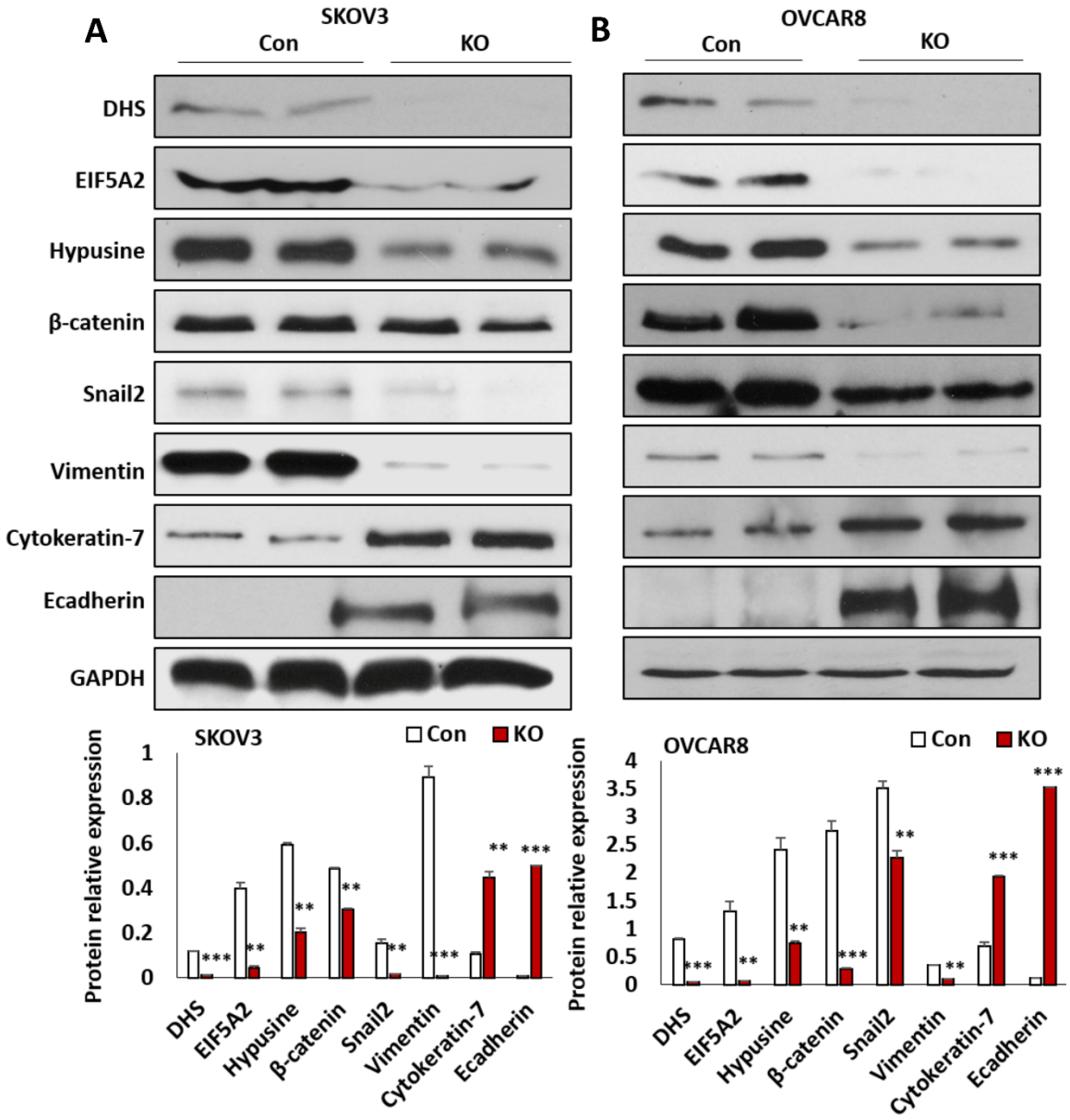

Figure 4-1. Disruption of DHS expression using lentiviral CRISPR/Cas9 nickase-mediated editing resulted in the inhibition of hypusinated EIF5A, EIF5A2 and EMT in ovarian cancer cells.

(A, B) Hypusinated EIF5A, EIF5A2, and EMT marker gene expression was examined in DHS knockout and control SKOV3 and OVCAR8 cells by using Western blot (n=3, **p<0.01, ***p<0.001). One representative Western blot was presented from three similar independent experiments. Band intensity was measured using ImageJ and the significance was determined by student's T-test.

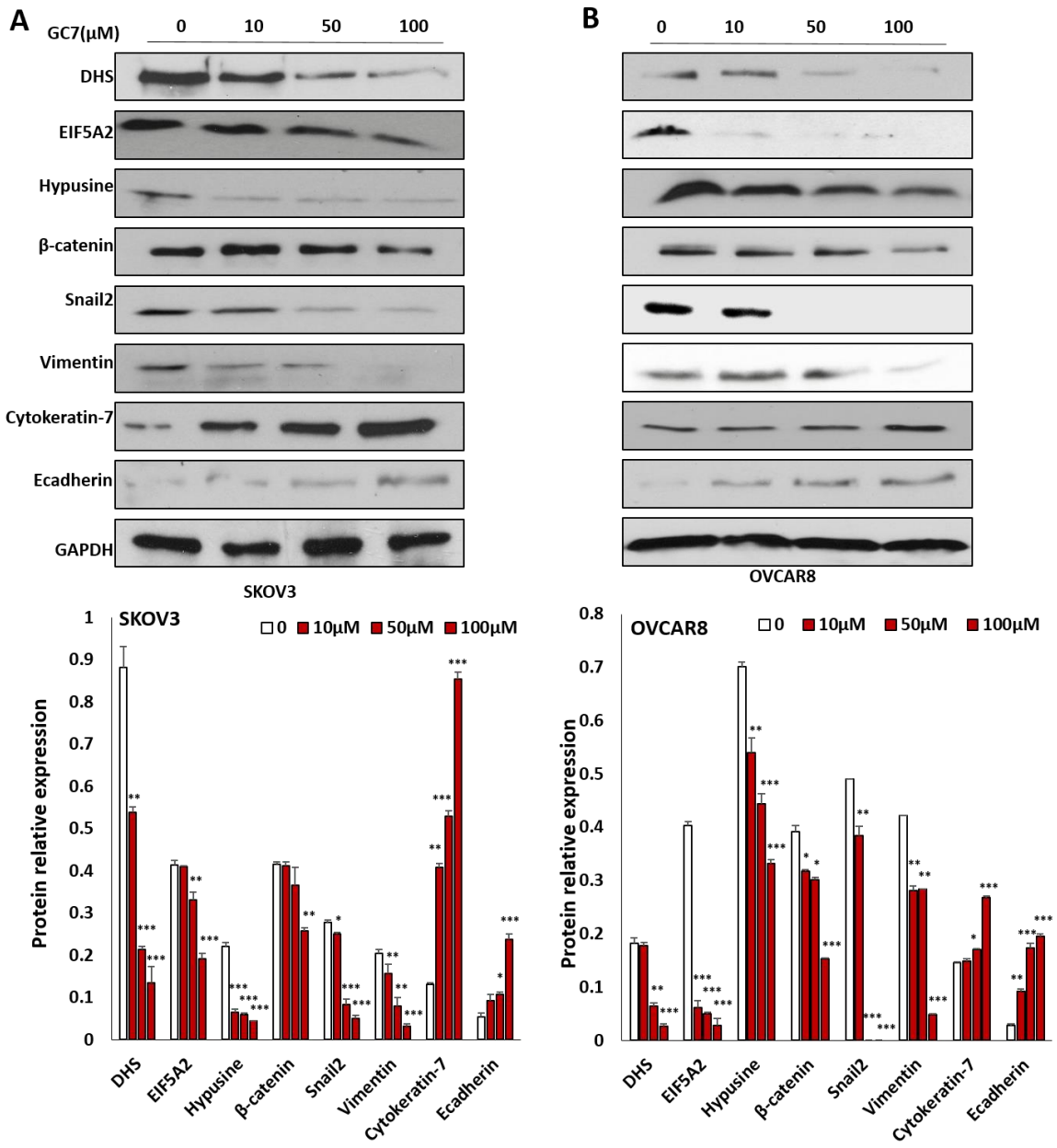

Figure 4-2. GC7 inhibited hypusinated EIF5A, EIF5A2 and EMT in ovarian cancer cells.

(A, B) Hypusinated EIF5A, EIF5A2 and EMT marker gene expression was examined in (0, 10, 50, 100 μM) GC7- and vehicle- treated SKOV3 and OVCAR8 cells by using Western blot (n=3, **p<0.01, ***p <0.001). One representative Western blot was presented from three independent experiments. Band intensity was measured using ImageJ and the significance was determined by student's T-test.

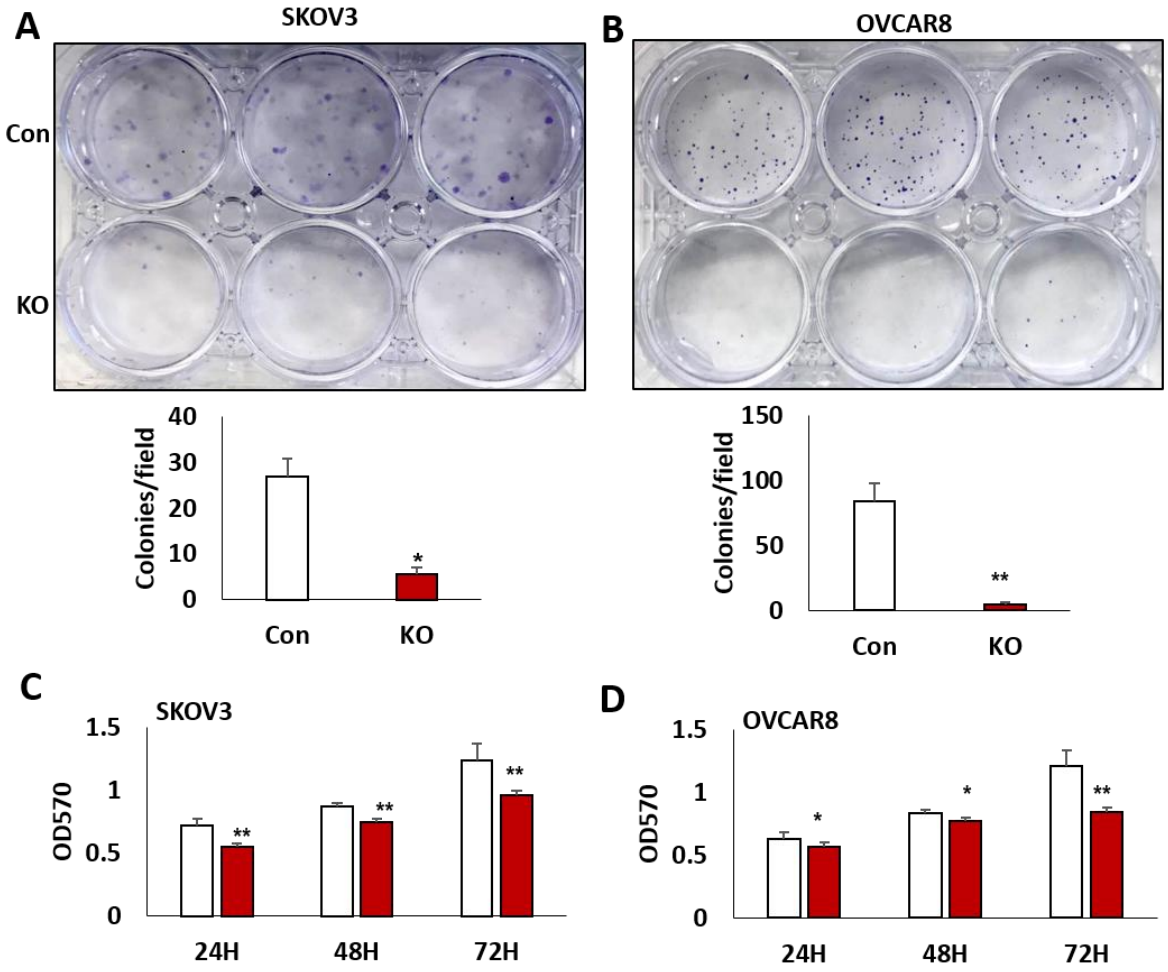

Figure 4-3. Disruption of DHS expression led to the inhibition of cell survival and proliferation in ovarian cancer cells.

(A, B) Cell survival in DHS KO and control SKOV3 and OVCAR8 cells was determined by colony formation assay (n=3, *p<0.05; **p <0.01). (C, D) Cell proliferation in DHS KO and control SKOV3 and OVCAR8 cells was determined by MTT assay (n=3, *p <0.05; **p <0.01).

to control cells at all three different time points (24, 48, and 72 h) in both SKOV3 and OVCAR8 cells (**Figure 4-3 C, D**). In addition, we tested the effect of GC7 on cell survival by treating SKOV3 and OVCAR8 cells with 20 μM of GC7 and found that GC7 significantly inhibited cell survival based on the colony formation assay (**Figure 4-4A, B**). To examine how GC7 affects cell proliferation, we treated both SKOV3 and OVCAR8 cells with three different doses of GC7 (0, 10, 20 μM) at four different time points (24, 48, 72 and 96 h). Results showed that cell proliferation was significantly inhibited in both SKOV3 and OVCAR8 cells at those time points (**Figure 4-4C, D**).

Disruption of DHS expression inhibits cell migration and invasion in ovarian cancer cells

Loss of DHS inhibits EMT in ovarian cancer cells, suggesting that blocking of hypusination of EIF5A2 affects cell motility and invasion. Using transwell plates, we examined cell migration in DHS KO and control cells and found that cell migration was significantly reduced in both DHS KO and control SKOV3 and OVCAR8 cells (**Figure 4-5A**). Using Matrigel-coated transwells, we assessed cell invasion, which was also significantly reduced in both DHS KO SKOV3 and OVCAR8 compared to control cells (**Figure 4-5B**). To test whether GC7 has a similar effect on cell migration and invasion, wild type SKOV3 and OVCAR8 cells were treated with 20 μM GC7 for 4 h following pre-treatment of 20 μM Z-VAD for 2 h by inhibiting cell proliferation, and cell migration and invasion were determined with the same methods. Our results showed that inhibition of DHS with GC7 significantly reduced cell migration and invasion in both cell lines (**Figure 4-6A, B**).

Blocking of hypusination of EIF5A2 attenuates TGFβ signaling pathway in ovarian cancer cells

To examine whether blocking of hypusination affects the TGFβ pathway in ovarian cancer cells, we treated DHS KO and control SKOV3 and OVCAR8 cells with 6 ng/ml TGFβ at different time points (0, 10 and 20 mins) and then examined phospho-Smad2 and total Smad2 by using Western blot. Loss of DHS resulted in the attenuation of TGFβ signaling pathway as showed by reduced phospho-Smad2 (**Figure 4-7A, B**). We also determined the TGFβ pathway following 20 μM GC7 treatment and found that inhibition of DHS attenuated phospho-Smad2 in both SKOV3 and OVCAR8 cells (**Figure 4-7C, D**). Our data indicated that disruption of hypusination of EIF5A2 inhibited the TGFβ pathway in ovarian cancer cells.

KO of DHS using lentiviral CRISPR/Cas9 nickase vector suppresses primary ovarian tumor growth and metastasis in an orthotopic ovarian cancer mouse model

We found that KO of EIF5A2 in SKOV3 cells led to the suppression of primary ovarian tumor growth and metastasis. To test whether disruption of hypusination inhibits

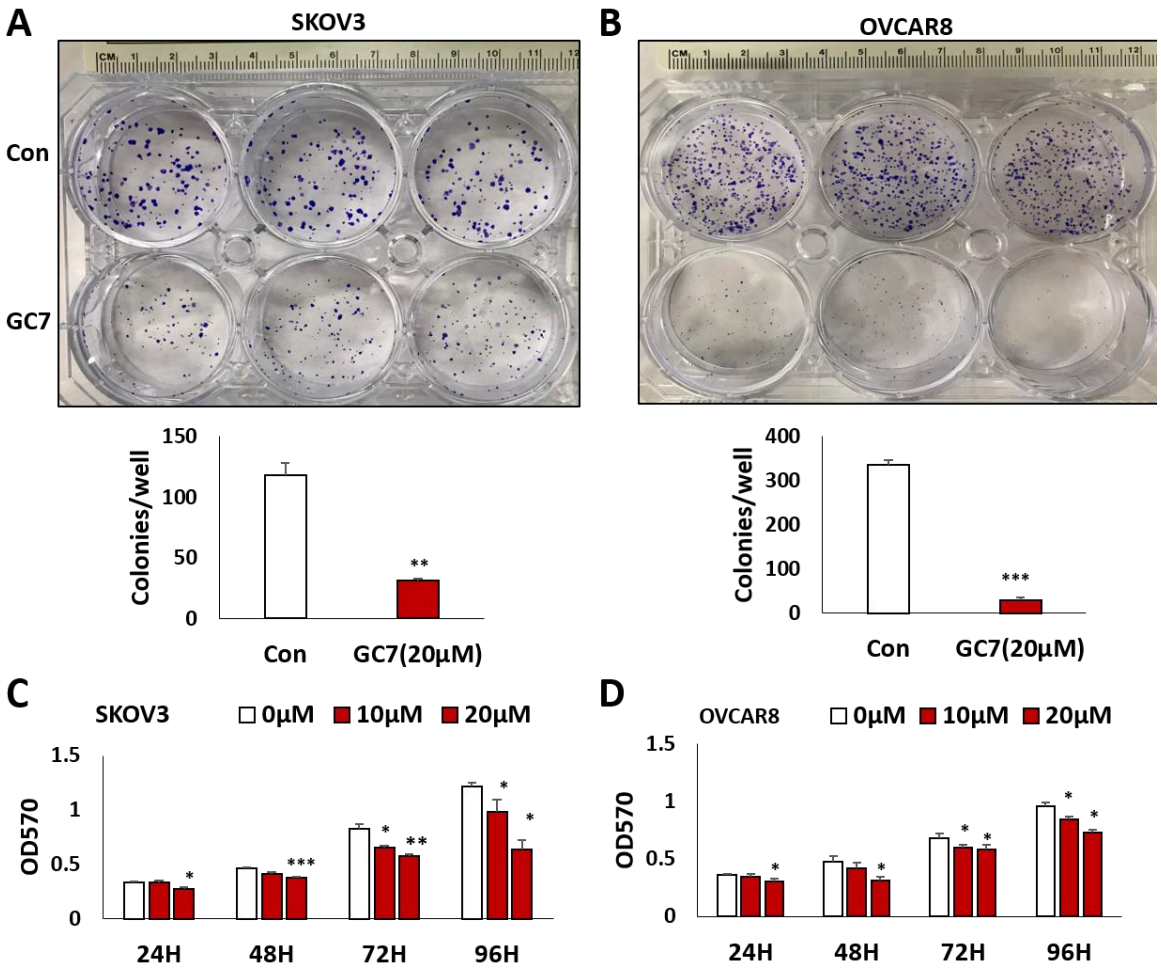

Figure 4-4. GC7 inhibited cell survival and proliferation in ovarian cancer cells. (A, B) Cell survival was determined in 20 μM GC7- and vehicle- treated SKOV3 and OVCAR8 cells by colony formation assay (n=3, **p <0.01; ***p <0.001). (C, D) Cell proliferation was determined using 10 and 20 μM of GC7 treatment at different time points in SKOV3 and OVCAR8 cells by MTT assay (n=3, *p <0.05; **p <0.01; ***p <0.001).

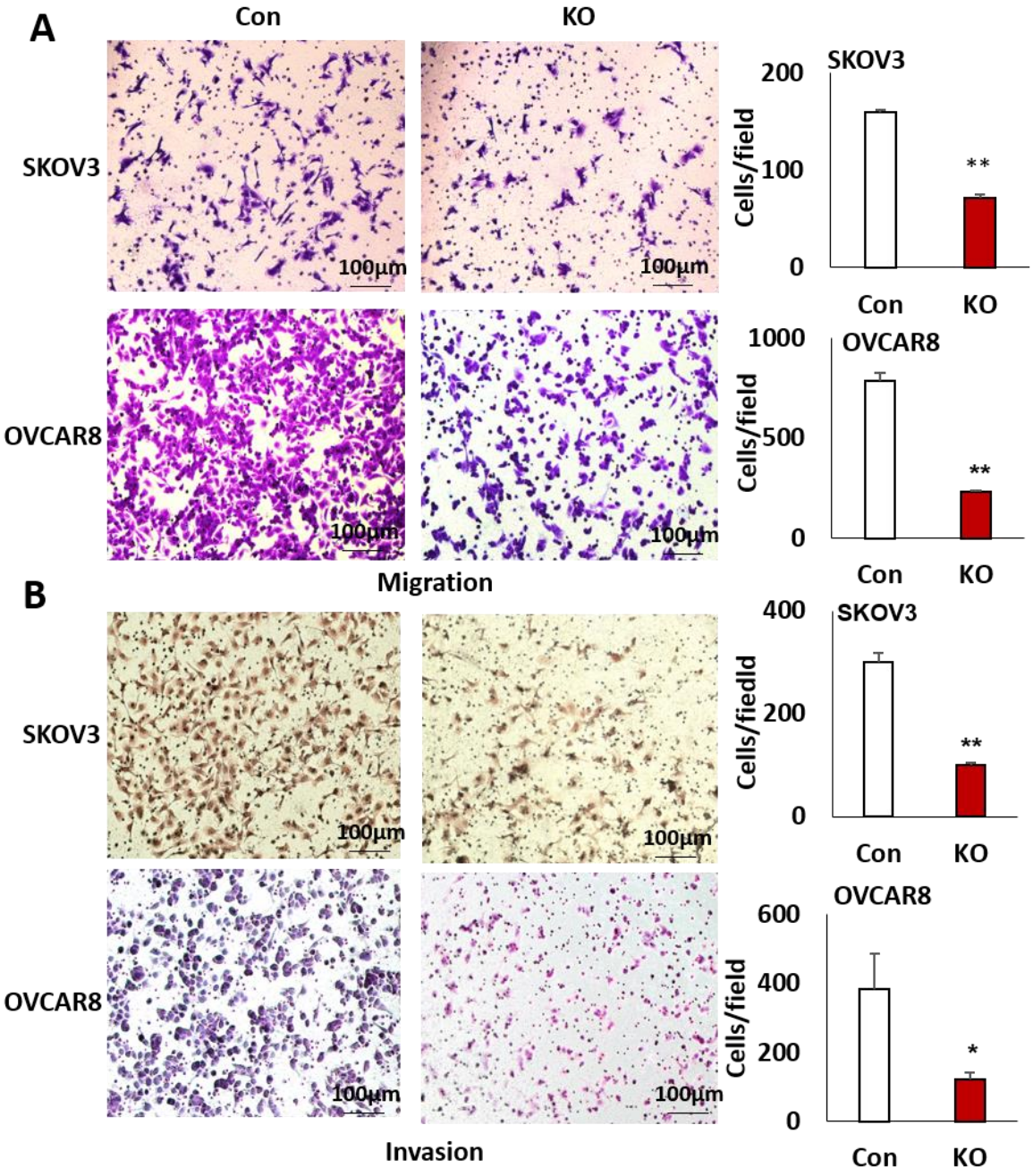

Figure 4-5. Disruption of DHS expression inhibited cell migration and invasion in ovarian cancer cells.

(A) Cell migration was examined in DHS KO and control SKOV3 or OVCAR8 cells using transwell plates, and migrated cells were stained with crystal violet and counted (n=3, **p<0.01; ***p <0.001). (B) Cell invasion in both DHS KO and control SKOV3 or OVCAR8 cells was examined using Matrigel-coated plates, and invaded cells were stained with H&E and counted (n=3, *p<0.05; **p <0.01).

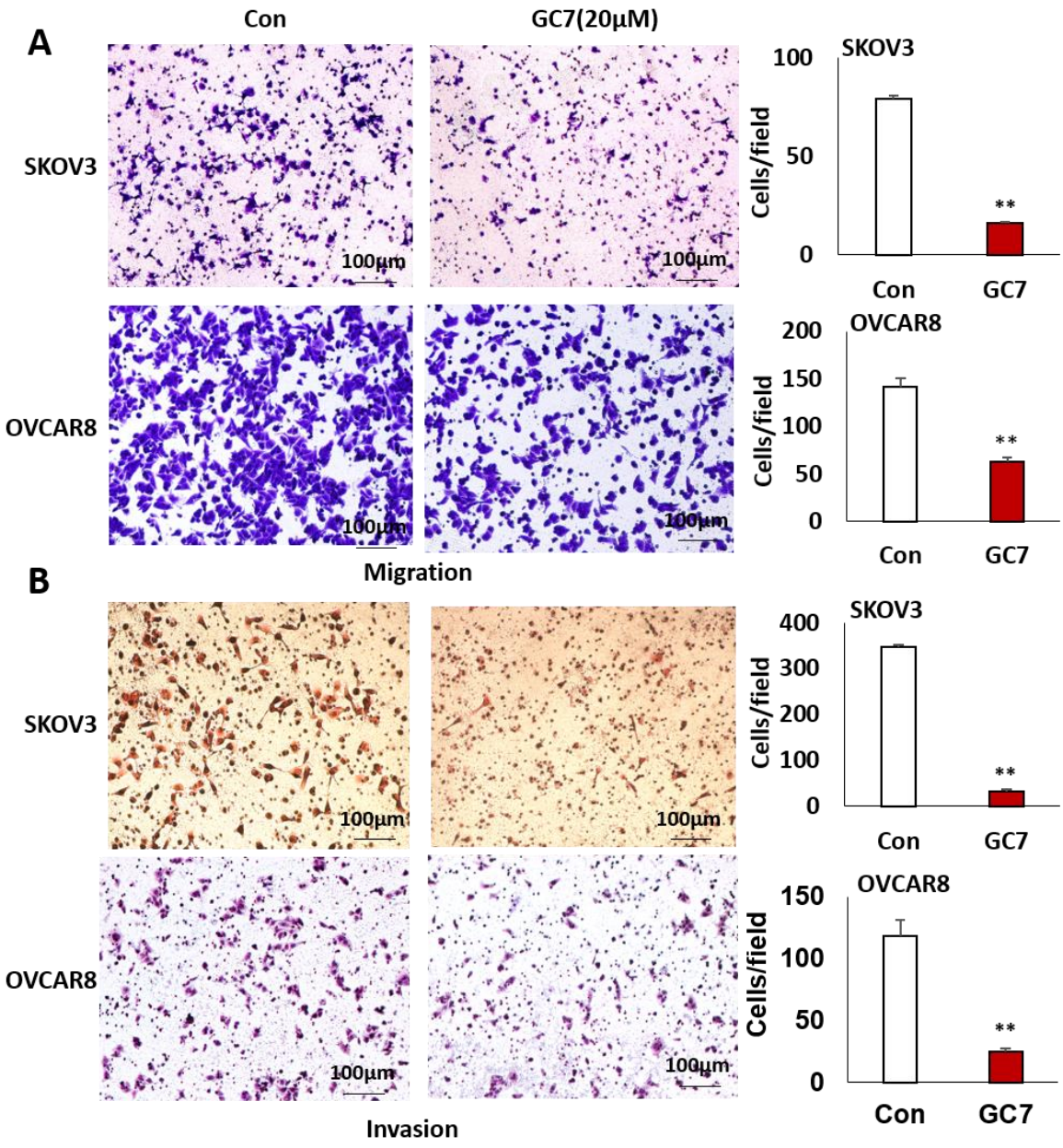

Figure 4-6. GC7 inhibited cell migration and invasion in ovarian cancer cells. (A) Cell migration was examined in 20 μM GC7- and vehicle- treated SKOV3 or OVCAR8 cells using transwell plates, and migrated cells were stained with crystal violet and counted (n=3, **p<0.01). (B) Cell invasion was examined in 20 μM GC7- and vehicle- treated SKOV3 or OVCAR8 cells using Matrigel-coated plates, and invaded cells were stained with H&E and counted (n=3, **p <0.01).

Figure 4-7. Inhibition of DHS attenuated the TGFβ signaling pathway in ovarian cancer cells.

(A, B) The expression of phospho- and total Smad2 in DHS KO and control SKOV3 and OVCAR8 cells was detected by Western blot following 6 ng/ml TGFβ treatment at the indicated time points (n=3, **p<0.01; *** p<0.001). (C, D) The expression of phospho- and total Smad2 was detected by Western blot in SKOV3 and OVCAR8 cells following 20 μM GC7 for 12 h and then treated with 6 ng/ml TGFβ at the indicated time points (n=3, *** p<0.001). Band intensity was measured using ImageJ and the significance was determined by student's T-test. One representative Western blot was presented from three similar independent experiments.

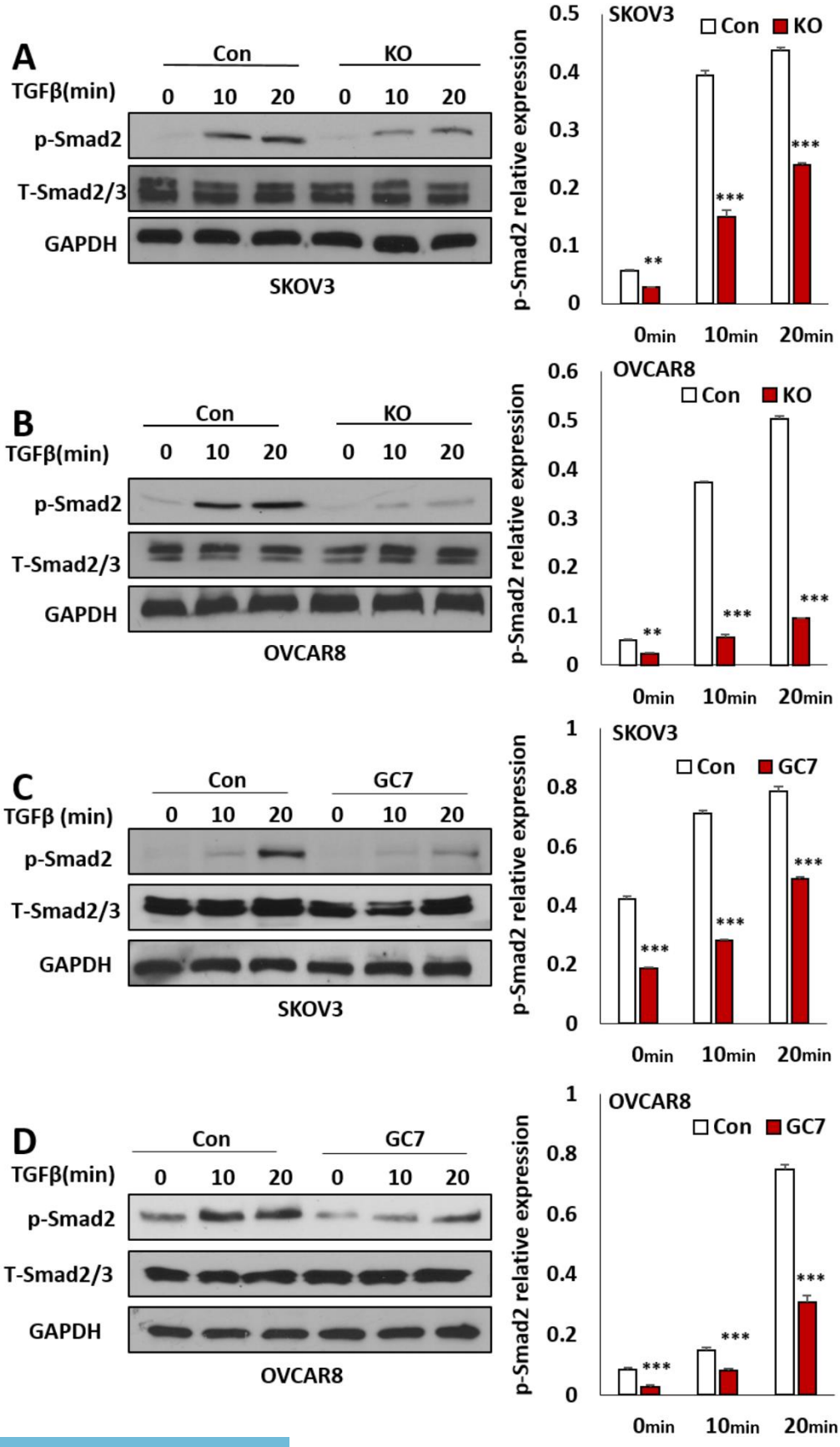

primary ovarian tumor growth and metastasis, we established a stable DHS KO OVCAR8 cell line with lentiviral CRISPR/Cas9 nickase vector as described in Chapter 2. We then intrabursally injected 5×10^5 ovarian cancer DHS KO and control OVCAR8 cells into two-month-old immunodeficient NSG female mice. Tumor growth and metastasis were monitored weekly using live animal imaging. After 5 weeks following cell injection, all mice xenografted with DHS KO OVCAR8 and control cells were sacrificed and tumors in ovaries were collected. Primary tumors were significantly smaller in mice injected with DHS KO cells compared to tumors injected with control cells when mice were either imaged using bioluminescence or sacrificed (**Figure 4-8A, B**). The primary tumors were characterized by H&E staining (**Figure 4-8C**).

We further examined multiple peritoneal organs and found that tumors mainly metastasized into the liver and spleen of mice injected with control cells (**Figure 4-9A**). In contrast, mice injected with DHS KO of OVCAR8 cells showed reduced metastatic tumors in those organs. The metastasized tumors were characterized by staining with H&E (**Figure 4-9B**). We examined hypusinated EIF5A, EIF5A2, EMT markers and p-Smad2 expression in primary ovarian tumors using Western blot. KO of DHS inhibited hypusinated EIF5A and EIF5A2 expression and downregulated the mesenchymal markers including β-catenin, Snail2, and Vimentin and p-Smad2 expression, and upregulated the epithelial marker Cytokeratin-7 and Ecadherin (**Figure 4-9C**). Tumor sections of mouse ovaries were immunostained with DHS, Vimentin, Cytokeratin-7 and hypusinated EIF5A antibodies, and the results were consistent with the Western blots (**Figure 4-10**). Our results indicated that blocking of hypusination suppressed primary ovarian tumor growth and metastasis by inhibiting EMT and attenuating the TGFβ pathway in orthotopic ovarian cancer mouse model.

GC7 suppresses primary ovarian tumor growth and metastasis in an orthotopic ovarian cancer mouse model

Knockout of DHS inhibited primary tumor growth in ovaries and tumor metastasis in multiple peritoneal organs (**Figure 4-8** through **4-10**). To test whether GC7 suppresses ovarian tumor metastasis by inhibiting DHS, we examined the efficacy of GC7 using an orthotopic ovarian cancer mouse model by intrabursally injecting OVCAR8- Luc2 cells into two-month-old immunodeficient NSG female mice and then treated mice with 16 mg/kg of GC7 for 5 days a week through intraperitoneal injection for 4 weeks. Tumor growth and metastasis were monitored using live animal imaging, and ovarian tumor metastasis was observed approximately two weeks after cell injection. At the 5th week following cell injection, tumors were dissected, and primary ovarian tumors were significantly reduced in GC7 treated mice compared to control mice (**Figure 4-11A, B**). The primary tumors were characterized by H&E staining (**Figure 4-11C**). We further examined multiple peritoneal organs and found that tumors metastasized into the liver and spleen of mice injected with control cells. In contrast, mice treated with GC7 did not display detectable metastatic tumors in those organs (**Figure 4-12A**). The metastasized tumors were characterized by H&E (**Figure 4-12B**). We examined hypusinated EIF5A, EIF5A2, EMT markers, and p-Smad2 expression in primary ovarian

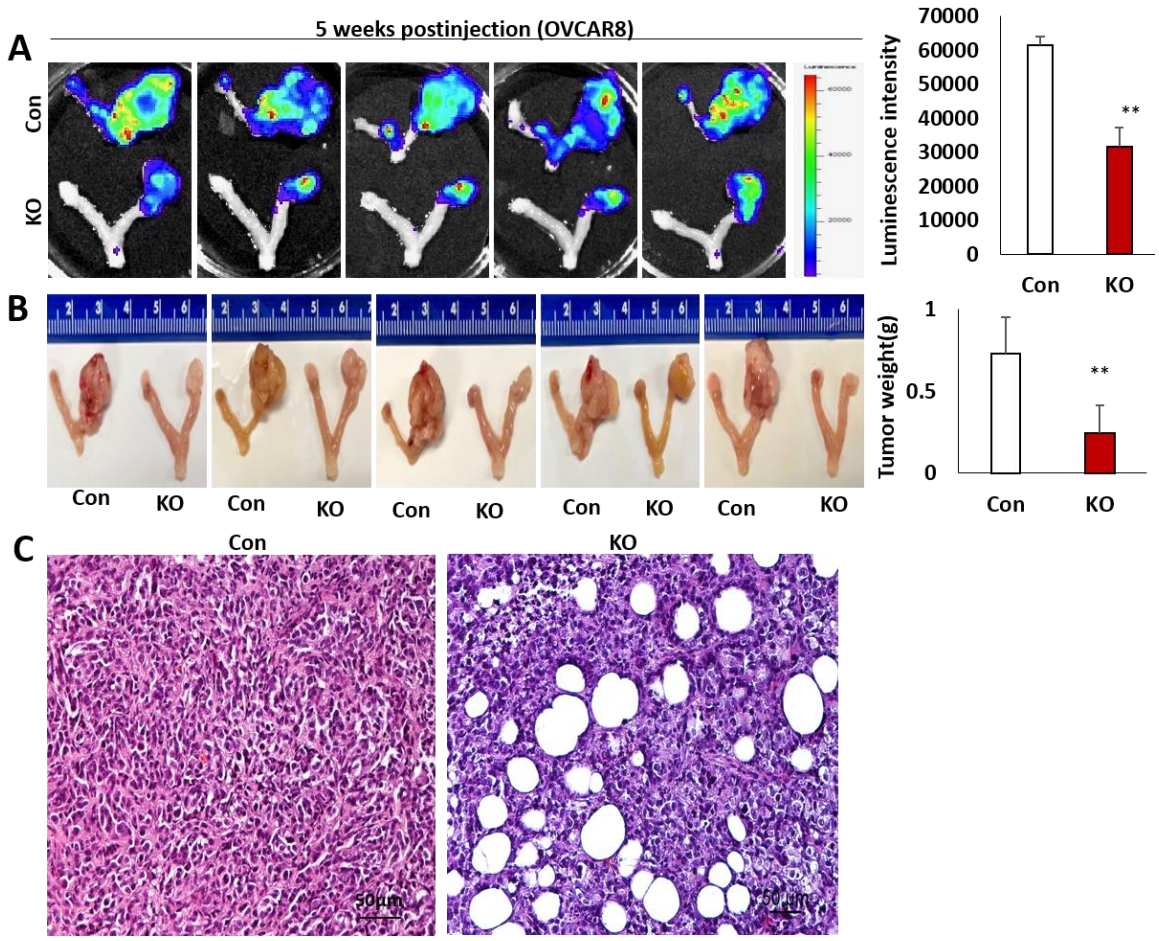

Figure 4-8. Knockout of DHS using lentiviral CRISPR/Cas9 nickase vector suppressed primary ovarian tumor growth in an orthotopic ovarian cancer mouse model.

(A) Bioluminescence of primary ovarian tumors dissected at one month following intrabursally injection of DHS KO and control OVCAR8 cells (n=5, **p <0.01). (B) Primary ovarian tumors dissected at 5 weeks following intrabursally injection of DHS KO and control OVCAR8 cells. Tumor weight in DHS KO is significantly less than in control (n=5, **p <0.01). (C) Primary tumors of mice xenografted with DHS KO and control cells were stained by H&E.

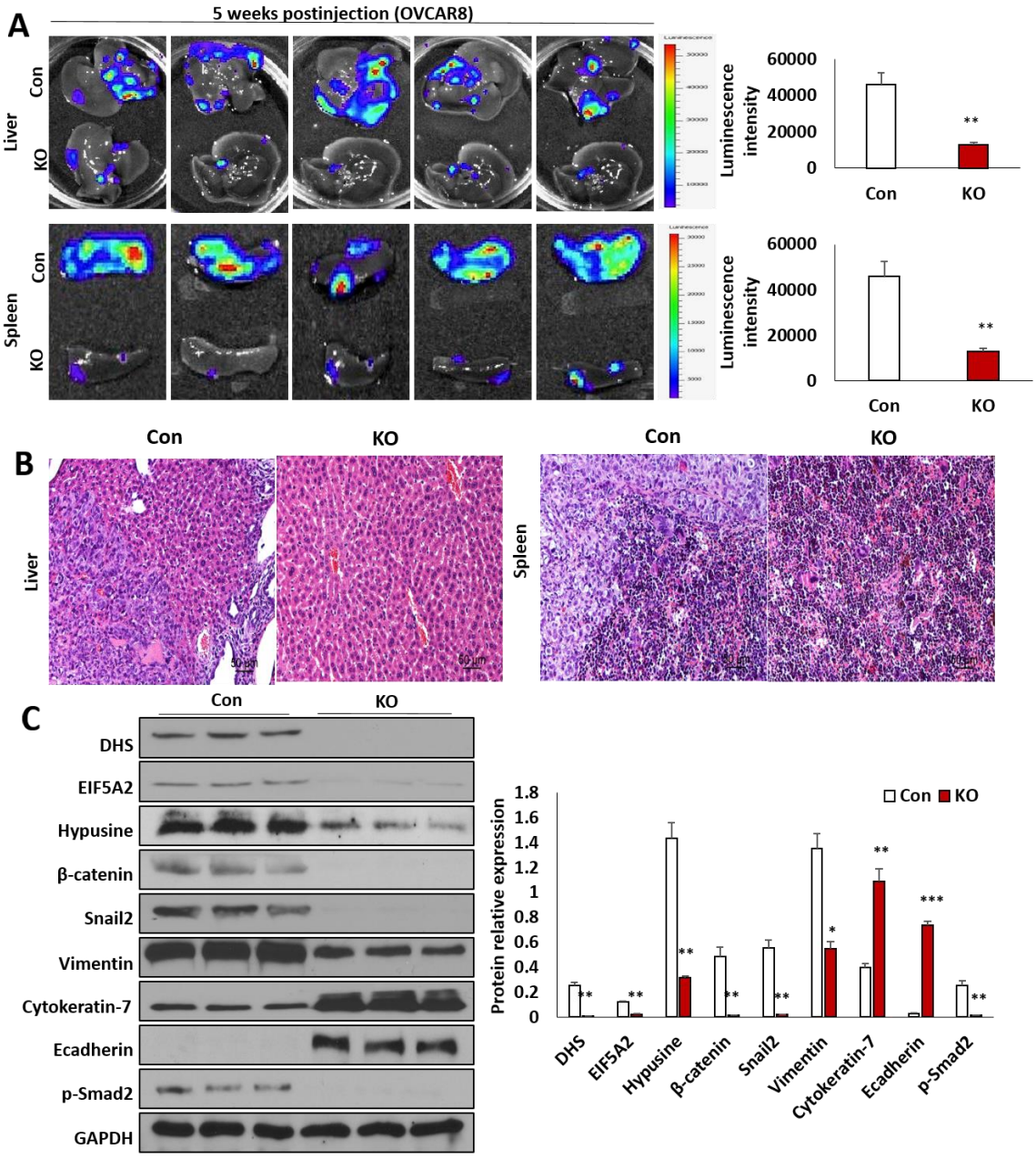

Figure 4-9. Knockout of DHS using lentiviral CRISPR/Cas9 nickase vector suppressed ovarian tumor metastasis in an orthotopic ovarian cancer mouse model. (A) Metastatic tumors in liver and spleen of mice xenografted with DHS KO and control cells were shown by bioluminescence images (n=5, **p <0.01). (B) Metastatic tumors in liver and spleen of mice xenografted with DHS KO and control cells were stained by H&E. (C) Western blot and densitometry analysis of DHS, hypusinated EIF5A, EIF5A2, p-Smad2 and EMT markers from primary ovarian tumor in mice xenografted with DHS KO and control cells (n=3, *p <0.05;**p <0.01;***p <0.001). Band intensity was measured using ImageJ and the significance was determined by the student's T-test.

Figure 4-10. DHS and EMT markers were stained in sections of ovarian tumor of DHS KO and control mice.

(A, B, C, D) DHS and Hypusinated EIF5A (green) was stained in cell cytoplasm, PCNA (red) was stained in cell nuclei and Cytokeratin-7 (green) and Vimentin (green) were stained in cell membranes of tumors from xenografted mice with DHS KO and control OVCAR8 cells. The sections of ovarian tumors were also stained with H&E.

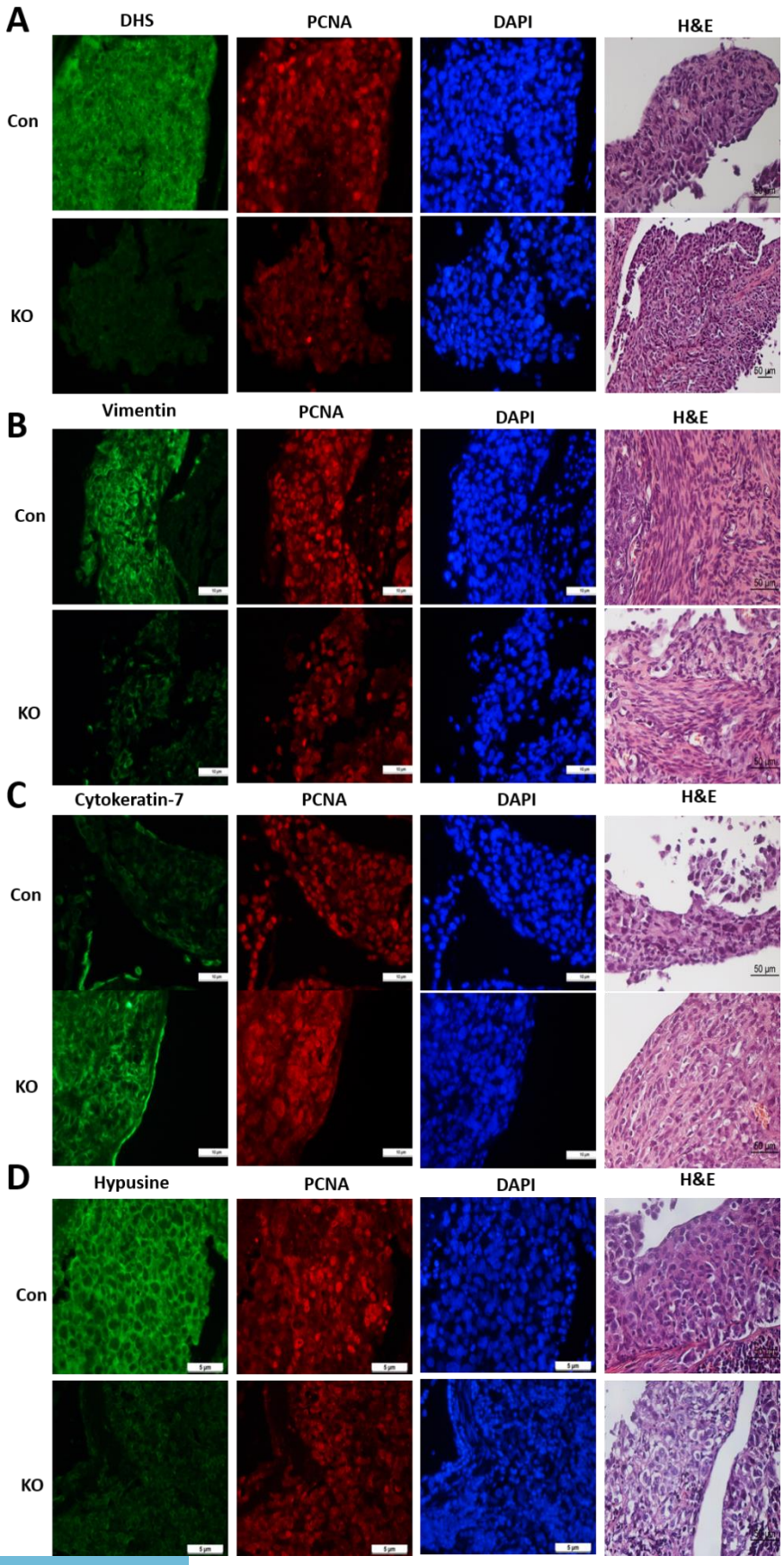

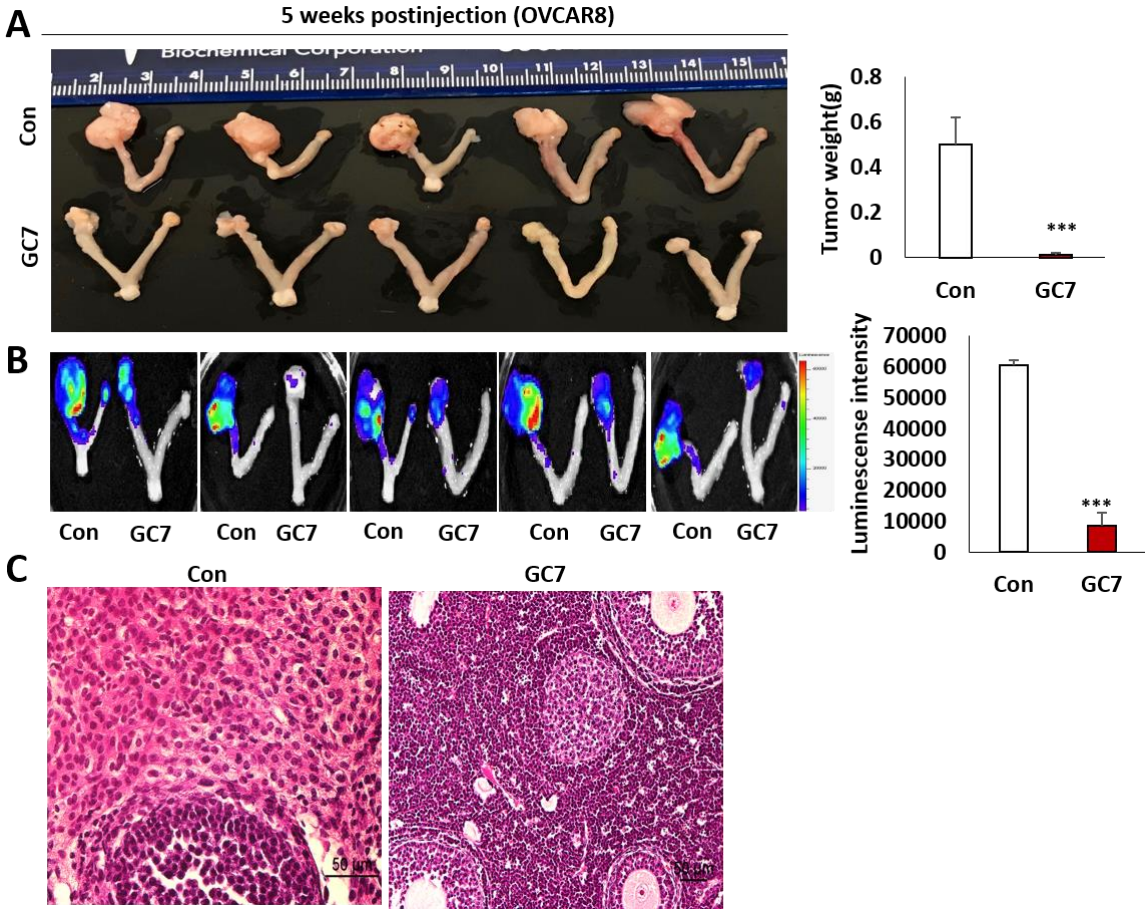

Figure 4-11. GC7 suppressed primary ovarian tumor growth in an orthotopic ovarian cancer mouse model.

(A) Primary ovarian tumor weight in GC7 and vehicle treated mice (n=5, ***p <0.001). (B) Primary ovarian tumors were shown using bioluminescence images (n=5, ***p <0.001). (C) Primary ovarian tumors were stained with H&E in GC7 and vehicle treated mice.

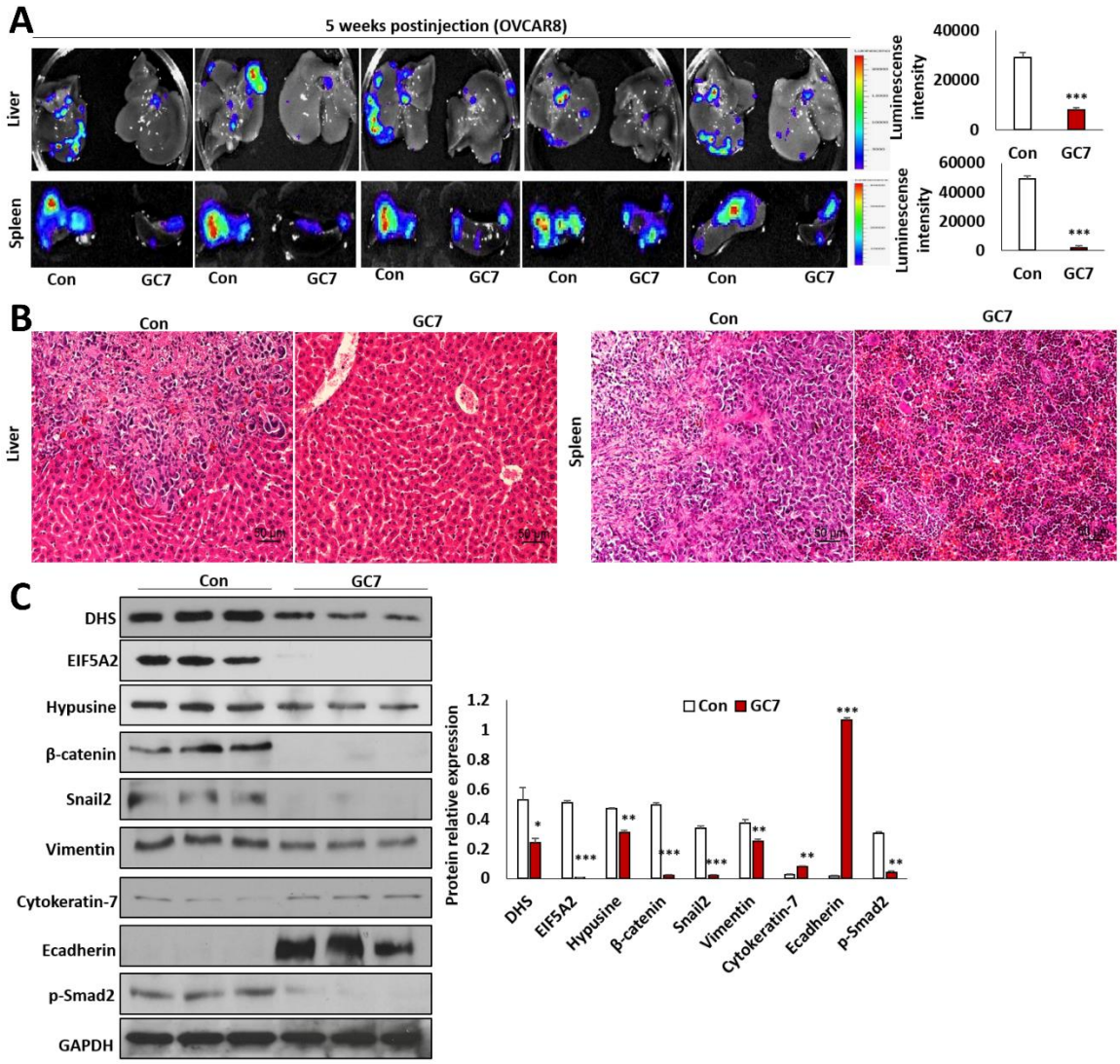

Figure 4-12. GC7 suppressed ovarian tumor metastasis in an orthotopic ovarian cancer mouse model.

(A) Metastatic tumors in liver and spleen of mice xenografted treated with GC7 and vehicle were shown by bioluminescence images (n=5, ***p <0.001). (B) Metastatic tumors in liver and spleen of mice xenografted treated with GC7 and vehicle were stained by H&E. (C) Western blot and densitometry analysis of DHS, hypusinated EIF5A, EIF5A2, p-Smad2 and EMT markers from primary ovarian tumors in three different mice xenografted with DHS KO and control cells (n=3, *p <0.05;**p <0.01;***p <0.001). Band intensity was measured using ImageJ and significance was determined by student's T-test.

tumors using Western blot. **Figure 4-12C** showed that GC7 treatment inhibited hypusinated EIF5A and EIF5A2 expression and downregulated the mesenchymal marker including β-catenin, Snail2, and Vimentin and p-Smad2 expression and upregulated the epithelial marker Cytokeratin-7 and Ecadherin. Ovary tumor sections were immunostained with DHS, Vimentin, Cytokeratin-7 and hypusinated EIF5A antibodies, and the results were consistent with the Western blots (**Figure 4-13**).

Discussion

DHS is the enzyme in the first step of hypusination and determines the activation and maturation of EIF5A (Caraglia et al., 2013). Either KO of DHS using lentiviral CRISPR/Cas9 nickase or inhibition of DHS with GC7 successfully blocked the hypusination pathway in both SKOV3 and OVCAR8 cell lines (**Figures 4-1** and **4-2**). The alterations of EMT markers after KO of DHS or GC7 treatment showed that mesenchymal markers are downregulated while epithelial cell markers are upregulated in ovarian cancer cells (**Figures 4-1** and **4-2**), suggesting that inhibition of EIF5A2 maturation by blocking the hypusination pathway suppresses EMT. Blocking hypusination pathway by KO of DHS or GC7 treatment also lead to significant reduction of cell survival, proliferation, migration, and invasion in both SKOV3 and OVCAR8 (**Figures 4-3** through **4-6**).

Our data show that KO of DHS or inhibition of DHS with GC7 suppressed ovarian primary tumor growth and metastasis into other organs, such as liver and spleen, by inhibiting EMT (**Figure 4-8** through **4-13**). Our findings are consistent with previous reports that blocking DHS inhibits EMT and reduces tumor growth and metastasis in several caner types including HCC, oral squamous cell carcinoma, breast cancer, and bladder cancer (Zhou et al., 2017; Fang et al., 2018a; Guan et al., 2019; Yang et al., 2014). Our results demonstrate that DHS is a potential therapeutic target for ovarian cancer treatment. Previous studies also showed that DHS disruption by GC7 treatment inhibits neuroblastoma cell growth (Bandino et al., 2014) and enhances the chemosensitivity in leukemia and lung cancer (Nakanishi and Cleveland, 2016). Therefore, targeting EIF5A2 hypusination with GC7 provides a novel approach for ovarian cancer therapy by reversing EMT.

Interestingly, we found that KO of DHS or GC7 treatment not only inhibited hypusinated EIF5A, but also reduced the total EIF5A2 expression in ovarian cancer cells (**Figure 4-1** and **4-2**). Our finding is consistent with a previous report in breast cancer (Guan et al., 2019) but is different from reports of hepatocellular carcinoma (HCC) and bladder cancer (BC) (Zhou et al., 2017; Lou et al., 2013; Yang et al., 2014). GC7 only reduced hypusinated EIF5A, but not the total EIF5A2 expression in HCC and BC. The different effects of GC7 on EIF5A2 expression may be related to the different cancer types.

Figure 4-13. DHS and EMT markers were stained in sections of ovarian tumor in GC7 and vehicle-treated mice.
(A, B, C, D) DHS and hypusinated EIF5A (green) were stained in cytoplasm, PCNA (red) was stained in cell nuclei and Cytokeratin-7 (green) and Vimentin (green) were stained in cell membranes from ovarian tumor sections in xenografted mice with DHS KO and control OVCAR8-Luc2 cells. Ovarian tumor sections were also stained by H&E.

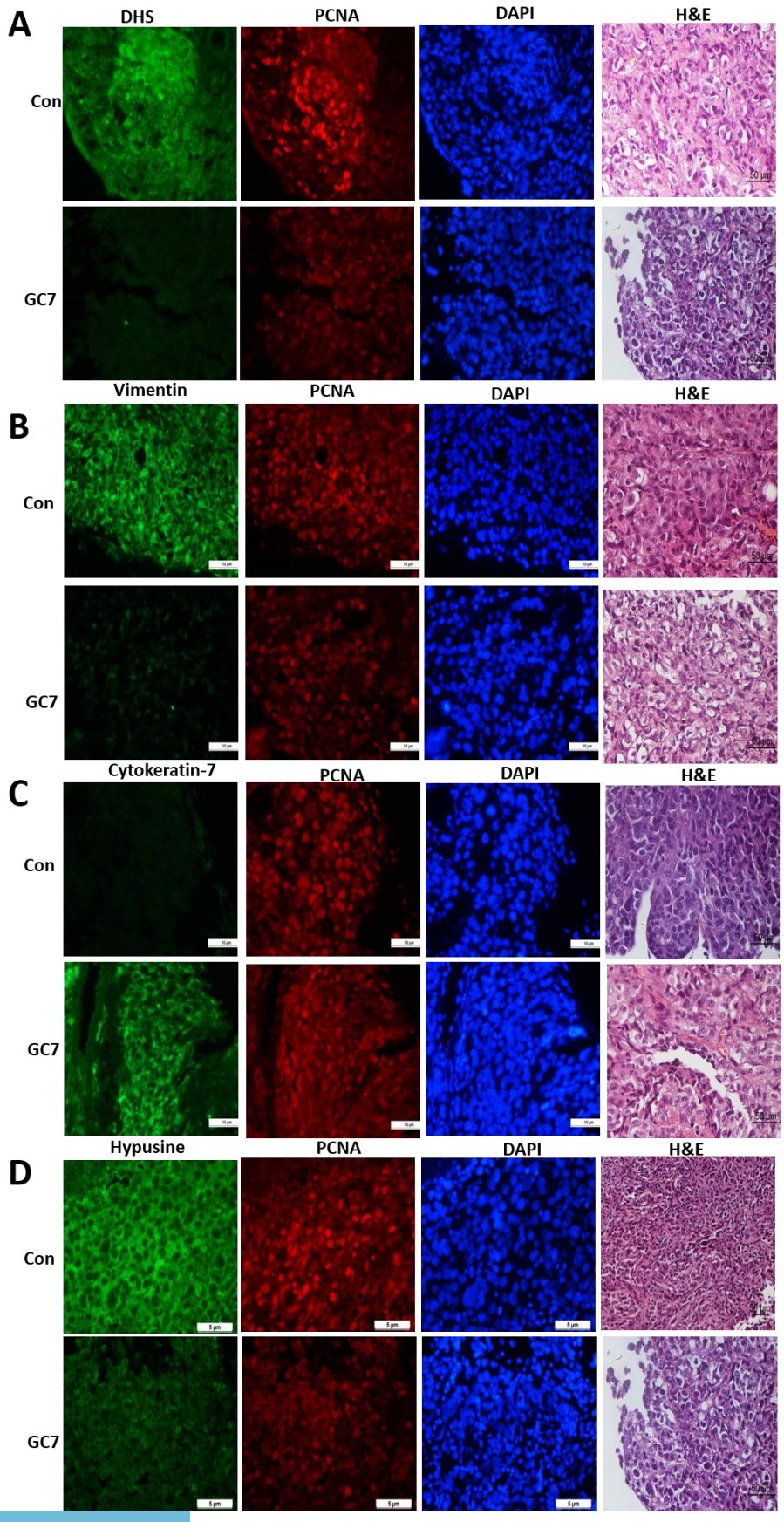

As shown in **Figure 4-11,** GC7 displayed high anti-tumor efficacy as an inhibitor of DHS in ovarian cancer and one of the most effective DHS inhibitors. GC7 has also been shown to inhibit tumor progression in other cancer types (Zhou et al., 2017; Fang et al., 2018a; Guan et al., 2019; Yang et al., 2014). However, GC7 has poor pharmacokinetic and pharmacodynamic properties due to its unstable molecular structure (Nakanishi and Cleveland, 2016). GC7 has also been reported to inhibit EIF5A1 activation (Lou et al., 2013). Since KO of EIF5A1 causes embryonic lethality and other side-effects, further work is needed to improve the selectivity of GC7 to specifically targeting EIF5A2 for ovarian cancer therapy.

Disruption of DHS blocks both EIF5A1 and EIF5A2 activation during the hypusination process. In Chapter 3, our results showed that KO of EIF5A2 attenuates Smad-dependent TGFβ signaling in ovarian cancer cells. In this study, inhibition of DHS also attenuated phospho-Smad2 in both SKOV3 and OVCAR8 cells (**Figure 4-7**). It is possible that inhibition of DHS attenuates the TGFβ pathway, which may be through suppressing EIF5A activation. Further investigation is needed to determine how DHS is involved in Smad-dependent TGFβ signaling pathway.

In conclusion, we reported that disruption of DHS expression using CRISPR/Cas9 nickase or GC7 blocks the hypusination pathway and leads to the inhibition of EIF5A2 and EMT in ovarian cancer cells. Disruption of DHS also leads to the inhibition of cell proliferation, survival, migration and invasion in ovarian cancer cells, possibly through inhibiting EIF5A2 and EMT and attenuating the TGFβ signaling pathway. Our results are consistent with previous reports that found hypusination is required for the activation and function of EIF5A2 in cancer cells and blocking hypusine synthesis using DHS inhibitors is a novel approach for ovarian cancer therapy.

CHAPTER 5. DISCUSSION

The lack of early biomarkers for clinical diagnosis is a contributing factor in the high mortality rate of ovarian cancer patients (Visintin et al., 2008). The current screening strategy for ovarian cancer uses a combinatorial approach of transvaginal ultrasound and blood testing for CA125, which has limited diagnostic efficacy due to poor specificity and insensitivity (Olivier et al., 2006). Therefore, it is important to identify an effective biomarker for early-stage diagnosis.

EIF5A2 is one of the two EIF5A isoforms and was first detected in the ovarian cancer cell line UACC-1598 (Clement et al., 2003b). In normal tissues, EIF5A2 is only present in testis and brain (Nishimura et al., 2012). A growing number of studies found that EIF5A2 is highly expressed in multiple types of human cancers (Wu et al., 2020). We analyzed 607 serous ovarian carcinomas and 561 normal tissues in the Oncomine database and found that EIF5A2 expression is amplified and upregulated in ovarian adenocarcinomas and is predictive of poor patient survival. These findings suggest that EIF5A2 is a potential biomarker for early diagnosis of ovarian cancer and also a prognostic indicator following chemotherapy.

Ovarian tumors are more metastatic than any other cancers because ovarian cancer cells disseminate directly to other abdominal organs (Lengyel, 2010). During cancer progression, EOC tumor cells undergo EMT and gain the motility for cancer metastasis. Detached ovarian tumor cells dissociate into single cells or form spheroids in the peritoneal fluid (Lengyel, 2010). We found that KO of EIF5A2 using CRISPR/Cas9 nickase inhibits EMT, while overexpression of EIF5A2 promotes EMT in ovarian cancer cells. For the first time, we show that KO of EIF5A2 inhibits primary ovary tumor growth and metastasis, which is consistent with previous findings that EIF5A2 promotes EMT, metastasis, and invasion in several other human cancer types (Tang et al., 2010; Zhu et al., 2012; Wei et al., 2014; Lin et al., 2020).

EIF5A1 is the other isoform of EIF5A and, similar to EIF5A2, is also highly expressed in ovarian cancer where its expression promotes EMT (Zhang et al., 2018). However, the two EIF5A isoforms have different biological functions. Homozygous deletion of EIF5A2 in mice doesn't affect body weight, fertility, or survival (Pällmann et al., 2015). In contrast, homozygous deletion of EIF5A1 causes embryonic lethality in mice (Nishimura et al., 2012). The functional similarity and difference between the two isoforms can be explained by their crystallographic structures. EIF5A1 and EIF5A2 share the same N-terminal domain containing the hypusination site, suggesting that the functional similarity might be linked to the hypusine modification. However, structures of the two isoforms differ at their C-terminal domains (Tong et al., 2009). Although EIF5A1 and EIF5A2 compensate each other in yeast cells (Clement et al., 2003), their functional similarity and differences in eukaryotic cells, especially in human cancers, are still obscure. Future work should address whether KO of EIF5A2 induces EIF5A1 upregulation or activation that compensates for loss of EIF5A2 in signaling pathways in ovarian cancer cells.

We previously showed that the TGFβ pathway stimulates EMT in ovarian cancer cells (Chen et al., 2014). The TGFβ pathway affects cell division, differentiation, migration, adhesion, and death by transcriptionally regulating downstream target genes through the Smad2/3/4 complex (Massagué et al., 2005). Possible correlations between the TGFβ pathway and EIF5A2 in ovarian carcinoma cells were studied by examining both EIF5A2 KO or overexpression cells following TGFβ treatment. We found that TGFβ upregulates EIF5A2 expression in a time-dependent manner, and KO of EIF5A2 attenuates TGFβ signaling in ovarian cancer cells, suggesting a positive feedback loop between the TGFβ pathway and EIF5A2 in ovarian cancer cells. The correlations between EIF5A2 and the TGFβ pathway have been reported to be either positive or negative depending on cancer type (Hao et al., 2020; Wei et al., 2014). Our study based on luciferase reporter gene assays suggests that Smad2/3/4 may bind to the promoter of EIF5A2 and activate EIF5A2 expression. To directly verify that Smad2/3/4 transcriptionally upregulates EIF5A2 in ovarian cancer cells, CHIP-PCR assays should be performed in the future. Since hypusinated EIF5A2 is localized primarily in the cytoplasm of ovarian cancer cells, EIF5A2 may potentially interact, either directly or indirectly, with TGFβ signaling components including the TGFβ receptors, Smad2, Smad3 and Smad4. Immunoprecipitation assays can be used to investigate whether EIF5A2 directly interacts with TGFβ receptor or the Smad protein complex. However, it is also possible that EIF5A2 indirectly regulates the TGFβ signaling pathway. In either case, our results indicate that EIF5A2 promotes primary ovarian tumor growth and metastasis by promoting EMT and activating the TGFβ pathway.

Inhibiting the hypusination pathway has been shown to suppress tumor progression in various cancer (Nakanishi and Cleveland, 2016). However, whether disruption of the hypusination pathway inhibits ovarian tumor growth is still unclear. DHS has been shown to be an anti-tumor target (Bandino et al., 2014) and is required for EIF5A maturation (**Figure 1-2**) (Maier et al., 2010). KO or inhibition of DHS using CRISPR/Cas9 nickase or GC7 successfully inhibited the expressions of hypusinated EIF5A, EIF5A2, and EMT in ovarian cancer cells. OC cell proliferation, survival, migration, and invasion are significantly reduced following DHS KO or inhibition. For the first time, we show that inhibition of DHS significantly suppressed EMT and ovarian tumor growth and metastasis, consistent with previous findings that inhibition of hypusination pathway suppresses tumor progression (Nakanishi and Cleveland, 2016). Whether inhibition of DHS affects EIF5A2 expression is depending on different cancer types (Zhou et al., 2017; Lou et al., 2013; Yang et al., 2014; Guan et al., 2019). Disruption of DHS may also affect EIF5A2 protein stability. Furthermore, we show that GC7 is an effective DHS inhibitor to block the hypusination pathway and inhibit primary ovarian tumor growth and metastasis. GC7 may potentially affect EIF5A1 function and thereby induce nonselective effects (Lou et al., 2013). Therefore, improvement of the specificity of DHS inhibitors is needed in the future, in order to selectively target EIF5A2 hypusination for ovarian cancer therapy.

Blocking the hypusination of EIF5A2 in ovarian cancer cells also inhibits EMT and attenuates the TGFβ signaling pathway using GC7, consistent with our findings in DHS KO ovarian cancer cells and orthotopic ovarian cancer mouse models. KO of DHS

disrupts primary ovarian tumor growth and metastasis by reversing EMT and attenuating the TGFβ pathway. Our results show that targeting EIF5A2 hypusination using DHS inhibitor is a new approach for ovarian cancer therapy.

In conclusion, this study revealed a novel mechanism underlying EIF5A2 mediated EMT in ovarian cancer progression and metastasis (**Figure 5-1**). Ligand TGFβ binds to the complex of TGFβ receptor-1 and receptor-2, followed by phosphorylation of TGFβ receptor dimers and Smads. The activated Smad complex translocates into the nucleus where it binds to the promoter of EIF5A2 and transcriptionally regulates EIF5A2 expression. Highly expressed EIF5A2 acts in EMT regulation and promotes tumor progression in ovarian cancer by activating the TGFβ signaling pathway. In addition, we found that disrupting the hypusination of EIF5A inhibits the expression of both hypusinated EIF5A and EIF5A2. Disruption of the hypusination process also inhibits EMT and suppresses ovarian primary tumor growth and metastasis. Taken together, our findings shed new light on potential treatment strategies of ovarian cancer and improve our understanding of the potential mechanisms underlying EIF5A2 mediated ovarian cancer progression.

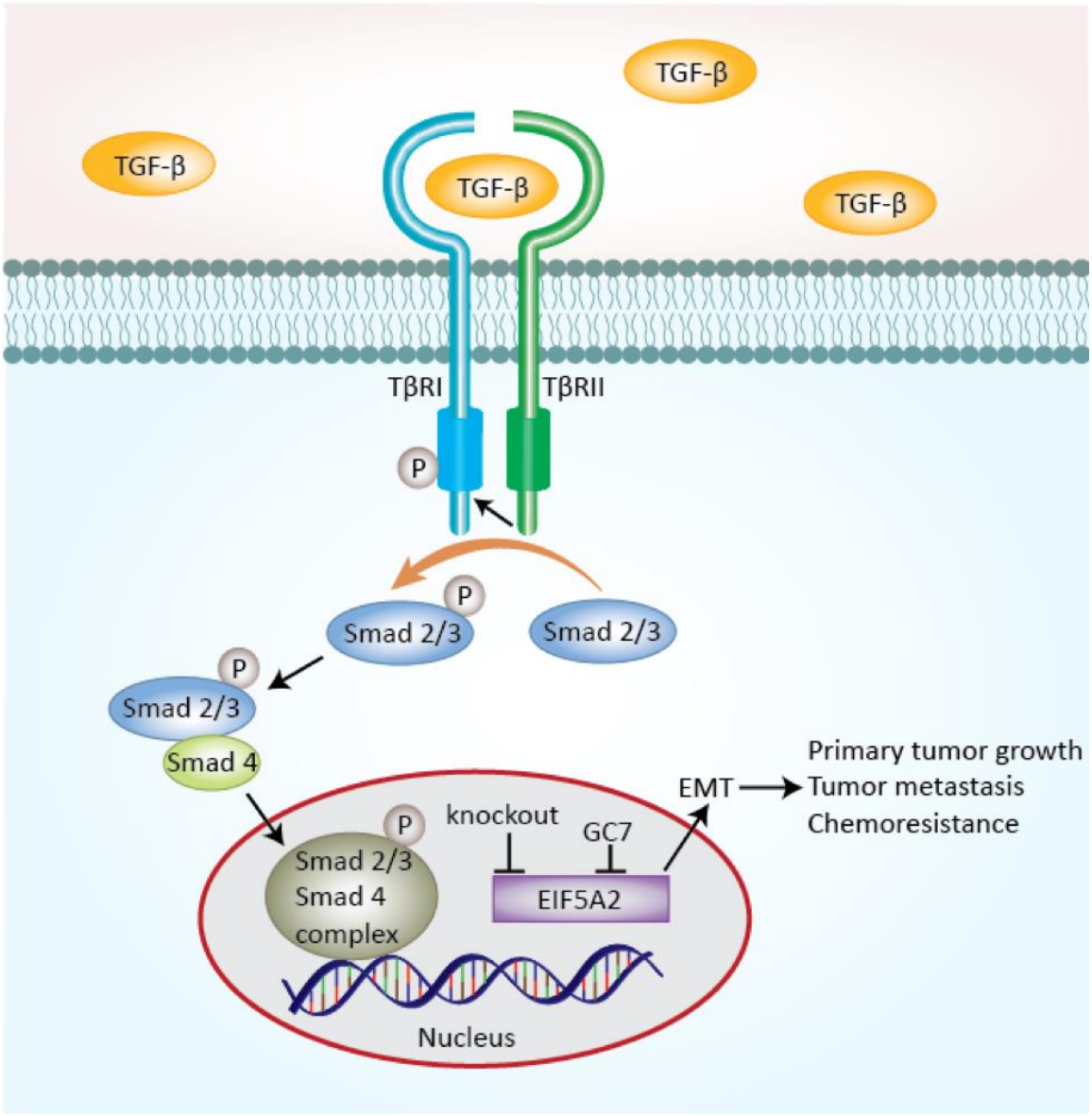

Figure 5-1. Potential molecular mechanism underlying EIF5A2 mediated tumor metastasis.

LIST OF REFERENCES

Aguirre-Gamboa, R., Gomez-Rueda, H., Martínez-Ledesma, E., Martínez-Torteya, A., Chacolla-Huaringa, R., Rodriguez-Barrientos, A., Tamez-Pena, J. G. & Trevino, V. (2013). SurvExpress: an online biomarker validation tool and database for cancer gene expression data using survival analysis. *PloS One,* 8 (9), e74250.

Ahmed, N., Abubaker, K., Findlay, J. & Quinn, M. (2010). Epithelial mesenchymal transition and cancer stem cell-like phenotypes facilitate chemoresistance in recurrent ovarian cancer. *Curr. Cancer Drug Targets,* 10 (3), 268-278.

Ahmed, N. & Stenvers, K. (2013). Getting to know ovarian cancer ascites: opportunities for targeted therapy-based translational research. *Front. Oncol.,* 3, 256.

Ahmed, N., Thompson, E. W. & Quinn, M. A. (2007). Epithelial–mesenchymal interconversions in normal ovarian surface epithelium and ovarian carcinomas: an exception to the norm. *J. Cell. Physiol.,* 213 (3), 581-588.

Antony, J., Thiery, J. P. & Huang, R. Y.-J. (2019). Epithelial-to-mesenchymal transition: Lessons from development, insights into cancer and the potential of EMT-subtype based therapeutic intervention. *Physical Biology,* 16 (4), 041004.

Armstrong, D. K., Bundy, B., Wenzel, L., Huang, H. Q., Baergen, R., Lele, S., Copeland, L. J., Walker, J. L. & Burger, R. A. (2006). Intraperitoneal cisplatin and paclitaxel in ovarian cancer. *N. Engl. J. Med.,* 354 (1), 34-43.

Bandino, A., Geerts, D., Koster, J. & Bachmann, A. S. (2014). Deoxyhypusine synthase (DHPS) inhibitor GC7 induces p21/Rb-mediated inhibition of tumor cell growth and DHPS expression correlates with poor prognosis in neuroblastoma patients. *Cellular Oncol.,* 37 (6), 387-398.

Bast, R. C., Hennessy, B. & Mills, G. B. (2009). The biology of ovarian cancer: new opportunities for translation. *Nat. Rev. Cancer,* 9 (6), 415-428.

Bhuyan, G., Arora, R., Ahluwalia, C. & Sharma, P. (2019). Epithelial–mesenchymal transition in serous and mucinous epithelial tumors of the ovary. *J. Cancer Res. Ther.,* 15 (6), 1309.

Bozhkova, D. M. & Poryazova-Markova, E. G. (2019). The Epithelial-Mesenchymal Transition, E-cadherin and Tumor Progression in Ovarian Serous Tumors. *Fol. Med.,* 61 (2), 296-302.

Bristow, R. E., Tomacruz, R. S., Armstrong, D. K., Trimble, E. L. & Montz, F. (2002). Survival effect of maximal cytoreductive surgery for advanced ovarian carcinoma during the platinum era: a meta-analysis. *J. Clin. Oncol.,* 20(5), 1248-59.

Brown, P. O. & Palmer, C. (2009). The preclinical natural history of serous ovarian cancer: defining the target for early detection. *PLoS Med.*, 6 (7), e1000114.

Burger, R. A. (2008). A new model of ovarian carcinogenesis may influence early detection strategies. *Am. J. Obstet Gynecol.*, 198 (4), 349-350.

Cao, T.-T., Lin, S.-H., Fu, L., Tang, Z., Che, C.-M., Zhang, L.-Y., Ming, X.-Y., Liu, T.-F., Tang, X.-M. & Tan, B.-B. (2017). Eukaryotic translation initiation factor 5A2 promotes metabolic reprogramming in hepatocellular carcinoma cells. *Carcinogenesis*, 38 (1), 94-104.

Caraglia, M., Park, M., Wolff, E., Marra, M. & Abbruzzese, A. (2013). eIF5A isoforms and cancer: two brothers for two functions? *Amino Acids*, 44 (1), 103-109.

Chandra, A., Pius, C., Nabeel, M., Nair, M., Vishwanatha, J. K., Ahmad, S. & Basha, R. (2019). Ovarian cancer: Current status and strategies for improving therapeutic outcomes. *Cancer Med.*, 8 (16), 7018-7031.

Chen, C., Zhang, B., Wu, S., Song, Y. & Li, J. (2018). Knockdown of EIF5A2 inhibits the malignant potential of non-small cell lung cancer cells. *Oncol. Lett.*, 15 (4), 4541-4549.

Chen, W., Luo, J.-H., Hua, W.-F., Zhou, F.-J., Lin, M. C., Kung, H.-F., Zeng, Y.-X., Guan, X.-Y. & Xie, D. (2009). Overexpression of EIF-5A2 is an independent predictor of outcome in patients of urothelial carcinoma of the bladder treated with radical cystectomy. *Cancer Epidemiol. Biomarkers Prev.*, 18 (2), 400-408.

Chen, Z., Wang, Y., Liu, W., Zhao, G., Lee, S., Balogh, A., Zou, Y., Guo, Y., Zhang, Z. & Gu, W. (2014). Doxycycline inducible Kruppel-like factor 4 lentiviral vector mediates mesenchymal to epithelial transition in ovarian cancer cells. *PloS One*, 9 (8), e105331.

Clement, P. M., Henderson, C. A., Jenkins, Z. A., Smit‐McBride, Z., Wolff, E. C., Hershey, J. W., Park, M. H. & Johansson, H. E. (2003). Identification and characterization of eukaryotic initiation factor 5A‐2. *Eur. J. Biochem.*, 270 (21), 4254-4263.

Clement, P. M., Johansson, H. E., Wolff, E. C. & Park, M. H. (2006). Differential expression of eIF5A‐1 and eIF5A‐2 in human cancer cells. *FEBS J.*, 273 (6), 1102-1114.

Bhatla, N. & Jones, A. (2018). The world ovarian cancer coalition atlas. *The World Ovarian Cancer Coalit.* 4.

Cui, W., Fowlis, D. J., Bryson, S., Duffie, E., Ireland, H., Balmain, A. & Akhurst, R. J. (1996). TGFβ1 inhibits the formation of benign skin tumors, but enhances progression to invasive spindle carcinomas in transgenic mice. *Cell*, 86 (4), 531-542.

Daraï, E., Scoazec, J.-Y., Walker-Combrouze, F., Mlika-Cabanne, N., Feldmann, G., Madelenat, P. & Potet, F. (1997). Expression of cadherins in benign, borderline, and malignant ovarian epithelial tumors: a clinicopathologic study of 60 cases. *Hum. Pathol.*, 28 (8), 922-928.

Derynck, R., Akhurst, R. J. & Balmain, A. (2001). TGF-β signaling in tumor suppression and cancer progression. *Nat. Genet.*, 29 (2), 117-129.

DiMeo, T. A., Anderson, K., Phadke, P., Feng, C., Perou, C. M., Naber, S. & Kuperwasser, C. (2009). A novel lung metastasis signature links Wnt signaling with cancer cell self-renewal and epithelial-mesenchymal transition in basal-like breast cancer. *Cancer Res.*, 69 (13), 5364-5373.

Dochez, V., Caillon, H., Vaucel, E., Dimet, J., Winer, N. & Ducarme, G. (2019). Biomarkers and algorithms for diagnosis of ovarian cancer: CA125, HE4, RMI and ROMA, a review. *J. Ovarian Res.*, 12 (1), 28.

Dou, C., Lee, J., Liu, B., Liu, F., Massague, J., Xuan, S. & Lai, E. (2000). BF-1 interferes with transforming growth factor β signaling by associating with Smad partners. *Mol. Cell. Biol.*, 20 (17), 6201-6211.

Drasin, D. J., Robin, T. P. & Ford, H. L. (2011). Breast cancer epithelial-to-mesenchymal transition: examining the functional consequences of plasticity. *Breast Cancer Res.*, 13 (6), 1-13.

Eisenberg, T., Knauer, H., Schauer, A., Büttner, S., Ruckenstuhl, C., Carmona-Gutierrez, D., Ring, J., Schroeder, S., Magnes, C. & Antonacci, L. (2009). Induction of autophagy by spermidine promotes longevity. *Nat. Cell Biol.*, 11 (11), 1305-1314.

Eisenkop, S. M. & Spirtos, N. M. (2001). The clinical significance of occult macroscopically positive retroperitoneal nodes in patients with epithelial ovarian cancer. *Gynecol. Oncol.*, 82 (1), 143-149.

Espinoza, I., Pochampally, R., Xing, F., Watabe, K. & Miele, L. (2013). Notch signaling: targeting cancer stem cells and epithelial-to-mesenchymal transition. *Onco Targets Ther.*, 6, 1249.

Fang, L., Gao, L., Xie, L. & Xiao, G. (2018a). Eukaryotic translation initiation factor 5A-2 involves in doxorubicin-induced epithelial-mesenchymal transition in oral squamous cell carcinoma cells. *J. Cancer*, 9 (19), 3479.

Fang, L., Gao, L., Xie, L. & Xiao, G. (2018b). GC7 enhances cisplatin sensitivity via STAT3 signaling pathway inhibition and eIF5A2 inactivation in mesenchymal phenotype oral cancer cells. *Oncol. Rep.*, 39 (3), 1283-1291.

Farghaly, S. (2012). Anti-metastatic gene therapy in patients with advanced epithelial ovarian cancer (EOC). *J. Cell. Sci. Ther.*,S:15, 2.

Fujimura, K., Choi, S., Wyse, M., Strnadel, J., Wright, T. & Klemke, R. (2015). Eukaryotic translation initiation factor 5A (EIF5A) regulates pancreatic cancer metastasis by modulating RhoA and Rho-associated kinase (ROCK) protein expression levels. *J. Biol. Chem.,* 290 (50), 29907-29919.

Guan, X., Gu, S., Yuan, M., Zheng, X. & Wu, J. (2019). MicroRNA-33a-5p overexpression sensitizes triple-negative breast cancer to doxorubicin by inhibiting eIF5A2 and epithelial-mesenchymal transition. *Oncol. Lett.,* 18 (6), 5986-5994.

Güth, R., Adamian, Y., Geller, C., Molnar, J., Maddela, J., Kutscher, L., Bhakta, K., Meade, K., Kim, S. & Agajanian, M. (2019). DHPS-dependent hypusination of eIF5A1/2 is necessary for TGFβ/fibronectin-induced breast cancer metastasis and associates with prognostically unfavorable genomic alterations in TP53. *Biochem. Biophys. Res. Commun.,* 519 (4), 838-845.

Győrffy, B., Lánczky, A. & Szállási, Z. (2012). Implementing an online tool for genome-wide validation of survival-associated biomarkers in ovarian-cancer using microarray data from 1287 patients. *Endocr. Relat. Cancer,* 19 (2), 197-208.

Hamilton, T. (1992). Ovarian cancer, part I: biology. *Curr. Probl. Cancer,* 16 (1), 5-57.

Hao, F., Zhu, Q., Lu, L., Sun, S., Huang, Y., Zhang, J., Liu, Z., Miao, Y., Jiao, X. & Chen, D. (2020). EIF5A2 Is Highly Expressed in Anaplastic Thyroid Carcinoma and Is Associated With Tumor Growth by Modulating TGF-Signals. *Oncology Research Featuring Preclinical and Clinical Cancer Therapeutics*, 28 (4), 345-355.

Haque, S. & Morris, J. C. (2017). Transforming growth factor-β: A therapeutic target for cancer. *Hum Vaccin Immunother.,* 13 (8), 1741-1750.

He, L. R., Zhao, H. Y., Li, B. K., Liu, Y. H., Liu, M. Z., Guan, X. Y., Bian, X. W., Zeng, Y. X. & Xie, D. (2011). Overexpression of eIF5A‐2 is an adverse prognostic marker of survival in stage I non‐small cell lung cancer patients. *Int. J. Cancer,* 129 (1), 143-150.

Hoffmeyer, K., Raggioli, A., Rudloff, S., Anton, R., Hierholzer, A., Del Valle, I., Hein, K., Vogt, R. & Kemler, R. (2012). Wnt/β-catenin signaling regulates telomerase in stem cells and cancer cells. *Science,* 336 (6088), 1549-1554.

Huang, P.-Y., Zeng, T.-T., Ban, X., Li, M.-Q., Zhang, B.-Z., Zhu, Y.-H., Hua, W.-F., Mai, H.-Q., Zhang, L. & Guan, X.-Y. (2016). Expression of EIF5A2 associates with poor survival of nasopharyngeal carcinoma patients treated with induction chemotherapy. *BMC Cancer,* 16 (1), 669.

Hussey, G. S., Link, L. A., Brown, A. S., Howley, B. V., Chaudhury, A. & Howe, P. H. (2012). Establishment of a TGFβ-induced post-transcriptional EMT gene signature. *PloS One,* 7 (12), e52624.

Imai, T., Horiuchi, A., Wang, C., Oka, K., Ohira, S., Nikaido, T. & Konishi, I. (2003). Hypoxia attenuates the expression of E-cadherin via up-regulation of SNAIL in ovarian carcinoma cells. *Am. J. Pathol.,* 163 (4), 1437-1447.

Jakus, J., Wolff, E. C., Park, M. H. & Folk, J. (1993). Features of the spermidine-binding site of deoxyhypusine synthase as derived from inhibition studies. Effective inhibition by bis-and mono-guanylated diamines and polyamines. *J. Biol. Chem.,* 268 (18), 13151-13159.

Kalluri, R. & Weinberg, R. A. (2009). The basics of epithelial-mesenchymal transition. *J. Clin. Invest.,* 119 (6), 1420-1428.

Kandoth, C., McLellan, M. D., Vandin, F., Ye, K., Niu, B., Lu, C., Xie, M., Zhang, Q., McMichael, J. F. & Wyczalkowski, M. A. (2013). Mutational landscape and significance across 12 major cancer types. *Nature,* 502 (7471), 333-339.

Khosravi, S., Martinka, M., Zhou, Y. & Ong, C. J. (2016). Prognostic significance of the expression of nuclear eukaryotic translation initiation factor 5A2 in human melanoma. *Oncol. Lett.,* 12 (5), 3089-3100.

Khosravi, S., Wong, R., Ardekani, G., Zhang, G., Martinka, M., Ong, C. & Li, G. (2014). Role of EIF5A2, a downstream target of Akt, in promoting melanoma cell invasion. *Br. J. Cancer,* 110 (2), 399-408.

Kim, J., Park, E. Y., Kim, O., Schilder, J. M., Coffey, D. M., Cho, C.-H. & Bast, R. C. (2018). Cell origins of high-grade serous ovarian cancer. *Cancers,* 10 (11), 433.

Kindelberger, D. W., Lee, Y., Miron, A., Hirsch, M. S., Feltmate, C., Medeiros, F., Callahan, M. J., Garner, E. O., Gordon, R. W. & Birch, C. (2007). Intraepithelial carcinoma of the fimbria and pelvic serous carcinoma: evidence for a causal relationship. *Am. J. Surg. Pathol.,* 31 (2), 161-169.

Kurman, R. J., Visvanathan, K., Roden, R., Wu, T. C. & Shih, I.-M. (2008). Early detection and treatment of ovarian cancer: shifting from early stage to minimal volume of disease based on a new model of carcinogenesis. *Am. J. Obstet. Gynecol.,* 198 (4), 351-356.

Lee, N. P., Tsang, F. H., Shek, F. H., Mao, M., Dai, H., Zhang, C., Dong, S., Guan, X. y., Poon, R. T. & Luk, J. M. (2010). Prognostic significance and therapeutic potential of eukaryotic translation initiation factor 5A (eIF5A) in hepatocellular carcinoma. *Int. J. Cancer,* 127 (4), 968-976.

Lee, S. K., Lee, J., Lee, S. I., Bae, W. J., Lee, Y. M., Park, J. S., Lee, S. K., Park, S. J., Min, S. K. & Kim, E. C. (2009). N1 ‐ guanyl ‐ 1, 7, ‐ diamineoheptane, an inhibitor of deoxyhypusine synthase, suppresses differentiation and induces apoptosis via mitochondrial and AMPK pathways in immortalized and malignant human oral keratinocytes. *J. Oral Pathol Med.*, 38 (10), 792-800.

Lengyel, E. (2010). Ovarian cancer development and metastasis. *Am. J. Pathol.*, 177 (3), 1053-1064.

Li, Y., Fu, L., Li, J.-B., Qin, Y., Zeng, T.-t., Zhou, J., Zeng, Z.-L., Chen, J., Cao, T.-T. & Ban, X. (2014). Increased expression of EIF5A2, via hypoxia or gene amplification, contributes to metastasis and angiogenesis of esophageal squamous cell carcinoma. *Gastroenterology*, 146 (7), 1701-1713. e9.

Lili, L. N., Matyunina, L. V., Walker, L. D., Wells, S. L., Benigno, B. B. & McDonald, J. F. (2013). Molecular profiling supports the role of epithelial-to-mesenchymal transition (EMT) in ovarian cancer metastasis. *J. Ovarian Res.*, 6 (1), 1-7.

Lin, Y.-M., Chen, M.-L., Chen, C.-L., Yeh, C.-M. & Sung, W.-W. (2020). Overexpression of EIF5A2 Predicts Poor Prognosis in Patients with Oral Squamous Cell Carcinoma. *Diagnostics*, 10 (7), 436.

Liu, T.-A., Chang, H.-K. & Shieh, R.-C. (2012a). Revisiting inward rectification: K ions permeate through Kir2. 1 channels during high-affinity block by spermidine. *J. Gen. Physiol.*, 139 (3), 245-259.

Liu, Y.-N., Abou-Kheir, W., Yin, J. J., Fang, L., Hynes, P., Casey, O., Hu, D., Wan, Y., Seng, V. & Sheppard-Tillman, H. (2012b). Critical and reciprocal regulation of KLF4 and SLUG in transforming growth factor β-initiated prostate cancer epithelial-mesenchymal transition. *Mol. Cell. Biol.*, 32 (5), 941-953.

Liu, Y., Du, F., Chen, W., Yao, M., Lv, K. & Fu, P. (2015a). EIF5A2 is a novel chemoresistance gene in breast cancer. *Breast Cancer*, 22 (6), 602-607.

Liu, Y., Liu, R., Fu, P., Du, F., Hong, Y., Yao, M., Zhang, X. & Zheng, S. (2015b). N1-guanyl-1, 7-diaminoheptane sensitizes estrogen receptor negative breast cancer cells to doxorubicin by preventing epithelial-mesenchymal transition through inhibition of eukaryotic translation initiation factor 5A2 activation. *Cell. Physiol. Biochem.*, 36 (6), 2494-2503.

López-Casillas, F., Wrana, J. L. & Massagué, J. (1993). Betaglycan presents ligand to the TGFβ signaling receptor. *Cell*, 73 (7), 1435-1444.

Lou, B., Fan, J., Wang, K., Chen, W., Zhou, X., Zhang, J., Lin, S., Lv, F. & Chen, Y. (2013). N1-guanyl-1, 7-diaminoheptane (GC7) enhances the therapeutic efficacy of doxorubicin by inhibiting activation of eukaryotic translation initiation factor 5A2

(eIF5A2) and preventing the epithelial–mesenchymal transition in hepatocellular carcinoma cells. *Exp. Cell Res.*, 319 (17), 2708-2717.

Lu, J., Zhao, H. W., Chen, Y., Wei, J. H., Chen, Z. H., Feng, Z. H., Huang, Y., Chen, W., Luo, J. H. & Fang, Y. (2019). Eukaryotic translation initiation factor 5A2 is highly expressed in prostate cancer and predicts poor prognosis. *Exp. Ther. Med.*, 17 (5), 3741-3747.

Luo, J. H., Hua, W. F., Rao, H. L., Liao, Y. J., Kung, H. F., Zeng, Y. X., Guan, X. Y., Chen, W. & Xie, D. (2009). Overexpression of EIF‐5A2 predicts tumor recurrence and progression in pTa/pT1 urothelial carcinoma of the bladder. *Cancer Sci.*, 100 (5), 896-902.

Maier, B., Tersey, S. A. & Mirmira, R. G. (2010). Hypusine: a new target for therapeutic intervention in diabetic inflammation. *Discov. Med.*, 10 (50), 18-23.

Marchet, A., Mocellin, S., Belluco, C., Ambrosi, A., De Marchi, F., Mammano, E., Digito, M., Leon, A., D'Arrigo, A. & Lise, M. (2007). Gene expression profile of primary gastric cancer: towards the prediction of lymph node status. *Ann. Surg. Oncol.*, 14 (3), 1058-1064.

Massagué, J., Seoane, J. & Wotton, D. (2005). Smad transcription factors. *Genes Dev.*, 19 (23), 2783-2810.

Mathews, M. B. & Hershey, J. W. (2015). The translation factor eIF5A and human cancer. *Biochim. Biophys. Acta Gene Regul. Mech.*, 1849 (7), 836-844.

Micalizzi, D. S., Farabaugh, S. M. & Ford, H. L. (2010). Epithelial-mesenchymal transition in cancer: parallels between normal development and tumor progression. *J. Mammary Gland Biol. Neoplasia*, 15 (2), 117-134.

Miettinen, P. J., Ebner, R., Lopez, A. R. & Derynck, R. (1994). TGF-beta induced transdifferentiation of mammary epithelial cells to mesenchymal cells: involvement of type I receptors. *J. Cell Biol.*, 127 (6), 2021-2036.

Miyamoto, S., Nakanishi, M. & Rosenberg, D. W. (2013). Suppression of colon carcinogenesis by targeting Notch signaling. *Carcinogenesis*, 34 (10), 2415-2423.

Muraoka, R. S., Dumont, N., Ritter, C. A., Dugger, T. C., Brantley, D. M., Chen, J., Easterly, E., Roebuck, L. R., Ryan, S. & Gotwals, P. J. (2002). Blockade of TGF-β inhibits mammary tumor cell viability, migration, and metastases. *J. Clin. Invest.*, 109 (12), 1551-1559.

Nakanishi, S. & Cleveland, J. L. (2016). Targeting the polyamine-hypusine circuit for the prevention and treatment of cancer. *Amino Acids*, 48 (10), 2353-2362.

Nauseef, J. T. & Henry, M. D. (2011). Epithelial-to-mesenchymal transition in prostate cancer: paradigm or puzzle? *Nat. Rev. Urol.,* 8 (8), 428.

Nieto, M. A. (2013). Epithelial plasticity: a common theme in embryonic and cancer cells. *Science,* 342 (6159).

Nieto, M. A., Huang, R. Y.-J., Jackson, R. A. & Thiery, J. P. (2016). EMT: 2016. *Cell,* 166 (1), 21-45.

Nik, N. N., Vang, R., Shih, I.-M. & Kurman, R. J. (2014). Origin and pathogenesis of pelvic (ovarian, tubal, and primary peritoneal) serous carcinoma. *Annu. Rev. Pathol.,* 9, 27-45.

Nishimura, K., Lee, S. B., Park, J. H. & Park, M. H. (2012). Essential role of eIF5A-1 and deoxyhypusine synthase in mouse embryonic development. *Amino Acids,* 42 (2-3), 703-710.

Oliverio, S., Corazzari, M., Sestito, C., Piredda, L., Ippolito, G. & Piacentini, M. (2014). The spermidine analogue GC7 (N1-guanyl-1, 7-diamineoheptane) induces autophagy through a mechanism not involving the hypusination of eIF5A. *Amino Acids,* 46 (12), 2767-2776.

Olivier, R., Lubsen-Brandsma, M., Verhoef, S. & Van Beurden, M. (2006). CA125 and transvaginal ultrasound monitoring in high-risk women cannot prevent the diagnosis of advanced ovarian cancer. *Gynecol. Oncol.,* 100 (1), 20-26.

Pällmann, N., Braig, M., Sievert, H., Preukschas, M., Hermans-Borgmeyer, I., Schweizer, M., Nagel, C. H., Neumann, M., Wild, P. & Haralambieva, E. (2015). Biological relevance and therapeutic potential of the hypusine modification system. *J. Biol. Chem.,* 290 (30), 18343-18360.

Park, M. H., Cooper, H. L. & Folk, J. (1981). Identification of hypusine, an unusual amino acid, in a protein from human lymphocytes and of spermidine as its biosynthetic precursor. *Proc. Natl. Acad. Sci.,* 78 (5), 2869-2873.

Park, M. H. & Wolff, E. C. (2018). Hypusine, a polyamine-derived amino acid critical for eukaryotic translation. *J. Biol. Chem.,* 293 (48), 18710-18718.

Park, M. H., Wolff, E. C. & Folk, J. (1993). Hypusine: its post-translational formation in eukaryotic initiation factor 5A and its potential role in cellular regulation. *BioFactors (Oxford, England),* 4 (2), 95.

Pegg, A. E. (2008). Spermidine/spermine-N 1-acetyltransferase: a key metabolic regulator. *Am. J. Physiol. Endocrinol. Metab.,* 294 (6), E995-E1010.

Rafehi, S., Ramos, V. Y., Bertrand, M., McGee, J., Prefontaine, M., Sugimoto, A., DiMattia, G. E. & Shepherd, T. G. (2016). TGFβ signaling regulates epithelial-mesenchymal plasticity in ovarian cancer ascites-derived spheroids. *Endoc. Relat. Cancer*, 23 (3), 147.

Ruggero, D. (2013). Translational control in cancer etiology. *Cold Spring Harb. Perspect. Biol.*, 5 (2), a012336.

Saini, P., Eyler, D. E., Green, R. & Dever, T. E. (2009). Hypusine-containing protein eIF5A promotes translation elongation. *Nature*, 459 (7243), 118-121.

Sankar, S., Mahooti-Brooks, N., Centrella, M., McCarthy, T. L. & Madri, J. A. (1995). Expression of transforming growth factor type III receptor in vascular endothelial cells increases their responsiveness to transforming growth factor β2. *J. Biol. Chem.*, 270 (22), 13567-13572.

Scalici, J. M., Arapovic, S., Saks, E. J., Atkins, K. A., Petroni, G., Duska, L. R. & Slack‐Davis, J. K. (2017). Mesothelium expression of vascular cell adhesion molecule‐1 (VCAM‐1) is associated with an unfavorable prognosis in epithelial ovarian cancer (EOC). *Cancer*, 123 (6), 977-984.

Schnier, J., Schwelberger, H., Smit-McBride, Z., Kang, H. A. & Hershey, J. (1991). Translation initiation factor 5A and its hypusine modification are essential for cell viability in the yeast Saccharomyces cerevisiae. *Mol. Cell. Biol.*, 11 (6), 3105-3114.

Shek, F. H., Fatima, S. & Lee, N. P. (2012). Implications of the use of eukaryotic translation initiation factor 5A (eIF5A) for prognosis and treatment of hepatocellular carcinoma. *Int. J. Hepatol.*, 2012.

Shiba, T., Mizote, H., Kaneko, T., Nakajima, T. & Yasuo, K. (1971). Hypusine, a new amino acid occurring in bovine brain: Isolation and structural determination. *Biochim. Biophys. Acta Gen. Subj.*, 244 (3), 523-531.

Siegel, R. L., Miller, K. D. & Jemal, A. (2019). Cancer statistics, 2019. *CA Cancer J. Clin.*, 69 (1), 7-34.

Solheim, O., Førsund, M., Tropé, C. G., Kraggerud, S. M., Nesland, J. M. & Davidson, B. (2017). Epithelial–mesenchymal transition markers in malignant ovarian germ cell tumors. *Apmis*, 125 (9), 781-786.

Sun, J., Xu, Z., Lv, H., Wang, Y., Wang, L., Ni, Y., Wang, X., Hu, C., Chen, S. & Teng, F. (2018). eIF5A2 regulates the resistance of gastric cancer cells to cisplatin via induction of EMT. *Am. J. Transl. Res.*, 10 (12), 4269.

Tang, D. J., Dong, S. S., Ma, N. F., Xie, D., Chen, L., Fu, L., Lau, S. H., Li, Y., Li, Y. & Guan, X. Y. (2010). Overexpression of eukaryotic initiation factor 5A2 enhances cell

motility and promotes tumor metastasis in hepatocellular carcinoma. *Hepatology,* 51 (4), 1255-1263.

Terraneo, N., Jacob, F., Dubrovska, A. & Grünberg, J. (2020). Novel Therapeutic Strategies for Ovarian Cancer Stem Cells. *Front. Oncol.,* 10, 319.

Tong, Y., Park, I., Hong, B. S., Nedyalkova, L., Tempel, W. & Park, H. W. (2009). Crystal structure of human eIF5A1: insight into functional similarity of human eIF5A1 and eIF5A2. *Proteins: Struct., Funct., Bioinf.,* 75 (4), 1040-1045.

Torre, L. A., Trabert, B., DeSantis, C. E., Miller, K. D., Samimi, G., Runowicz, C. D., Gaudet, M. M., Jemal, A. & Siegel, R. L. (2018). Ovarian cancer statistics, 2018. *CA Cancer J. Clin.,* 68 (4), 284-296.

Tsang, F. H., Au, V., Lu, W.-J., Shek, F. H., Liu, A. M., Luk, J. M., Fan, S.-T., Poon, R. T. & Lee, N. P. (2014). Prognostic marker microRNA-125b inhibits tumorigenic properties of hepatocellular carcinoma cells via suppressing tumorigenic molecule eIF5A2. *Dig. Dis. Sci.,* 59 (10), 2477-2487.

Visintin, I., Feng, Z., Longton, G., Ward, D. C., Alvero, A. B., Lai, Y., Tenthorey, J., Leiser, A., Flores-Saaib, R. & Yu, H. (2008). Diagnostic markers for early detection of ovarian cancer. *Clin. Cancer Res.,* 14 (4), 1065-1072.

Wang, F.-W., Guan, X.-Y. & Xie, D. (2013). Roles of eukaryotic initiation factor 5A2 in human cancer. *Int. J. Biol. Sci.,* 9 (10), 1013.

Webb, P. M. & Jordan, S. J. (2017). Epidemiology of epithelial ovarian cancer. *Best Pract. Res. Clin. Obstet. Gynaecol.,* 41, 3-14.

Wei, J., Cao, J., Zhang, D., Liao, B., Zhong, W., Lu, J., Zhao, H., Zhang, J., Tong, Z. & Fan, S. (2014). EIF5A2 predicts outcome in localised invasive bladder cancer and promotes bladder cancer cell aggressiveness in vitro and in vivo. *Br. J. Cancer,* 110 (7), 1767-1777.

Winter, W. E., Maxwell, G. L., Tian, C., Carlson, J. W., Ozols, R. F., Rose, P. G., Markman, M., Armstrong, D. K., Muggia, F. & McGuire, W. P. (2007). Prognostic factors for stage III epithelial ovarian cancer: a Gynecologic Oncology Group Study. *J. Clin. Oncol.,* 25 (24), 3621-3627.

Wolff, E. C., Lee, Y. B., Chung, S. I., Folk, J. & Park, M. H. (1995). Deoxyhypusine synthase from rat testis: purification and characterization. *J. Biol. Chem.,* 270 (15), 8660-8666.

Wu, G.-Q., Xu, Y.-M. & Lau, A. T. (2020). Recent insights into eukaryotic translation initiation factors 5A1 and 5A2 and their roles in human health and disease. *Cancer Cell Int.,* 20, 1-13.

Xie, D., Ma, N.-F., Pan, Z.-Z., Wu, H.-X., Liu, Y.-D., Wu, G.-Q., Kung, H.-F. & Guan, X.-Y. (2008). Overexpression of EIF-5A2 is associated with metastasis of human colorectal carcinoma. *Hum. Pathol.*, 39 (1), 80-86.

Xu, J., Lamouille, S. & Derynck, R. (2009). TGF-β-induced epithelial to mesenchymal transition. *Cell Res.*, 19 (2), 156-172.

Yan, H. & Sun, Y. (2014). Evaluation of the mechanism of epithelial-mesenchymal transition in human ovarian cancer stem cells transfected with a WW domain-containing oxidoreductase gene. *Oncol. Lett.*, 8 (1), 426-430.

Yang, G.-F., Xie, D., Liu, J.-H., Luo, J.-H., Li, L.-J., Hua, W.-F., Wu, H.-M., Kung, H.-F., Zeng, Y.-X. & Guan, X.-Y. (2009). Expression and amplification of eIF-5A2 in human epithelial ovarian tumors and overexpression of EIF-5A2 is a new independent predictor of outcome in patients with ovarian carcinoma. *Gynecol. Oncol.*, 112 (2), 314-318.

Yang, H., Li, X.-d., Zhou, Y., Ban, X., Zeng, T.-t., Li, L., Zhang, B.-z., Yun, J., Xie, D. & Guan, X.-Y. (2015). Stemness and chemotherapeutic drug resistance induced by EIF5A2 overexpression in esophageal squamous cell carcinoma. *Oncotarget*, 6 (28), 26079.

Yang, J., Yu, H., Shen, M., Wei, W., Xia, L. & Zhao, P. (2014). N 1 - guanyl - 1, 7 - diaminoheptane sensitizes bladder cancer cells to doxorubicin by preventing epithelial – mesenchymal transition through inhibition of eukaryotic translation initiation factor 5 A 2 activation. *Cancer Sci.*, 105 (2), 219-227.

Yang, Q., Ye, Z., Zhang, Q., Zhao, Z. & Yuan, H. (2016a). Expression of eukaryotic translation initiation factor 5A-2 (eIF5A-2) associated with poor survival in gastric cancer. *Tumor Biol.*, 37 (1), 1189-1195.

Yang, S. S., Gao, Y., Wang, D. Y., Xia, B. R., Liu, Y. D., Qin, Y., Ning, X. M., Li, G. Y., Hao, L. X. & Xiao, M. (2016b). Overexpression of eukaryotic initiation factor 5A2 (EIF5A2) is associated with cancer progression and poor prognosis in patients with early - stage cervical cancer. *Histopathology*, 69 (2), 276-287.

Yue, J., Sheng, Y., Ren, A. & Penmatsa, S. (2010). A miR-21 hairpin structure-based gene knockdown vector. *Biochem. Biophys. Res. Commun.*, 394 (3), 667-672.

Zender, L., Xue, W., Zuber, J., Semighini, C. P., Krasnitz, A., Ma, B., Zender, P., Kubicka, S., Luk, J. M., Schirmacher, P., McCombie, W. R., Wigler, M., Hicks, J., Hannon, G. J., Powers, S. & Lowe, S. W. (2008). An oncogenomics-based in vivo RNAi screen identifies tumor suppressors in liver cancer. *Cell*, 135(5):852–64.

Zhang, J., Li, X., Liu, X., Tian, F., Zeng, W., Xi, X. & Lin, Y. (2018). EIF5A1 promotes epithelial ovarian cancer proliferation and progression. *Biomed. Pharmacother.*, 100, 168-175.

Zhao, G., Wang, Q., Gu, Q., Qiang, W., Wei, J.-J., Dong, P., Watari, H., Li, W. & Yue, J. (2017). Lentiviral CRISPR/Cas9 nickase vector mediated BIRC5 editing inhibits epithelial to mesenchymal transition in ovarian cancer cells. *Oncotarget*, 8 (55), 94666.

Zhao, G., Wang, Q., Wu, Z., Tian, X., Yan, H., Wang, B., Dong, P., Watari, H., Pfeffer, L. M. & Guo, Y. (2019). Ovarian primary and metastatic tumors suppressed by survivin knockout or a novel survivin inhibitor. *Mol. Cancer Ther.*, 18 (12), 2233-2245.

Zhou, Q.-Y., Tu, C.-Y., Shao, C.-X., Wang, W.-K., Zhu, J.-D., Cai, Y., Mao, J.-Y. & Chen, W. (2017). GC7 blocks epithelial-mesenchymal transition and reverses hypoxia-induced chemotherapy resistance in hepatocellular carcinoma cells. *Am. J. transl. Res.*, 9 (5), 2608.

Zhu, W., Cai, M.-Y., Tong, Z.-T., Dong, S.-S., Mai, S.-J., Liao, Y.-J., Bian, X.-W., Lin, M. C., Kung, H.-F. & Zeng, Y.-X. (2012). Overexpression of EIF5A2 promotes colorectal carcinoma cell aggressiveness by upregulating MTA1 through C-myc to induce epithelial–mesenchymaltransition. *Gut*, 61 (4), 562-575.

VITA

Guannan Zhao was born in Xinxiang, China in 1987. She received her bachelor's degree from Yangtze University in Jingzhou, China, with a major in Clinical Medicine. She received her master's degree from Zhengzhou University in Zhengzhou, China, with a major in Obstetrics and Gynecology. She moved to United States and started her doctoral study in the Integrated Biomedical Sciences Program at University of Tennessee Health Science Center in 2015. She is expected to receive her Ph.D. degree in November 2020.